UNIVERSIDADE FEDERAL DO CEARÁ
GRADUATE PROGRAM IN CHEMICAL ENGINEERING

DIÔGO PEREIRA BEZERRA

MODIFYING STATE-OF-ART ADSORBENTS FOR CO_2 CAPTURE BY AMINE INCORPORATION AND ION-EXCHANGE

FORTALEZA, CEARÁ, BRAZIL – 2014

DIÔGO PEREIRA BEZERRA

MODIFYING STATE-OF-ART ADSORBENTS FOR CO_2 CAPTURE BY AMINE INCORPORATION AND ION-EXCHANGE

Thesis submitted to the Graduate Program in Chemical Engineering as partial fulfillment of the requirements for the degree of Doctor in Chemical Engineering at Universidade Federal do Ceará

Supervisors:
Prof. Diana Cristina Silva de Azevedo
Prof. Rodrigo Silveira Vieira

FORTALEZA, CEARÁ, BRAZIL – 2014

MODIFYING STATE-OF-ART ADSORBENTS FOR CO_2 CAPTURE BY AMINE INCORPORATION AND ION-EXCHANGE

by
Diôgo Pereira Bezerra
Department of Chemical Engineering
Universidade Federal do Ceará, 2014

Thesis submitted to the Graduate Program in Chemical Engineering as partial fulfillment of the requirements for the degree of Doctor in Chemical Engineering at Universidade Federal do Ceará.

Certified by……
Prof. Diana Cristina Silva de Azevedo
Department of Chemical Engineering, Universidade Federal do Ceará
Thesis Supervisor

Certified by……
Prof. Rodrigo Silveira Vieira
Department of Chemical Engineering, Universidade Federal do Ceará
Thesis Co-Supervisor

Accepted by…….....
Prof. Hosiberto B. Sant'Ana
Department of Chemical Engineering, Universidade Federal do Ceará

Accepted by…….....
Prof. Moises Bastos Neto
Department of Chemical Engineering, Universidade Federal do Ceará

Accepted by…….....
Prof. Jussara Lopes de Miranda
Department of Inorganic Chemistry, Universidade Federal do Rio de Janeiro

Accepted by…….....
Dr. Wilson Mantovani Grava
Centro de Pesquisa e Desenvolvimento Leopoldo Américo Miguêz de Mello, Petrobras

MAY 8, 2014

ABSTRACT

CO_2 is the major Greenhouse Gas (GHG), which may cause undesired consequences to the environment, such as global warming. There are many options for CO_2 separation, among which adsorption on porous materials is highlighted in this work. Activated carbons and zeolites have been proposed as potential adsorbents due to their natural affinity for CO_2 and to the possibility of tailoring textural properties and surface chemistry to enhance capacity and selectivity under specific capture scenarios. This thesis focuses on changing the surface chemistry of conventional adsorbents, by means of amine impregnation and ion-exchange, so as to examine the effect of such modifications on their performance for CO_2 capture. The experimental section was divided into three distinct studies. Initially, CO_2 adsorption isotherms were obtained on X zeolite functionalized with increasing concentrations of 2-aminoethanol (monoethanolamine, abbreviated as MEA). Subsequently, activated carbon was investigated as a support for amine impregnation for CO_2 capture. Lastly, a study of ion exchange in X zeolite was conducted in order to investigate the influence of different compensation cations in CO_2 capture. In general, MEA impregnation led to a deterioration in the textural properties of the examined adsorbents, which are essentially microporous. It seems the amines fill completely the micropores, as the concentration of impregnating solution increases. There is experimental evidence that part of the loaded amine covalently bonds to the zeolitic framework. CO_2 adsorption capacity is always lower for MEA impregnated solids than for the pristine support at 298 K, but the same is not true at 348 K. X zeolite keeps texture and crystalline structure intact upon ion-exchange. CO_2 adsorption is enhanced for smaller and lighter compensating cations, such as Li, reaching 4.82 mmol/g at 348 K and 1 bar. In terms of working capacity (between 0.1 and 1 bar) at 298 K, Ba exchanged X zeolite performs better than the other solids. It remains to be studied in future work the CO_2/N_2 and CO_2/CH_4 selectivity of such materials in dry and humid conditions.

KEYWORD: CO_2 adsorption; zeolite; activated carbon**.**

RESUMO

CO_2 é o principal Gás de Efeito Estufa (GEE), que pode causar consequências indesejáveis ao meio ambiente, como o aquecimento global. Há muitas opções para a separação de CO_2, entre as quais a adsorção em materiais porosos é destaque neste trabalho. Carbonos ativados e zeólitos têm sido propostas como potenciais materiais adsorventes, devido à sua afinidade natural com o CO_2 e para a possibilidade de adaptar as propriedades texturais e química de superfície para aumentar a capacidade e seletividade em cenários de captura específicos. Esta tese se concentra em modificar a química da superfície de adsorventes convencionais, por meio de impregnação de amina e troca-iônica, de modo a avaliar o efeito de tais modificações sobre o seu desempenho de captura de CO_2. A secção experimental foi dividida em três estudos distintos. Inicialmente, isotermas de adsorção de CO_2 foram obtidos em zeólito X funcionalizado com concentrações crescentes de 2-aminoetanol (Monoetanolamina, MEA). Subsequentemente, o carbono ativado, foi investigado como um suporte para a impregnação de amina para a captura de CO_2. Por último, um estudo de troca iônica em zeólito X foi realizada a fim de investigar a influência de diferentes cátions de compensação na captura de CO_2. Em geral, MEA impregnação conduziu a uma deterioração nas propriedades texturais dos adsorventes estudados, que são essencialmente microporosos. Quanto maior a concentração da solução de impregnação aumenta, maior é o preenchimento dos microporos por aminas. Há evidências experimentais de que parte da amina carregada liga covalentemente à estrutura zeolítica. A capacidade de adsorção de CO_2 é sempre menor para amostras impregnadas do que para o suporte puro a 298 K, contudo em temperatura maiores, 348 K, é possível observar melhorias. Zeólito X mantém textura e estrutura cristalina intacta nas amostras de troca-iônica. Adsorção de CO_2 é reforçada por cátions de compensação menores e mais leves, como Lítio, atingindo 4,82 mmol/g a 348 K e 1 bar. Em termos de capacidade de trabalho (entre 0,1 e 1 bar) a 298 K, o Ba em zeólito X tem um desempenho melhor do que os outros sólidos. Ele continua a ser estudado em trabalhos futuros a CO_2/N_2 e CO_2/CH_4 seletividade de tais materiais em condições secas e úmidas.

PALAVRAS-CHAVE: Adsorção de CO_2; zeolito; carbono ativado

LIST OF FIGURES

CHAPTER 1 – INTRODUCTION

CHAPTER 3 – LITERATURE REVIEW

CHAPTER 4 – AMINE-GRAFTED X ZEOLITE

CHAPTER 5 – AMINE-GRAFTED ACTIVATED CARBON

LIST OF TABLE

ABREVIATION

Greenhouse Gases	GHG
Energy Information Administration	EIA
United States	US
Intergovernmental Panel for Climate Change	IPCC
Environmental Protection Agency	EPA
Carbon Capture and Storage	CCS
Density Functional Theory	DFT
Non Local Density Functional Theory	NLDFT
Polyethyleneimine	PEI
X-ray Photoelectron Spectroscopy	XPS
Fourier Transform Infrared Spectroscopy	FTIR
Thermo-Gravimetric Analysis	TGA
Activated Carbon	AC
Pore Size Distribution	PSD
Thermo-Gravimetric Analysis – Mass Spectrometry	TGA-MS

SUMMARY

CHAPTER 1 - INTRODUCTION

1.1 Introduction

The emissions of pollutants from combustion of fossil fuels, including air toxics and greenhouse gases (GHGs), have become a global issue. The use of fossil fuels to meet energy demands contributes to a number of environmental problems in global scale (**Olajire, 2010**). Moreover, EIA (Energy Information Administration, of the U.S. Department of Energy) predicts a 57 % increase in energy demand from 2004 to 2030 (**EIA, 2003**), which has been one of the main drives for studies on new energy sources and ways to mitigate greenhouse gas effects.

According to the second report of the Intergovernmental Panel for Climate Change (**IPCC, 2007**), human activities initiated in the industrial era have caused the emission of four main greenhouse gases: carbon dioxide (CO_2), methane (CH_4), nitrous oxide (N_2O) and halocarbons (a group of gases containing fluorine, chlorine and bromine) (see **Table 1.1**).

Table 1.1. Emission sources of greenhouse gases (**IPCC, 2007**).

GHGs	**Emissions From**
Methane (CH_4)	Agriculture, natural gas distribution landfills
Carbon Dioxide (CO_2)	fossil fuel manufacture of cement
Nitrous Oxide (N_2O)	fertilizer fossil fuel
Halocarbons (X/F,Cl,Br)	refrigeration agents industrial processes
Ozone (O_3)	chemical reactions in the troposphere through the release of carbon monoxide, hydrocarbons and nitrogen oxide

Among anthropogenic greenhouse gases, methane is thought to have the second greatest effect on the climate, after carbon dioxide (**IPCC, 1995**). Methane emissions from anthropogenic sources account for 70 % of all methane emissions worldwide,

contributing significantly to global warming (**Ritzkowski and Stegmann, 2007**). After 1750, atmospheric CH4 levels rose almost exponentially with time, reaching 1650 ppb by the mid-1980s and 1803 ppb by 2011. Between 1980s and 2000s the atmospheric concentration of CH4 remained stable, increasing again more recently since 2006 (Dlugokencky et al., 2009; Frankenberg et al., 2011; IPCC, 2013).

The fossil fuel combustion and fertilizer use are emission sources of nitrous oxide (**IPCC, 2005; IPCC, 2007; IPCC, 2013; Snyder et al., 2009**). Its emission has increased since the pre-industrial era, estimated at $1.88 \cdot 10^{13}$ g per year (**EPA, 2010**). Other greenhouse gases such as ozone and water are also studied; however, they exhibit structural instability (short half-life) and hence they do not contribute significantly to the greenhouse effect (**IPCC, 2005; IPCC, 2007**).

Among these GHGs, CO_2 is the largest contributor in regards to its concentration in the atmosphere, contributing to nearly 60 % of global warming effects (**Yamasaki, 2003; IPCC, 2013**). Moreover, the largest absorption of infrared radiation by carbon dioxide and its longer residence time in the atmosphere determine its higher contribution to the greenhouse effect (see **Figure 1.1**).

Large quantities of carbon dioxide are released in the atmosphere around the globe every day, from several important industries, such as power generation, steel and cement manufacturing (**Yadav et al., 2010**). CO_2 emission from anthropogenic activity was within the order of magnitude of 7 Gt/yr only in the late 1990's (**Yamasaki, 2003**).

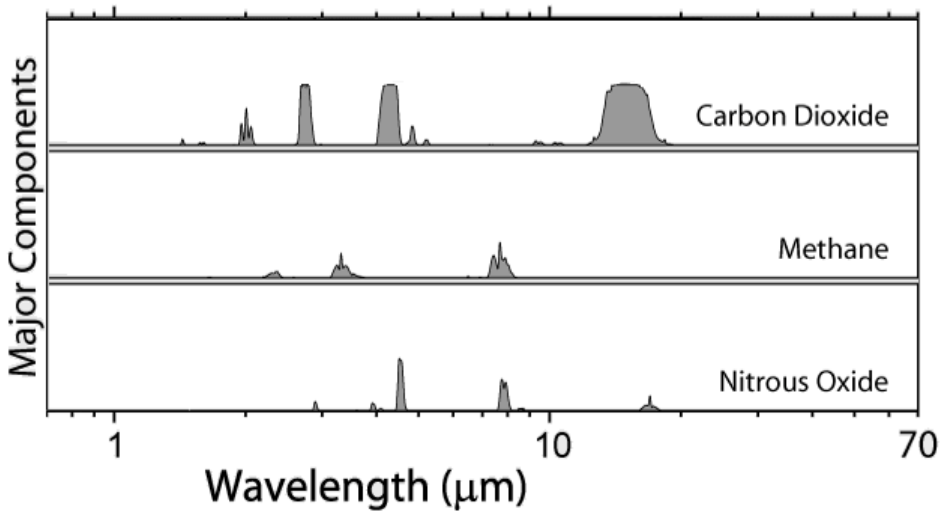

Figure 1.1. Infrared absorption by greenhouse gases (adapted image of Global Warming Art - Robert A. Rohde).

Given the growing CO_2 emissions and increasing global energy demand (**IEA, 2003; IEA 2002**), concerted action is necessary in order to stabilize the atmospheric concentration of CO_2. Among the available technologies, Carbon Capture and Storage (CCS) processes have been receiving significant attention in recent years and are being recognized as promising options for CO_2 emission reductions (**Beecy and Kuuskraa, 2001; Thiruvenkatachari et al., 2009**).

Under this CCS concept, carbon dioxide would be captured from emission point sources (such as pre- and post-combustion power plants, and in large industrial process, for instance, separating it from natural gas, coal bed methane or biogas) and injected into geologic formations, mature petroleum and gas reservoirs, saline formations, unmineable coal seams, among others (**Klara et al., 2003; Figueroa et al., 2008**).

In CCS, there are three main technological pathways that can be pursued for CO_2 capture from fossil fuel-derived power generation plants: post-combustion, pre-combustion and oxy-fuel combustion. The scenario of post-combustion is typical of current power plants, CO_2 being separated from other exhaust gas constituents leaving the cracking-furnace (see **Figure 1.2 (a)**). The major obstacle in post-combustion is the

low pressure of the flue gas (atmospheric pressure). Moreover, low CO_2 concentration (14-15 %), presence of steam and other components (N_2, H_2O, O_2, CO, SO_X and NO_X) and high temperatures (ca. 348 K) make it particularly difficult to capture CO_2.

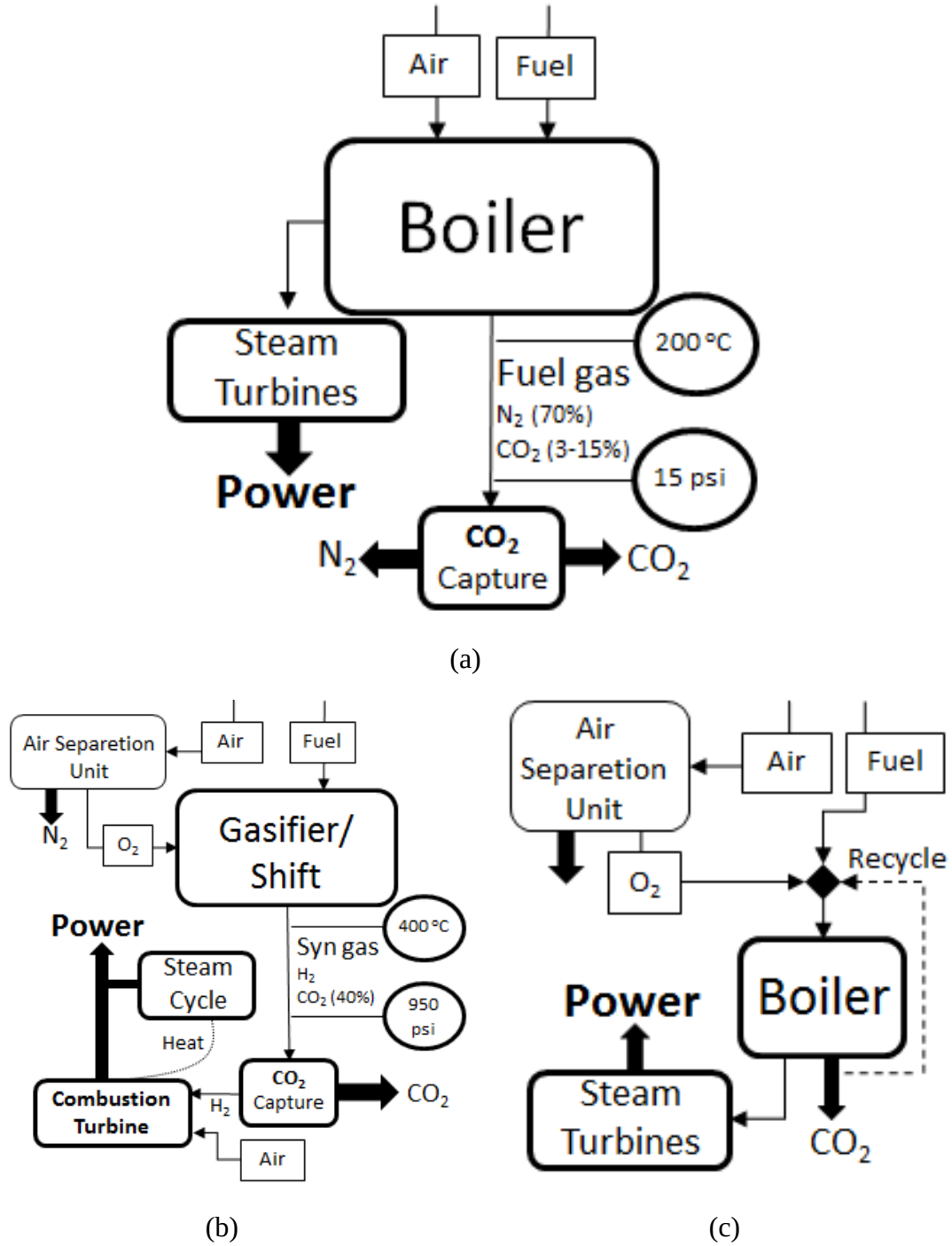

Figure 1.2. Block diagrams illustrating post-combustion (a), pre-combustion (b), and oxy-combustion (c) systems (Adapted from **Figueroa et al., 2008**).

The scenario of pre-combustion is typical of power plants on a hydrogen-based energy matrix, where the CO_2 is generated by water-gas shift reactions (see **Figure 1.2 (b)**). In pre-combustion, generated CO_2 is under high pressure (30-50 atm), about 40 % v/v and temperatures around 313 K. Other gases are usually also present (H_2, CO, H_2S, N_2 and H_2O), which may pose additional separation challenges.

For the scenario of oxy-fuel combustion, the energy production is carried out by burning fuel in oxygen-enriched air, resulting in a flue gas rich in CO_2 (see **Figure 1.2 (c)**). In such scenario, combustion is highly exothermic, requiring structural changes in the equipment or adjustments for cooling. In this process, there is also formation of other gases (H_2O, SO_2, NO_X and HCl), which should be separated from CO_2.

Within this context, post-combustion CO_2 capture can be regarded as an add-on solution with minor changes to existing power plants, allowing for its medium to short-term application. According to **IPCC (2007)** estimates, CO_2 emissions to the atmosphere could be reduced by 80-90 % in a post-combustion power plant equipped with CCS facilities. However, its current implementation may increase the energy requirements of the plant up to 25-40 % (without compression), requiring advances in capture technologies and material developments for its implementation (**IPCC, 2005; Haszeldine, 2009; D'Alessandro et al., 2010**).

There are many options for CO_2 separation, and these include absorption, adsorption, membranes and cryogenics. The cryogenic method of purification involves the separation of the gas mixtures by fractional condensation and distillation of CO_2 at temperatures as low as 200 K, implying a high energy cost (**Olajire, 2010**). In membrane processes, the permeating materials, either organic or inorganic, porous or non-porous, act as filters to separate one or more gases from a feed mixture by distinct mechanisms

(solution/diffusion, adsorption/diffusion, molecular sieving and ionic transport), may be advantageous for natural gas purification by high pressure.

Among these technologies, absorption is promising because it can be easily implemented for large-scale CO_2 capture from point sources, being a currently commercial technology. However, it still requires improvements in reducing energy consumption involved in absorbent regeneration (**Onoda, 2009**).

Adsorption is another well-known separation technology that makes use of porous solids with high selectivity. These materials, called adsorbents, can operate via weak physisorption processes (van der Waals forces, repulsion and dispersion, and electrostatic interactions including the interaction of polarization, dipole and quadrupole) or strong chemical interactions (with formation of chemical bonds or complexation). Separation processes are usually employed in cyclic, multi-module processes of adsorption and desorption, with desorption induced by a pressure or temperature swing (**Choi et al., 2009**).

The adsorbents typically investigated for gas adsorption include activated carbons, zeolites, modified mesoporous silica, metal oxides, mixed hydroxides and metal-organic frameworks. Among these, amine-grafted adsorbents have gained increased attention in the capture of CO_2 from flue gases because of their potential to maintain adsorption capacity at temperatures around 373 K. The modification increases the strong interactions between adsorbate and adsorbent (chemisorption) even at high temperature.

Significant advances have been reported for these adsorbents and this thesis will review the methodologies of impregnation, the characterization techniques and results of CO_2 capture using amine-grafted adsorbents.

1.2 References

Beecy, D.J., Kuuskraa, V.A. Status of U.S. geologic carbon sequestration research and technology. Environmental Geosciences 8 (2001) 152–159.

Choi, S., Drese, J.H., Jones, C.W. Adsorbent Materials for Carbon Dioxide Capture from Large Anthropogenic Point Sources. ChemSusChem 2 (2009) 796–854.

D'Alessandro, D.M., Smit, B., Long, J.R. Carbon Dioxide Capture: Prospects for New Materials. Angewandte Chemie International 49 (2010) 6058–6082.

EIA – U.S. Energy Information Administration. International Energy Outlook Washington, 2003.

EPA. Inventory of U.S. Greenhouse Gas Emissions and Sinks: 1990-2008. 430-R-10-006. U.S. Environmental Protection Agency, N.W. Washington, 2010.

Figueroa, J.D., Fout, T., Plasynski, S., McIlvried, H., Srivastava, R.D. Advances in CO_2 capture technology—The U.S. Department of Energy's Carbon Sequestration Program. International Journal of Greenhouse Gas Control 2 (2008) 9–20.

Haszeldine, R.S. Carbon Capture and Storage: How Green Can Black Be. Science 325 (2009) 1647–1652.

IEA. CO_2 emissions from fossil fuel combustion 1971–2000. International Energy Agency (IEA), Paris, 2002.

IEA. Prospects for CO_2 capture and storage. Energy technology analysis, OECD/IEA. International Energy Agency (IEA), France, 2003.

IPCC, Climate Change 1995: Impacts, Adaptations, and Mitigation of Climate Change: Scientific-Technical Analyses. Contribution of Working Group II to the Second Assessment Report of the Intergovernmental Panel on Climate Change. Cambridge: Cambridge University Press, 1995.

IPCC. Climate Change 2005: Carbon Dioxide Capture and Storage. Intergovernmental Panel on Climate Change. Cambridge: Cambridge University Press, 2005.

IPCC, Climate Change 2007: The Physical Science Basis. Contribution of Working Group I to the Fourth Assessment Report of the Intergovernmental Panel on Climate Change. Cambridge: Cambridge University Press, 2007.

Klara, S.M., Srivastavab, R.D., McIlvriedb, H.G. Integrated collaborative technology development program for CO_2 sequestration in geologic formations—United States Department of Energy R&D. Energy Conversion and Management 44 (2003) 2699–2712.

Olajire, A.A. CO_2 capture and separation technologies for end-of-pipe applications – A review. Energy 35 (2010) 2610–2628.

Onoda, M. Recent CO_2 capture technology. Journal of the Japan Institute of Energy 88 (2009) 278–283.

Ritzkowski, M., Stegmann, R. Controlling greenhouse gas emissions through landfill in situ aeration. International Journal of Greenhouse Gas Control 1 (2007) 281–288.

Snyder, C.S., Bruulsema, T.W., Jensen, T.L., Fixen, P.E. Review of greenhouse gas emissions from crop production systems and fertilizer management effects. Agriculture. Ecosystems and Environment 133 (2009) 247–266.

Thiruvenkatacharia, R., Su, S., Ana H., Yua, X.X. Post combustion CO_2 capture by carbon fibre monolithic adsorbents. Progress in Energy and Combustion Science 35 (2009) 438–455.

Yadav, V.S., Prasad, M., Khan, J., Amritphale, S.S., Singh, M., Raju, C.B. Sequestration of carbon dioxide (CO_2) using red mud. Journal of Hazardous Materials 176 (2010) 1044–1050.

Yamasaki, A. An Overview of CO_2 Mitigation Options for Global Warming—Emphasizing CO_2 Sequestration Options. Journal of Chemical Engineering of Japan 36 (2003) 361–375.

CHAPTER 2 – RESEARCH OBJECTIVE AND OUTLINE

2.1 Objectives

This thesis is intended to provide an assessment of adsorption in some classes of porous solids as a CO_2 uptake technology, focusing on the development of efficient adsorbents for CO_2 capture, by evaluating the adsorption characteristic of amine-based materials with different chemical nature and ion-exchanged zeolites.

2.2 Outline

Chapter 3 focuses on a literature review of the possible interaction mechanisms between an amine and a support and on the identification of the physical-chemical characteristics of an adsorbent influencing on its performance for CO_2 capture. In Chapter 4 the experimental results obtained of the adsorption for CO_2 on X zeolite functionalized with MEA in different concentrations will be presented. In Chapter 5, the use of activated carbon as a support for amino impregnation was investigated for CO_2 capture. Lastly, in Chapter 6, a study of ion exchange in binder-free X zeolite pellets – a state-of-the-art CO_2 adsorbent - was conducted in order to investigate the influence of different compensation cations in CO_2 capture.

CHAPTER 3 – LITERATURE REVIEW

Relevant advancements have been reported for amine-loaded adsorbents and this chapter will summarize the methodologies of impregnation, the characterization techniques, as well as the main results reported in the literature concerning these issues.

3.1 Materials

3.1.1 Support

A variety of microporous and mesoporous materials have been considered to be used as support for amine-impregnation aiming at CO_2 capture: carbon-based sorbents such as activated carbon, carbon molecular sieves and carbon nanotubes, zeolites, and mesoporous silica-based materials (SBA, MCM, KIT etc.).

3.1.2 Amines

Amines are organic molecules of basic character, generally used to absorb acid gases in industrial processes. However, these industrial processes of carbon dioxide capture using liquid amines suffer from several disadvantages, such as solvent degradation, corrosion, and foaming. A fraction of the amine and its decomposition products is also lost by evaporation, posing severe operational problems (**Knöfel et al., 2009**). In order to overcome these disadvantages, adsorption on amino-functionalized solids has been claimed to be a promising alternative. Amino modifications on the surface, incorporate new adsorption sites and the more intense interaction forces may remain unchanged even at high temperatures (**Aroua et al., 2008; Bacsik et al., 2010; Bezerra et al., 2011; Khalil et al., 2012**).

The most widely studied amine in acid gas solvent scrubbing is monoethanolamine (MEA). Despite being commercially utilized for CO_2 absorption, there are few reports of its immobilization in porous supports. A large variety of other molecules containing amino groups has been evaluated to be incorporated in porous

solids, seeking for a better compromise between structural and chemical interactions (amine, polyamine, aminoalcohol, aminosilane, polyamidoamine etc.).

3.2 Impregnation Methods

3.2.1 Wet Impregnation Method

Aqueous amine solutions are added to appropriate amounts of support in a given solid–liquid ratio. Some authors report that the theoretical value for the maximum amount of amines that can be impregnated into a support is equal to the pore volume ($cm^3\ g^{-1}$) of a given support multiplied by the specific mass of the amine ($g\ cm^{-3}$) (**Choi et al., 2009**). In some cases, this theoretical amount is added gradually so that the solid is only slightly soaked by the amine solution, which is called by some authors as incipient wet impregnation or dry impregnation (**Choi et al., 2009**).

The wet impregnation is very easy as compared to other methods. In a typical preparation, the desired amount of amine is dissolved in some solvent (water, methanol, benzene, toluene etc.) under stirring for a given time until a homogeneous mixture is obtained. Then, the adsorbent is added to the amine solution. The resulting slurry is continuously stirred long enough to reach reaction equilibrium (variable for each solution and adsorbent). Some studies add a heating step during this process. Then the slurry is dried at a temperature next to the boiling point of the solvent by a certain time under reduced pressure or a flow of inert gas (nitrogen, helium, etc.) (**Xu et al., 2003**).

Some studies report a drastic reduction in the textural characteristics of the adsorbents after the impregnation of amines following this methodology. The impregnation process leads to a decrease in the surface areas, indicating blocking of the pores due to the amine filling. However, the mechanism of pore filling using different amines is not well understood, but it is assumed that the different pore filling effects are

due to the differences in the molecular size and shape of the amines used (**Lin et al. 2013; Yaumi et al., 2013**).

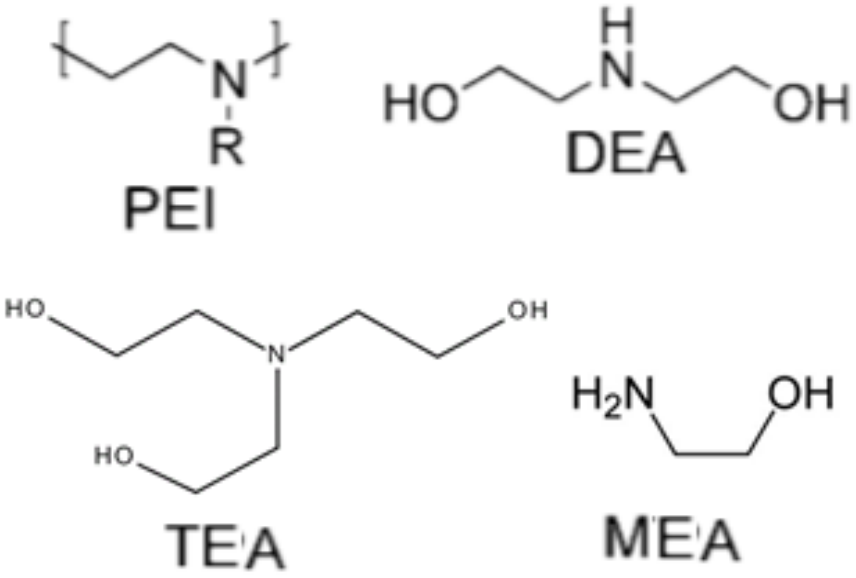

Figure 3.1. Amines used in the synthesis of solid supported amine adsorbents (Adapted from **Choi et al., 2009**).

For example, MEA, a primary amine with low molecular weight (69 g/mol), is very specific towards filling micropores, whereas branched structures with higher molecular weight and size (e.g. polyamines) appear to build up in the mesopores and may block off the micropores without actually filling them (**Choi et al., 2009**). It should also be considered that the loaded amount of amine may also affect the pore coverage and blockage. Theoretically, this filling effect is justified by the incorporation of amine into the adsorbent, restricting the access of gases into the pores (**Chatti et al., 2009; Xu et al., 2003**).

3.2.2 Thermal Treatment in the Presence of Ammonia.

The samples are obtained by placing them under ammonia pure flow at high temperatures for a given time. This may be carried out in a vertical tube furnace at temperatures higher than 673 K. Dried carbon is placed in a quartz reactor and held under N_2 flow (**Plaza et al., 2009**). Once the sample reaches the desired temperature, the flow is changed from N_2 to NH_3, or to NH_3 in air, and held at least for 2 h. Finally, the flow is changed back to N_2 until room temperature is reached.

3.2.3 Electrophilic Aromatic Substitution

The first step involves aromatic nitration of the support (activated carbon): a mixture of concentrated acids is prepared by adding sulfuric acid and nitric acid. Next, the selected support is added to the acid mixture and stirred 323 K. The mixture is filtered, washed with distilled water, and then air dried. The second step consists of reducing the attached nitro groups to amine functionalities using sodium hydrosulfite ($Na_2S_2O_4$), as a reducing agent in basic media. Then, the nitrated sample is added to a mixture of ammonia solution and stirred. Then, $Na_2S_2O_4$ is added to the mixture, which is left to stir at room temperature. The resulting product is filtered and washed. In order to eliminate a possible excess of sodium hydrosulfite in the filtrate, the carbon may be allowed to stir in distilled water for after be filtered and washed again. This process is repeated three times in order to purify the product. Finally, the carbon is air dried (**Plaza et al., 2009**).

3.3 Possible Reaction Mechanisms

The loading of the amine to a solid support may overcome such disadvantages or limitations associated with the liquid-amine-based scrubbing systems. The identified limitations are the corrosive nature of the amines being used, high-energy costs in

regenerating the scrubbing units and problems associated with the viscous nature of the amine solutions (**Franchi et al., 2005; Chatti et al., 2009**).

It is envisaged that the amine exists as a confined solvent in the porous solid matrix, which plays the role of micro-reactors for the capture of carbon dioxide. Studies reveal (**Bacsik et al., 2010**) that the interaction of amines with silica-based supports, after to wet impregnation, occurs by reaction of the silanol and aluminol groups with a carbon atom of the amine, according to reaction 1. Another source of basic strength is required to remove the weak H of silanol.

$$SiOH + C_nH_{2n+1}–NH_2 \rightleftharpoons Si–(C_nH_{2n})–NH_2 + H_2O \quad (1)$$

Some authors (**Chatti et al., 2009**) recommend a pretreatment of the support only with solvent (methanol, generally) so that silanol and aluminol groups present in the support react with methanol to form $Si–O–CH_3$ and water. It is necessary to force the removal of water. The use of benzene in the pre-treatment will result in a greater electron-donor effect, raising the basic character of the adsorbent.

$$Si + CH_3–CH_2–OH \rightleftharpoons Si–O–CH_3 + H_2O \quad (2)$$

The $Si–O–CH_3$ group then reacts with the amine molecule:

$$Si–O–CH_3 + RNH_n \rightleftharpoons Si–O–(CH_n)NH_n \quad (3)$$

The reactions taking place between CO_2 and the amine-grafted adsorbents are similar to the reactions with aqueous amine, wherein there is formation of carbonates, bicarbonates, carbamate species depending to the conditions of humidity, temperature, pressure etc. as shown in reaction 4 and 5 (**Filburn et al., 2005; Chatti et al., 2009**):

$$2RNH_2 + CO_2 \rightleftharpoons RNHCOO^- + RNH_3^+ \quad (4)$$

$$RNHCOO^- + H_2O \rightleftharpoons RNH_2 + HCO_3^- \quad (5)$$

The enhancement in the adsorption capacity of the amine loaded support materials can be attributed to this chemisorptive interaction of CO_2 with amine, which may

theoretically be evenly dispersed in the pores of adsorbents with high surface area. However, studies are not conclusive with reference the reactions/interactions that occur in this system and to which extent chemisorption and physisorption may act synergistically at high temperatures. Further studies are therefore in progress to elucidate this mechanism.

3.4 Characterization Techniques

3.4.1 Nitrogen Adsorption/Desorption Isotherms at 77 K

From N_2 adsorption/desorption isotherms at cryogenic temperature (77 K), textural parameters (surface area, total volume pore, volume of meso or micropores, pore diameter and pore size distribution) may be obtained.

The specific surface area, S_{BET}, can be calculated by the Brunauer–Emmett–Teller (BET) equation; average pore size can be estimated by means of the expression $f.V_P / S_{BET,}$ where f is dependent on the pore format; total pore volume, V_P, were evaluated using Gurvitch's rule at P/P_o=0.99; micropore volume, V_M, can be determined by using the Dubunin–Radushkevich equation; the mesopore volume and pore size distribution can be calculated by applying the Density Functional Theory (DFT) methods (**Rouquerol et al., 1999**). These methods are classic and suitable for textural characterization of the samples.

The textural properties of amino-grafted adsorbents tend to deteriorate as the amine loading increases. A likely explanation is the presence of amine inside the pores, impeding access of the probe-molecule (e.g., nitrogen with 1.57 Å).

Aroua et al. (2008) reports the impregnation of 0.28 % poliethyleneimine (PEI) on commercial activated carbon. It is interesting to note that the volume of adsorbed nitrogen (in micropores) is higher for PEI/AC than for virgin AC. The authors suggest that the large PEI molecules may have adsorbed predominantly on macro- and mesopores

of the AC and as a result, reduces and constrict them. This subsequently results in creation of additional meso- microporous and the higher volume of adsorbed nitrogen.

Impregnation with high concentrations of amine can lead to a drastic reduction in the volume of adsorbed nitrogen, and consequently a worsening of the textural characteristics. **Son el al. (2008)** reported a reduction in the textural characteristics of mesoporous silicas (MCM-41, MCM-48, SBA-15, SBA-16 and KIT-6) for concentrations of PEI higher than 50% in the impregnating solution.

Plaza et al. (2010) used heat treatment with gaseous ammonia to both activate and generate basic sites in carbon. They report a development of the porous structure of the carbonaceous material although to a lesser extent than that usually obtained by conventional activation procedures (with CO_2). Amine-impregnation showed two advantages over activation with CO_2: a shorter soaking time and a greater carbon yield.

Zukal et al. (2009) studied the impregnation of aminosilane in SBA-15 and zeolite ITQ-6, a kind of mesoporous zeolitic material. They also reported a reduction of the textural characteristics (surface area, mesopore volume and pore size), after amine impregnation.

Xu et al. (2009) studied the impregnation of zeolite beta with monoethanolamine (MEA) varying concentrations (5, 15, 40 and 60 % wt). They reported that very small surface areas (15−17 m^2/g) and pore volumes (0.063−0.090 cm^3/g) were obtained when the MEA concentration in the impregnating solution was higher than 15 % wt. Upon further increase of the MEA loading, the micropores of zeolite beta were filled with MEA, thus restricting access of nitrogen at its condensation temperature. **Table 3.1** summarizes textural characteristics of amine modified adsorbents reported on some previous studies.

Table 3.1. Textural Characteristics of samples reported in the literature.

Sample	Amine	Surface Area (m^2/g)	Pore volume (cm^3/g)	Pore size (nm)	Reference
AC	-	941	0.524	-	**Aroua et al., 2008**
	PEI 0.28wt%	1052	0.605	-	
MCM-41	-	1042	0.85	2.8	**Son et al., 2008**
	PEI 50wt%	4	0.01	-	
MCM-48	-	1162	1.17	3.1	
	PEI 50wt%	26	0.10	-	
SBA-15	-	753	0.94	5.5	
	PEI 50wt%	13	0.04	-	
KIT-6	-	895	1.22	6.0	
	PEI 10wt%	430	0.68	5.9	
	PEI 30wt%	251	0.49	5.4	
	PEI 50wt%	86	0.18	5.3	
AOS Char (AC)	-	859	0.420	1.0	**Plaza et al., 2010**
	NH_3 (gas)	853	0.395	0.9	
ITQ-6 Zeolite (1 - 4 mmol of amine/g ITQ-6)	-	580.4	0.318	9.5	**Zukal et al., 2009**
	AP	102.6	0.118	9.5	
	MAP	121.9	0.129	9.3	
	PAP	58.3	0.102	9.8	
SBA-15 (1 - 4 mmol of amine/g SBA-15)	-	790.1	0.810	6.2	
	AP	561.7	0.785	5.8	
	MAP	445.3	0.572	5.6	
	PAP	307.2	0.472	4.8	
Zeolite Beta	-	574	0.230	0.65	**Xu et al., 2009**
	MEA 5wt%	209	0.190	0.57	
	MEA 15wt%	17	0.090	-	
	MEA 40wt%	15	0.074	-	
	MEA 60wt%	15	0.063	-	
SBA-15 (1)	-	528.9	0.760	5.7	**Fadhel et al., 2009**
	PAMAM	19.9	0.030	6.9	
SBA-15 (2)	-	660.1	0.820	4.8	
	PAMAM	36.1	0.060	6.3	

3.4.2 Spectroscopic Techniques (IR and XPS)

IR spectroscopy is an important technique to study the adsorbent after impregnation and it has been mainly used for two purposes: structural elucidation and compound identification. This technique is mostly based on absorption spectroscopy within the infrared region of the electromagnetic spectrum. X-ray Photoelectron Spectroscopy (XPS) is capable of identifying qualitatively all chemical elements present on the surface of the adsorbent and their oxidation states, among other information, such as metal arrangement (tetrahedral, octahedral, etc.) XPS spectra are obtained by irradiating of the adsorbent with a beam of X-rays and measuring the binding energy and number of electrons that escape from the surface (**Guo et al., 2013; Yu et al., 2012**).

Bacsik et al. (2010) studied certain aspects of propylamine-modified silica using FTIR spectroscopy. The IR spectra revealed the presence of primary amino groups in all impregnated samples. In-situ temperature-programmed adsorption of CO_2 was also studied by IR spectroscopy. As expected, the authors observed that the amount of physisorbed CO_2 is lower at high temperatures. Some chemisorbed species formed at 308 K do not occur at 343 K, as the bands of NH_3^+ groups decreased in intensity. **Knöfel et al. (2009)** obtained similar results for mesoporous silicas impregnated with aminopropylsilane (APS) and they postulated the formation of chemisorption products: carbamate, and carbonate.

Chang et al. (2009) evaluated the impregnation of mono, di and tri-amines in SBA-15 for the adsorption of CO_2. They reported a decrease in IR absorption of silanol groups followed by the appearance of absorption peaks of N–H bonds, C–H bonds and Si–C bonds, thus suggesting the formation of aminosilanes on the surface of SBA-15.

The IR spectra of N-enriched activated carbons studied by **Zhang et al. (2010)** showed some marked similarities among samples (modified and unmodified) assigned to

aliphatic C–H stretching modes, C–O (carboxylic and lactones) and C–C. New IR absorbance bands related to N-containing species were observed in the spectra of the modified ACs, implying that the heat treatment of samples under ammonia flux produced new nitrogen surface complexes. The amine groups were related to the detected vibrational modes of bonds C–N and C–N–C. In this study, XPS confirmed significant increment of nitrogen atomic concentration on their surfaces, from 1.80 to 2.56 N % atomic composition.

Arrigo et al. (2010) reported the formation of nitrogen species in nanocarbons functionalized with NH_3 at different temperatures by XPS analyses. Oxidized nitrogen groups (amide) were also identified depending on the temperature of the impregnation process, rising from 1.3 to 10 N % atomic composition.

3.4.3 Thermo-Gravimetric Analysis (TGA)

Thermo-gravimetric analysis (TGA) measures changes in sample weight as a function of temperature. It may be performed under inert, reducing or oxidative atmosphere and is usually intended to assess sample thermal stability.

Xu et al. (2009) studied beta zeolite impregnated with monoethanolamine in varying concentrations by wet impregnation. The thermo-gravimetric analysis on the parent zeolite showed a unique weight loss up to 450 K, which is assigned to the desorption of physically adsorbed water. For the MEA-modified zeolites, similar weight losses attributed to water desorption were also detected. Another weight loss event is evident at temperatures higher than 450 K, which increased in magnitude with the increase of MEA loading. Such weight losses can thus be attributed to the desorption and/or decomposition of impregnated amine species.

Wei et al. (2008) studied CO_2 adsorption in amine (APTES, N-(2-aminoethyl)-3-aminopropyltrimethoxysilane) supported in SBA-16 by wet impregnation. The results

showed that a significant mass loss occurred when the parent and functionalized SBA-16 was heated at 403 K, attributed to the loss of physically adsorbed water. Up to 403 K, Wei reported superior mass loss for the functionalized silica, about 10 %, as compared to 5 % of the parent sample. The introduction of amino groups possibly increased the hydrophilicity of the sample. For functionalized samples, another weight loss event of about 15 % was present at temperatures 473 K, related to amine-grafting.

Knöfel et al. (2007) reported diamine (TEDA) supported SBA-16 for CO_2 adsorption and they obtained 27 % mass loss, assigned to the loaded amine at temperatures above 473 K.

3.5 CO_2 Equilibrium Adsorption

Most porous adsorbents (activated carbon, zeolite, mesoporous silica etc.) have good potential for CO_2 capture, but their adsorption capacity or selectivity over other gases becomes insufficient especially at high temperature and in the presence of humidity, NOx and SOx (typical in post-combustion scenario). Functionalization with amines tends increasing or maintaining adsorption capacity in the temperature range typical of flue gas emissions.

Leal et al. (1995) was one of the first authors to report the functionalization of the silica surface with an aminosilane for the adsorption of carbon dioxide. Following this publication, further work was carried out to investigate the adsorption of carbon dioxide on amine-functionalized materials using different amine molecules and different techniques (**Choi et al., 2009; D'Alessandro et al., 2010; Olajire, 2010**).

The studies reported by **Aroua et al. (2008)** with PEI-impregnated activated carbons showed an increase in the adsorption capacity of CO_2 at 298 K and 1 bar from 0.48 to 2.28 mmol/g. The enhanced adsorption of CO_2 is attributed to increased

concentration of nitrogen functional groups on the surface of the AC, as introduced by impregnation of PEI. Increase in adsorption capacities of all gases in PEI-impregnated samples, as compared to virgin AC may perhaps be attributed to two predominant factors, namely creation of additional meso- and micropores from PEI constriction of larger pores as well as chemisorption due to increased presence of PEI molecules.

Chatti et al. (2009) performed impregnation in X zeolite with distinct amines. The adsorption capacities obtained at 1 bar and 348 K were 0.71 mmol/g for unmodified zeolite, 0.89 and 1.01 mmol/g for zeolite modified with monoethanolamine and isopropanolamine, respectively. The decrease in surface area and pore volume of the amine-modified adsorbent was expected to reduce the adsorption capacity of the adsorbent. However, the increase in uptake, though small, despite the worsening of textural properties, may be due to enhanced chemisorption at 348 K. At lower (room) temperature, physisorption is dominant over chemisorption and available surface area of the adsorbent, thus plays vital role in the adsorption process. However, at higher temperatures, chemisorption on sites introduced by the incorporation of the amine groups in the zeolite seems to be the dominant process. Thus, we observe an increase in the adsorption capacity at higher temperature, due to increase in the chemisorption process.

A recent study on CO_2/CH_4 separation by amino-functionalized MIL-53 (metal-organic framework) by **Couck et al. (2009)** brought about important results. According to the authors, a drastic increase in the adsorbed amount of CO_2 occurs at significantly high pressure (5 bar) attributed to breathing effect (enlarged pores under certain conditions of temperature and pressure). The temperature change shifts the breathing effect towards lower or higher pressures. In contrast to CO_2, CH_4 is essentially not adsorbed at pressures below 2 bar. This differentiates amino-MIL-53(Al) from MIL-53(Al), which adsorbs significant amounts of CH_4 at low pressure. The presence of amino

groups on the aromatic ring of the organic linker in the framework of amino-MIL-53(Al) reduces the number of apolar adsorption sites, leading to reduced CH_4 uptake.

Zukal et al. (2009) studied mesoporous silica SBA-15 and zeolite ITQ-6 loaded with aminosilane. The adsorption isotherms were measured at 293 K and an increase in CO_2 uptake was observed after the impregnation of amine, mainly at low pressures. In this study the formation of ammonium carbamates species was observed at low CO_2 pressures of (chemisorption), whereas at higher pressures, adsorption on the bare surface prevails (physisorption).

Fadhel et al. (2009) evaluated mesoporous SBA-15 impregnated with PAMAM (polyamidoamine) 50 % v/v. The impregnation improved CO_2 adsorption capacity significantly, especially at 348 and 378 K. According to the authors, impregnation seems to break down internal H-bonding and allow for the amine groups within the dendrimer interacting with CO_2. In addition, higher temperatures enhance CO_2 diffusion within the impregnated adsorbents, presumably due to improved mobility of the dendrimers.

Knöfel et al. (2009) functionalized mesoporous silica and titania with APS (aminopropylsilane) by wet impregnation method. Amine-loaded samples, Si-APS and Ti-APS, adsorbed more carbon dioxide than the respective parent support materials at low carbon dioxide coverage. The enhancement in carbon dioxide uptake is attributed to the acid-base interaction between the CO_2 molecules and the amine sites. There was also another important point, the Ti-APS sample adsorbs significantly more carbon dioxide then the Si-APS sample, although a similar quantity of amine sites per surface area were present on both materials. The interaction of carbon dioxide with titania is much stronger then with silica. Therefore, in case of the Ti-APS sample, carbon dioxide will interact not only with the amine sites but also with other surface sites, such as Ti cations or hydroxyl

groups from the support. The **Table 3.2** shows comparison of CO_2 adsorption capacity on some previous studies.

Table 3.2. Adsorption capacity of CO_2 at 1 bar in some adsorbents cited.

Samples	Amine	Temperature (K)	Adsorption Capacity of CO_2 (mmol/g)	Reference
AC	-	298	0.48	**Aroua et al., 2008**
	PEI	298	2.28	
Zeolite Type X	-	348	0.71	**Chatti et al., 2009**
	MEA	348	0.89	
	IPA	348	1.01	
Zeolite Type ITQ-6	-	298	1.09	**Zukal et al., 2009**
	AP	298	1.19	
	MAP	298	0.94	
	PAP	298	0.49	
SBA-15	-	298	0.92	
	AP	298	0.84	
	MAP	298	0.99	
	PAP	298	0.50	
SBA-15 (pore-expanded)	DT	318	3.83	**Olea et al., 2013**
	PEI	318	6.16	
	TEPA	318	7.32	

* PEI = polyethyleneimine; TEPA = tetraethylenepentamine; DT = diethylenetriamine; PAP = phenylaminopropyl; MAP = methylaminopropyl; AP = aminopropyl; IPA = isopropylamine; MEA = Monoethanolamine.

As demonstrated in this section, several studies have been published about the development of adsorbents for CO_2 capture. Porous structures provide the support for impregnation of amine groups. It became evident that the incorporation of amines in state-of-art adsorbents (zeolite, activated carbon and mesoporous silicas) should take place by strong interactions (preferably by covalent reactions) in order to avoid leaching of the incorporated functionalities. Another important factor to evaluate is the type of amine

molecule. The size of the amine molecule (simple or polymeric) may obstruct the pores, preventing CO_2 from diffusing and being adsorbed. With simple amines (MEA, for example), it is *a priori* possible to increase the basicity of the adsorbent surface without compromising the textural characteristics. The microporous supports seem be more indicated for these processes, requiring an adequate relationship between amine size and adsorbent texture to avoid pore blocking.

3.6 Ion-Exchanged Binderless Zeolites

The influence of the structural characteristics of zeolites on CO_2 adsorption may be assigned to several factors. The intrinsic acidity of zeolites is generally derived from specific Al location in some sites, allowing for strong interaction with CO_2. The CO_2 adsorption in zeolites may be associated with the compensating cations and their distribution, size and concentration. All of these factors influence the active sites in a zeolite. (**Bonenfant et al. 2008; Yang et al., 2010; Barthomeuf et al., 2003**).

A significant number of papers dealing with CO_2 adsorption in ion-exchanged zeolites have been published (**Walton et al., 2006; Plant et al., 2006; Yang et al., 2010; Yu et al., 2013**).

Ion exchange may be carried out by dispersing the commercial X or Y in nitrate or chloride salts in aqueous solution, followed by stirring at room temperature. The mass ratio of zeolite microspheres to the metal ion solution was about 1:100. After being washed, the samples are dried and/or calcined in air (**Yu et al., 2013**).

Yu et al. (2013) reported ion-exchange between Na^+, K^+ and Ca^{2+} in synthetic zeolite X. Pure gas adsorption measurements showed that the NaX CaX and KX have high adsorption capacities for CO_2, between 3 and 5 mmol/g at 298 K. They observed that CO_2 capacity increased as Ca < Na < K. Some studies reported ion-exchange with

Li, K, Ba, Fe and NH_4^+ in X zeolite for CO_2 adsorption, however, they have not measured their performance at high temperatures.

3.7 References

Aroua, M.K., Daud, W.M.A.W., Yin, C.Y., Adinata, D. Adsorption capacities of carbon dioxide, oxygen, nitrogen and methane on carbon molecular basket derived from polyethyleneimine impregnation on microporous palm shell activated carbon. Separation and Purification Technology 62 (2008) 609–613.

Arrigo, R., Hävecker, M., Wrabetz, S., Blume, R., Lerch, M., McGregor, J., Parrott, E.P.J., Zeitler, J.A., Gladden, L.F., Knop-Gericke, A., Schlögl, R., Su, D.S. Tuning the Acid/Base Properties of Nanocarbons by Functionalization via Amination. Journal of the American Chemical Society 132 (2010) 9616–9630.

Bacsik, Z., Atluri, R., Garcia-Bennett, A.E. Hedin, N. Temperature-Induced Uptake of CO_2 and Formation of Carbamates in Mesocaged Silica Modified with n-Propylamines. Langmuir 26 (2010) 10013–10024.

Barthomeuf, D. Framework induced basicity in zeolites. Microporous and Mesoporous Materials 66 (2003) 1–14.

Bezerra, D.P., Oliveira, R.S., Vieira, R.S., Cavalcante Jr., C.L., Azevedo, D.C.S. Adsorption of CO_2 on nitrogen-enriched activated carbon and zeolite 13X.Adsorption 17 (2011) 235–246.

Bonenfant, D., Kharoune, M., Niquette, P., Mimeault, M., Hausler, R. Advances in principal factors influencing carbon dioxide adsorption on zeolites. Science and Technology of Advanced Materials 9 (2008) 13007–130014.

Chang, F., Chao, K., Cheng, H., Tan, C. Adsorption of CO_2 onto amine-grafted mesoporous silicas. Separation and Purification Technology 70 (2009) 87–95.

Chatti, R., Bansiwal, A.K., Thote, J.A., Kumar, V., Jadhav, P., Lokhande, S.K., Biniwale, R.B., Labhsetwar, N.K., Rayalu, S.S. Amine loaded zeolites for carbon dioxide capture: Amine loading and adsorption studies. Microporous and Mesoporous Materials 121 (2009) 84–89.

Choi, S., Drese, J.H., Jones, C.W. Adsorbent Materials for Carbon Dioxide Capture from Large Anthropogenic Point Sources. ChemSusChem 2 (2009) 796–854.

Couck, S., Denayer, J. F.M., Baron, G.V., Rémy, T., Gascon, J., Kapteijn, F. An Amine-Functionalized MIL-53 Metal-Organic Framework with Large Separation Power for CO2 and CH4. Journal of the American Chemical Society131 (2009) 6326–6327.

D'Alessandro, D.M., Smit, B., Long, J.R. Carbon Dioxide Capture: Prospects for New Materials. Angewandte Chemie International 49 (2010) 6058–6082.

Fadhel, B., Hearn, M., Chaffee, A. CO_2 adsorption by PAMAM dendrimers: Significant effect of impregnation into SBA-15. Microporous and Mesoporous Materials 123 (2009) 140–149.

Filburn, T., Helble, J. J., Weiss, R.A. Development of Supported Ethanolamines and Modified Ethanolamines for CO_2 Capture. Industrial & Engineering Chemistry Research 44 (2005) 1542–1546.

Franchi, R.S., Harlick, P.J.E., Sayari, A. Applications of Pore-Expanded Mesoporous Silica. 2. Development of a High-Capacity, Water-Tolerant Adsorbent for CO_2. Industrial and Engineering Chemistry Research 44 (2005) 8007–8013.

Guo, Y., Li, Y., Zhu, T., Ye, M., Wang, X. Adsorption of SO_2 and chlorobenzene on activated carbon. Adsorption 19 (2013) 1109–1116.

Khalil, S.H., Aroua, M.K., Daud, W.M.A.W. Study on the improvement of the capacity of amine-impregnated commercial activated carbon beds for CO_2 adsorbing. Chemical Engineering Journal 183 (2012) 15–20.

Knöfel, C., Descarpentries, J., Benzaouia, A., Zelenenák, V., Mornet, S., Llewellyn, P.L., Hornebecq, V. Functionalised micro-/mesoporous silica for the adsorption of carbon dioxide. Microporous and Mesoporous Materials 99 (2007) 79–85.

Knöfel, C., Martin, C., Hornebecq, V., Llewellyn, P.L. Study of Carbon Dioxide Adsorption on Mesoporous Aminopropylsilane-Functionalized Silica and Titania Combining Microcalorimetry and in Situ Infrared Spectroscopy. Journal of Physical Chemistry 113 (2009) 21726–21734.

Leal, O., Bolivar, C., Ovalles, C., Garcia, J.J., Espidel, Y. Reversible adsorption of carbon dioxide on amine surface-bonded silica gel. Inorganica Chimica Acta 240 (1995) 183–189.

Lin, C., Zhang, H., Lin, X. and Feng, Y. Adsorption CO_2 on activated carbon with surface modification. Advanced Materials Research 634 (2013) 746–750.

Olajire, A.A. CO_2 capture and separation technologies for end-of-pipe applications – A review. Energy 35 (2010) 2610–2628.

Olea, A., Sanz-Perez, E.S., Arencibia, A., Sanz, R., Calleja, G. Amino-functionalized pore-expanded SBA-15 for CO_2 adsorption. Adsorption 19 (2013) 589–600.

Plant, D.F., Maurin, G., Deroche, I., Gaberova, L., Llewellyn, L.P. CO_2 adsorption in alkali cation exchanged Y faujasites: A quantum chemical study compared to experiments. Chemical Physics Letters 426 (2006) 387–392.

Plaza, M. G., Pevida, C., Arias, B., Casal, M.D., Martín, C.F., Fermoso, J., Rubiera, F., Pis, J.J. Different Approaches for the Development of Low-Cost CO_2 Adsorbents. Journal of Environmental Engineering 135 (2009) 426–432.

Plaza, M.G., Pevida, C., Martín, C.F., Fermoso, J., Pis, J.J., Rubiera, F. Developing almond shell-derived activated carbons as CO_2 adsorbents. Separation and Purification Technology 71 (2010) 102–106.

Rouquerol, F., Rouquerol, J., Sing, K. Adsorption by Powders & Porous Solids, Academic Press, San Diego (1999).

Son, W., Choi, J., Ahn W. Adsorptive removal of carbon dioxide using polyethyleneimine-loaded mesoporous silica materials. Microporous and Mesoporous Materials 113 (2008) 31–40.

Walton, K.S., Abney, M.B., LeVan, M. D. CO_2 adsorption in Y and X zeolites modified by alkali metal cation exchange. Microporous and Mesoporous Materials 91 (2006) 78–84.

Wei, J., Shi, J., Pan, H., Zhao, W., Ye, Q., Shi, Y. Adsorption of carbon dioxide on organically functionalized SBA-16. Microporous and Mesoporous Materials 116 (2008) 394–399.

Xu, X., Song, C., Andrésen, J.M., Miller, B.G., Scaroni A.W. Preparation and characterization of novel CO_2 ‘‘molecular basket’’ adsorbents based on polymer-modified mesoporous molecular sieve MCM-41. Microporous and Mesoporous Materials 62 (2003) 29–45.

Xu, X., Zhao, X., Sun, L., Liu, X. Adsorption separation of carbon dioxide, methane and nitrogen on monoethanol amine modified β-zeolite. Journal of Natural Gas Chemistry 18 (2009) 167–172.

Yang, S., Kim, J., Ahn, W. CO_2 adsorption over ion-exchanged zeolite beta with alkali and alkaline earth metal ions. Microporous and Mesoporous Materials135 (2010) 90–94.

Yaumi, A.L., Hussien, I.A. andShawabkeh, R.A. Surface modification of oil fly ash and its application in selective capturing of carbon dioxide. Applied Surface Science 266 (2013) 118–125.

Yu, J., Le, Y., Chang, B. Fabrication and CO_2 adsorption performance of bimodal porous silica hollow spheres with amine-modified surfaces. RSC Advances 2 (2012) 6784–6791.

Yu, L., Gong, J., Zeng, C., Zhang, L. Synthesis of binderless zeolite X microspheres and their CO_2 adsorption properties. Separation and Purification Technology 118 (2013) 188–195.

Zhang, Z., Xu, M., Wang, H., Li, Z. Enhancement of CO_2 adsorption on high surface area activated carbon modified by N_2, H_2 and ammonia. Chemical Engineering Journal 160 (2010) 571–577.

Zukal, A., Dominguez, I., Mayerová, J., Cejka, J. Functionalization of Delaminated Zeolite ITQ-6 for the Adsorption of Carbon Dioxide. Langmuir 25 (2009) 10314–10321.

CHAPTER 4 – AMINE-GRAFTED X ZEOLITE

CO_2 ADSORPTION IN AMINE-GRAFTED X ZEOLITE

Abstract

The adsorption of CO_2 on X Zeolite functionalized with amino groups was studied. Adsorbent functionalization was carried out by grafting with monoethanolamine (MEA) in different concentrations. The adsorbents were characterized by N_2 adsorption/desorption isotherms at 77 K, X-ray diffraction, TGA, in situ FTIR, XPS and adsorption microcalorimetry. CO_2 isotherms were studied in a gravimetric device up to 10 bar at 298 and 348 K. It was found that increasing loads of amine to the adsorbent tend to reduce micropore volume of the resulting adsorbents by pore blocking with MEA. There is experimental evidence of that the loaded MEA is effectively covalently bonded to the zeolitic structure, whereas there is also physisorbed excess MEA which will eventually be desorbed by raising the temperature beyond MEA boiling point. Heats of adsorption at nearly zero coverage indicate that some of the adsorbed CO_2 reacts with available amino groups, which agrees with the finding that the adsorption capacity increases with increasing temperature for the modified zeolite with the highest MEA load.
Keywords: CO_2 adsorption; Zeolite; Amine.

4.1 Introduction

A wide variety of adsorbents has been investigated lately for CO_2 capture, which includes activated carbons, zeolites, mesoporous silicas, metal oxides, mixed hydroxides and metal-organic frameworks (**Choi et al., 2009; Shao et al., 2009; D'Alessandro et al., 2010; Bezerra et al., 2011**).

X zeolites are crystalline microporous oxides with pore size in the range of 11 to 14 Å. Although their chemical composition is limited to aluminosilicate tetrahedra, cations (usually Na) should be introduced to compensate the negative charge of oxygen linked to Al atoms in the framework. This chemical versatility allows for the modification of some physicochemical zeolite properties (such as acidity, redox properties, or hydrophobic−hydrophilic nature) and, consequently, tune them for a specific application (**Moliner, 2012**).

Adsorbents functionalized with basic groups, such as amines, are claimed to be potentially effective materials for the capture of CO_2 from flue gas mainly due to the relatively smaller decrease in adsorption capacity with rises in temperatures as compared to conventional physisorbents (**Choi et al., 2009; Bezerra et al., 2011; Aroua et al., 2008; Sumida et al., 2007**). The optimal functionalization or modification of inorganic materials has received considerable attention in the last few years (**Su et al., 2010; Chatti et al., 2009; Zukal et al., 2009; Nik et al., 2012; Jadhav et al., 2007; Lee et al., 2013**).

Modifying silicate and aluminosilicate surfaces with amino groups has been shown by some authors to lead to sorbents with increased capacity as compared to the pristine materials. **Chatti et al.** (**2009**) have measured CO_2 uptakes of 0.36 mmol/g for unmodified X zeolite and 0.45, and 0.52 mg/g for zeolite modified with monoethanolamine, and isopropanol amine at 1 bar and 25 °C. CO_2 adsorption capacity of amine-grafted mesoporous silicas has been investigated by **Vilarrasa-García et al.** (**2014**). At 1 bar and 25 °C, CO_2 uptakes of 2.4 mmol g^{-1} or 0.64 mol CO_2 per mol N were achieved. However, such CO_2 uptakes are still below those reached by commercial zeolite samples under the same conditions of pressure and temperature. **Bacsik et al.** (2010) also studied CO_2 adsorption on amine-grafted mesoporous silica (AMS-6 and MCM-48) at two temperatures (273 and 294 K). The authors observed that CO_2

adsorption capacity increases with temperature, which is distinct from what would be expected in physisorption alone. Such behavior has been attributed to the occurrence of chemisorption. As reported in a previous paper (**Bezerra et al., 2011**), the impregnation with dilute amine solutions and drying in inert atmosphere led to the same behavior. This study evaluated the adsorption capacity at two temperatures (298 and 348 K) and it was observed that, for a given impregnated sample with monoethanolamine, CO_2 uptake increases with a rise in temperature.

On a recent comprehensive review about the subject, **Ebner and Ritter** (**2009**) suggest that a near-term goal to be pursued concerning adsorbents for CO_2 capture should be to develop materials which can operate at elevated temperatures in the presence of sulfur bearing compounds and possibly steam, with working capacities in the range of 3-4 mmol of CO_2/g adsorbent, that is, 132-176 mg/g within the pressure range at which emissions occur.

Considerable experimental effort has been devoted in the last few years in the preparation of amine-functionalized adsorbents, however few studies discuss how each impregnation route affects CO_2 capacity, how amine species are attached to the adsorbent surface and their long-term stability upon pressure and temperature swings. Proposing to perform this study, commercial X zeolite was functionalized by immersing it in monoethanolamine (MEA) methanolic solutions under different amine concentrations (0 to 10 % v/v) and CO_2 adsorption isotherms were measured for the thus-prepared solids. The pristine adsorbent and modified materials were analyzed by N_2 adsorption/desorption isotherms at 77 K, thermo-gravimetric analysis (TGA), X-ray photoelectron spectroscopy (XPS) and CO_2 adsorption microcalorimetry, in order to characterize the textural, structural and surface modifications induced on the adsorbents by the impregnation

process. The adsorbents were tested for CO_2 adsorption at two temperatures (298 and 348 K) under the pressure range of 10^{-2} to 10 bar using a gravimetric setup.

4.2 Experimental

4.2.1 Adsorbents

Zeolite KÖSTROLITH 13X was supplied by CWK – Chemiewerk Bad Köstrite (Germany) in the form of spherical pellets of approximately 2 mm diameter.

4.2.2 *Wet Amine Impregnation*

MEA (VETEC, 99.9 %, Brazil) impregnation on zeolite type X was carried out following an experimental procedure reported by **Chatti et al.** (**2009**) and **Bezerra et al.** (**2011**) with different amine concentrations. About 2.0 g adsorbent, previously regenerated at 623 K, were soaked in 50 mL MEA solution in different concentrations (from 0.2 to 10 % (v/v), based on previous study) in methanol (VETEC, 99.9 %, Brazil) (**Bezerra et al., 2011**). The zeolites remained in contact with the MEA solution under slight agitation for 72 h and at 298 K. The solids were separated from the amine solution by filtration. One of the samples (blank) was prepared only with methanol, following the same procedure except for the absence of MEA. The modified sorbents were dried at 423 K under inert atmosphere (nitrogen flow). Table 1 shows the different MEA concentrations used for amine impregnation and the code to identify each of the samples.

Table 4.1. Summary of amine impregnation conditions on zeolite type X.

Support	Monoethanolamine/Methanol (concentration in % vol.)	Code
X Zeolite	No impregnation	ZX
	0 % (methanol only)	ZX0
	0.2 %	ZX0.2
	0.5 %	ZX0.5
	0.8 %	ZX0.8
	1.0 %	ZX1.0
	1.5 %	ZX1.5
	10.0 %	ZX10

4.2.3 Characterization of the Amine-functionalized Adsorbents

Nitrogen adsorption/desorption isotherms were measured using an Autosorb-1 MP apparatus (Quantachrome, U.S.A.) for the determination of textural properties such as surface area (S_{BET}), total pore volume (V_{TOTAL}) and micropore volume (V_{MICRO}). The impregnated adsorbents were initially outgassed at 423 K, to avoid amine volatilization (boiling point 443 K), and then subjected to stepwise N_2 relative pressure increases and decreases at 77 K. The specific surface area was calculated using the BET equation and micropore volume was determined by using the Dubunin–Radushkevich equation (**Rouquerol et al., 1999**) appropriate for this adsorbent.

The identification of the crystalline phases of the zeolite samples was performed by X-ray diffractometry in a Rigaku (DMAXB) X-ray Powder Diffractometer by using a Bragg–Brentano geometry. X-ray photoelectron spectroscopy (XPS) was carried out to

determine the atomic concentrations (%) of the elements on the surface of the pristine and amine-impregnated samples, especially the atomic concentration % of nitrogen induced by the chemical modification. Spectra were obtained at ultra high vacuum (10^{-12} bar) using a Physical Electronics spectrometer (model 5700). Thermogravimetric analyses (TGA) were carried out using as Shimadzu TGA 50 equipment, with a heating rate of 10 K/min, in a dynamic N_2 atmosphere with approximately 5.0 mg sample. The temperature range of 340–1000 K was used for TGA analyses. FTIR spectra were obtained using a Bruker IFS88 spectrometer and specially designed cells which were permanently connected to a gas or vacuum line. Spectra were obtained at two temperatures (298 and 348 K) and two pressures (vacuum and 1 bar pure CO_2).

CO_2 adsorption microcalorimetric experiments were carried out using an isothermal Tian–Calvet type microcalorimeter (model CA-100 from ITI Company, Del Mar, CA) combined with a homemade volumetric device. Thus, simultaneous measurement of isotherms and calorimetric curves for the adsorption of CO_2 were performed at 298 K up to 101 kPa. In order to evaluate the adsorption differential enthalpy from calorimetric data, the so-called discontinuous procedure was employed, which consists of injecting discrete quantities of gas in successive steps to the adsorbent. The adsorbed amount was calculated from mass balance of the gas phase by using pressure, volume and temperature measured data. Further details on the experimental procedure can be found in **Rouquerol et al.** (**1999**) and **Silva et al.** (**2012**).

4.2.4 CO_2 Adsorption Isotherms

Adsorption equilibrium isotherms for pure CO_2 were measured using a magnetic suspension balance by Rubotherm (Bochum, Germany). The adsorbents were degassed in situ at 423 K, lower temperature of the boiling point of MEA (except for pristine

zeolite 13X, which was regenerated at 623 K) until no mass variation in the system was observed. After that, the measuring chamber was cooled down to the experiment temperature (298 or 348 K) and the gas pressure (CO_2) was increased stepwise (UHV until approximately 10 bar).

4.3 Results and Discussion

4.3.1 Adsorbent Characterizations

4.3.1.1 Nitrogen Adsorption/Desorption Isotherms

The textural properties of the pristine and amino-impregnated zeolites are shown in **Table 4.2**. A progressive reduction of the specific surface area and pore volume were observed as the amine concentration increases, which indicates that MEA tends to fill and obstruct micropores, preventing nitrogen from being adsorbed. Only the textural characteristics for the pristine zeolite and that loaded with the lowest amine solution concentration were nearly the same. Note that, when MEA is absent (sample ZX0), rinsing with methanol (only) tends to increase surface area and micropore volume possibly due to solubilization of impurities (e.g. pellet binder). Therefore, the slightly higher nitrogen uptake observed for ZX0.2 (see **Figure 4.1**) suggests that the added MEA was little enough so that the solvent effect (methanol) in opening up porosity was nearly compensated by the obstruction effect of MEA.

Table 4.2. Textural characteristics of the investigated adsorbents.

Adsorbent	S_{BET} (m^2/g)	V_{TOTAL} (cm^3/g)	V_{MICRO} (cm^3/g)
ZX	515	0.454	0.298
ZX0	608	0.400	0.343
ZX0.2	491	0.456	0.277
ZX0.5	462	0.378	0.237
ZX0.8	436	0.312	0.227
ZX1.0	429	0.198	0.190
ZX1.5	419	0.236	0.168
ZX10	121	0.148	0.054

The nitrogen adsorption isotherms at 77 K for pristine and amine-impregnated X zeolite are shown in **Figure 4.1**. All isotherms may be classified as Type I, in accordance with the IUPAC classification, with predominant microporous characteristics as evidenced by the high volume of nitrogen adsorbed within very low relative pressures. A second sharp increase in relative pressures close to 1.0 present in some isotherms is probably due to the presence of macropores as a result of pellet conformation and addition of binding agent.

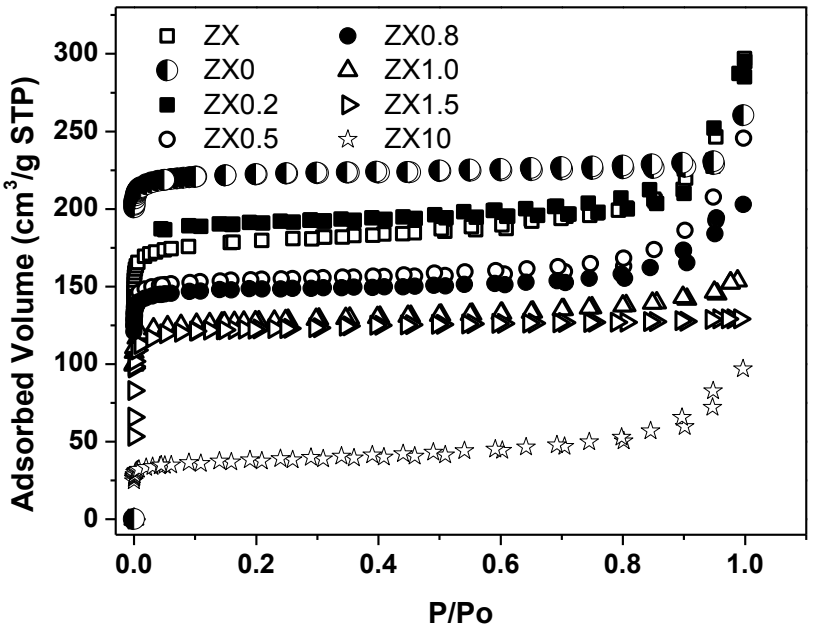

Figure 4.1. Nitrogen adsorption isotherms at 77 K of the studied samples.

For the other amine-impregnated zeolites loaded with different amine concentrations, nitrogen adsorption isotherms showed a progressive reduction in uptake as the concentration of the impregnating solution increases. The isotherm shapes indicate that ZX1.0 and ZX1.5 practically have no macropores, possibly because they were completely filled with amine. The samples impregnated with increasing amine concentration (up to 1.5% MEA) also showed a progressive decrease in the final uptake rise, which leads to the hypothesis that MEA fills not only micropores, but also larger pores to a certain extent.

4.3.1.2 X-Ray Diffraction Analysis

X-ray diffraction technique was used to determine the crystallinity of impregnated and fresh samples. The XRD patterns of parent (ZX) and MEA-modified zeolite (ZX10)

are shown in **Figure 4.2**. The reflection lines are well resolved and it can be seen that the location of the reflection lines remains constant, indicating that the structure of zeolite 13X was well preserved even with the highest load of MEA. Sample ZX10 was chosen because it was the most intensely affected sample in terms of its textural characteristics. Nevertheless, the crystalline zeolitic structure remained nearly intact, which suggests that the impregnation procedure did not affect the crystallinity of any of the other impregnated samples.

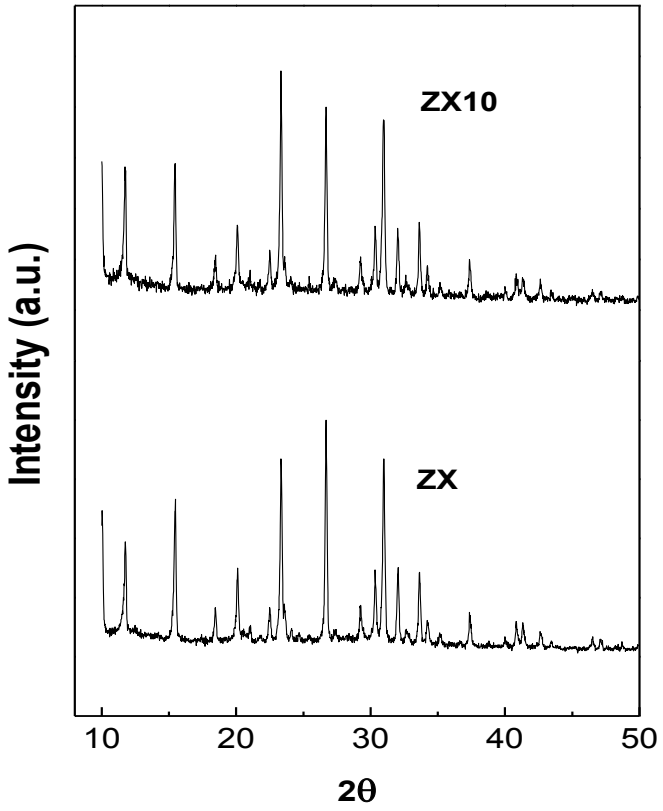

Figure 4.2. XRD patterns of the zeolite before and after modifiers loading MEA.

4.3.1.3 TGA Analysis

Mass loss profiles, as determined by TGA, are shown in **Figure 4.3** for ZX and ZX10. For both samples, there is the same continuous and smooth mass loss up to 443 K. Beyond this temperature, a higher variation in the mass loss profile was observed for the

amino-loaded zeolite, evidencing the presence of retained MEA (boiling temperature of 443 K). The adsorption sites in the pristine sample, usually occupied by water molecules, were mainly loaded with MEA in ZX10. This changes the hydrophilic character of the zeolite. In the inset of **Figure 4.3**, it is possible to observe the first peak at lower temperature (attributed to desorption of moisture) in ZX10 sample. The second peak, at 520 K, is ascribed to the volatilization of the entrapped organic material, MEA, ranging your weight loss between 90 and 85 % (**Bezerra et al., 2011**). This peak is absent for the pristine ZX.

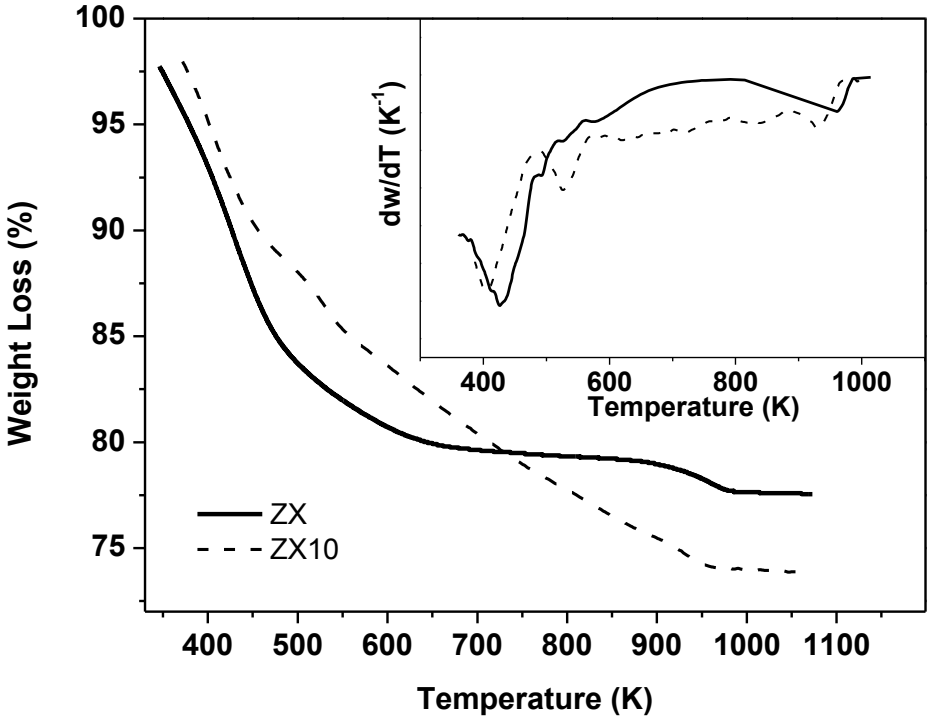

Figure 4.3. TGA and DTA curves for the parent and MEA-impregnated X zeolite in low and high concentration.

4.3.1.4 XPS Analysis

The surface atomic concentrations of elements nitrogen and carbon, as obtained by XPS measurements, are summarized in **Table 4.3** for the pristine and amino-loaded

samples ZX and ZX10. The atomic concentration percentages of C and N were 4.43 % and 0.89 %, respectively for sample ZX, and 18.99 % and 4.34 %, respectively for sample ZX10, respectively. These results are in accordance with TGA results shown previously. The observed increase in the carbon and nitrogen contents upon modification of the zeolite is due to the incorporation of the monoethanolamine. The presence of a small amount of N on the surface of the pristine zeolite is due to impurities containing nitrogen. These results suggests the successful incorporation of MEA ($CH_2(NH_2)CH_2OH$) in the solid. However, the observed percentage of carbon in sample ZX10 is higher than expected if the percentage of nitrogen is considered, being possible the MEA decomposition or methanol (used as solvent). This can be explained if the adsorption of atmospheric CO_2 is considered.

Table 4.3. Atomic concentration % for the studied samples.

Sample	**N**	**C**	**Binding energies (eV)**	
	a.c. %	a.c. %	C 1*s*	N 1*s*
ZX	0.83-	4.43	284.8 (adventitious C-C)	401.0
ZX10	4.34	18.99	284.8 (adventitious C-C)	399.8 (R-NH_2(N-alkylamine))
			286.1 (C-N) and (C-O)	401.4 (RNH_2-CO_2(carbamate),
			287.8 (O-C=O)	RNH_3^+(N-alkylammoniun))

Table 4.3 shows the binding energy values for C 1*s* and N 1*s* for ZX10 sample. For the pristine sample, which is essentially an aluminosilicate, only an almost symmetric C 1*s* peak was observed corresponding to adventitious carbon. In modified zeolites, the C 1*s* signal can be decomposed in three contributions (spectrum not shown) and the

corresponding binding energies (BE) allowed us to identify the presence of aliphatic carbons (284.8 eV), bonds C–N and C–O (286.1 eV) and O=C–O (about 288 eV).

XPS analysis was also performed for sample ZX10 after contact with CO_2 in high pressure gravimetric experiments. The corresponding atomic concentrations % are summarized in **Table 4.4** and spectra decomposition are shown in **Figure 4.4** for the N 1*s* and C 1*s* signals in the case of the impregnated sample after CO_2 adsorption at high pressure.

Upon MEA modification (sample ZX10), the N 1*s* signal was examined in a higher resolution XPS spectrum (**Figure 4.4a**). The asymmetrical and broad features of N 1*s* signal suggest the coexistence of distinguishable nitrogen bonds. The peak decomposition shown in **Figure 4.4** indicates the presence of several N-containing species in the impregnated sample, with their binding energies at 399.8 and 401.4 eV. The former corresponds to primary alkylamines ($R–NH_2$), and the latter to "zwitterions" carbamate ($R–NH–CO_2^-$) and n-alkylammonium ($R–NH_3^+$), respectively (**Yu et al., 2012**). From these, it can be inferred that part of the loaded amine, covalently attached to the zeolite through the sylanol, reacts with atmospheric CO_2 forming a carbamate and an alkylammonium, as previously reported (**Choi et al., 2009**).

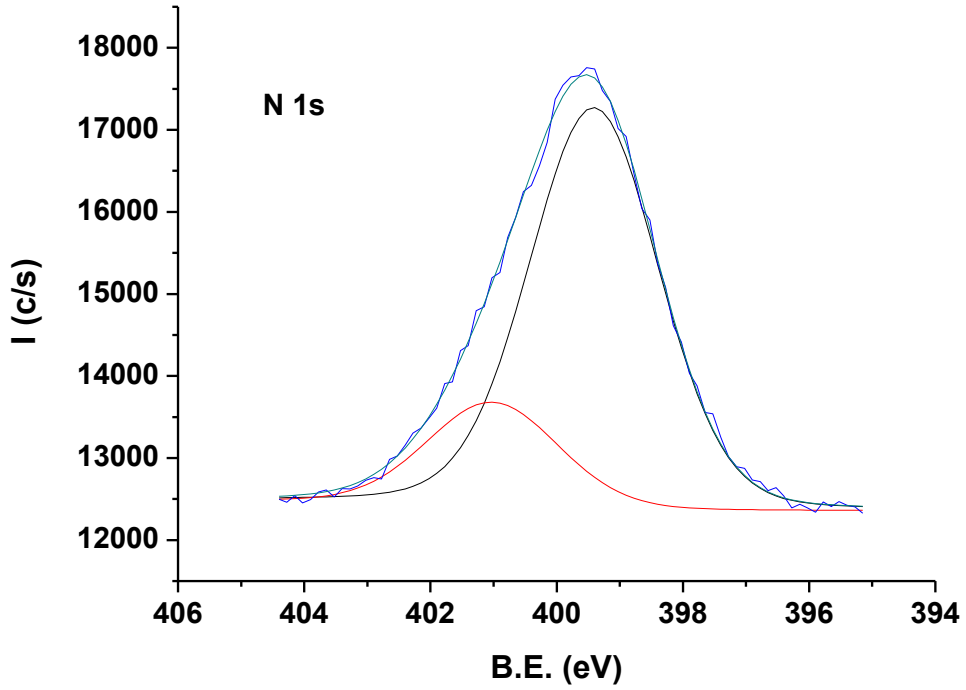

(a)

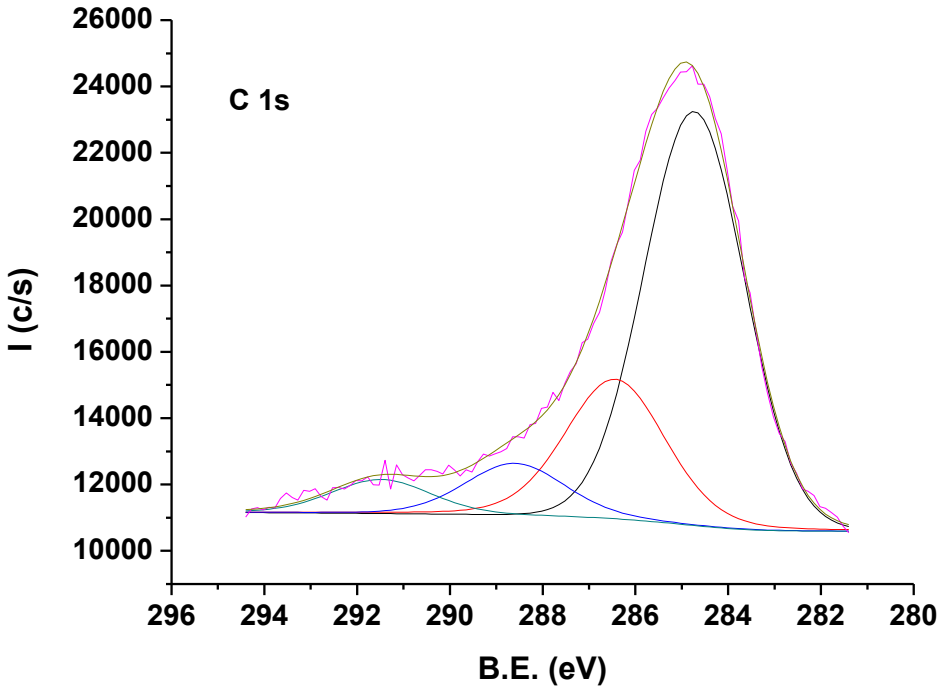

(b)

Figure 4.4. XPS spectrum of N 1*s* (a) and C 1*s* (b) for ZX10 after CO_2 capture.

The atomic concentration percentages of nitrogen for the sample ZX10 before and after CO_2 adsorption at 10 bar (4.34% and 4.30%, respectively) are essentially the same and this fact suggests that nitrogen is firmly anchored to the adsorbent surface (**Table 4.4**). In addition, there is an increase in the amount of fixed carbon after CO_2 adsorption at high pressure (from 18.99% to 24.00%), which is likely to be due to the interaction between the amine and CO_2. The analysis of the C 1*s* spectra is very complex. In the case of sample ZX10, the main contribution at 286.1 eV is derived from the presence of monoethanolamine (C–N and C–O bonds), and the contribution at 287.8 eV to the interaction of atmospheric CO_2 with the amine group. Upon CO_2 capture at high pressure, the C 1*s* signal is modified. More adventitious carbon is present and a new contribution at high binding energy (289.1 eV) is observed and assigned to the presence of surface carbonate.

Table 4.4. Binding energy values (in eV) of C 1*s*, O 1*s* and N 1*s* (in eV) for ZX10 and ZX10 after CO_2 capture at high pressure.

Element	ZX10			ZX10 after CO_2 capture		
	a.c. (%)		BE (eV)	a.c. (%)		BE (eV)
	Total	Deconvolution		Total	Deconvolution	
C1*s*	18.99%	37 %	284.8	24.00%	63 %	284.8
		52 %	286.1		23 %	286.4
		11 %	287.8		8 %	288.5
		-	-		6 %	291.4
O1*s*	48.50%	100%	531.7	45.79%	100%	531.2
N1*s*	4.34%	72 %	399.8	4.30%	80 %	399.4
		28 %	401.4		20 %	401.0

4.3.1.5 FTIR Analysis

In **Figure 4.5**, in situ FTIR spectra are shown for the pristine zeolite 13X and amine-grafted sample ZX10. The pristine sample presented peaks in the range of 3750 to

3500 cm^{-1} attributed to hydroxyl groups belonging to the surface of the adsorbent or physisorbed water. The spectrum also suggests the formation of hydrogen bonds, judging from the peaks observed in the range of 3250 to 3400 cm^{-1}. Note that at high temperature (pristine sample), the hydrogen bonds are not found. A large peak near 2330 cm^{-1} is related to physisorbed CO_2 in both samples (**Aziz et al., 2012; Stevens Jr. et al., 2008**), which is present in both temperatures with different intensities.

The peaks found in the region from 1200 to 1700 cm^{-1} (**Figure 4.5b**) are relevant because they provide important evidence of amine impregnation and formation of carbamate species (characteristic of chemical adsorption). By comparing the spectra of the pristine and grafted samples under vacuum, the presence of an additional peak is observed for ZX10 at 1615 cm^{-1}, relative to the incorporation of amine groups (protonated form) on the adsorbent surface (**Montanari et al., 2010; Montanari et al., 2011**).

The pristine sample in the presence of CO_2 presented peaks in the region from 1681 to 1650 cm^{-1}, which may be assigned to adsorbed CO_2 coordinated to the compensation cation (Na^+) in bidentate form, and around 1361 cm^{-1} in monodentate form (**Du et al., 2010**). In the case of ZX10, other observed bands account for unimpeded carbonate ion in the range of 1420 to 1450 cm^{-1} (**Stevens Jr. et al., 2008**).

Table 4.5. Peaks observed in FTIR spectra for zeolite (ZX) sample and the amine-grafted sample ZX10.

Peaks (cm^{-1})	Attribution
3750 to 3500	hydroxyl groups belonging to the surface of the adsorbent or physisorbed water
2330	physisorbed CO_2
1200 to 1700	formation of carbamate species
1615	amine groups (protonated form)
1681 to 1650	adsorbed CO_2 bidentate form
1361	adsorbed CO_2 monodentate form
1420 to 1450	unimpeded carbonate ion

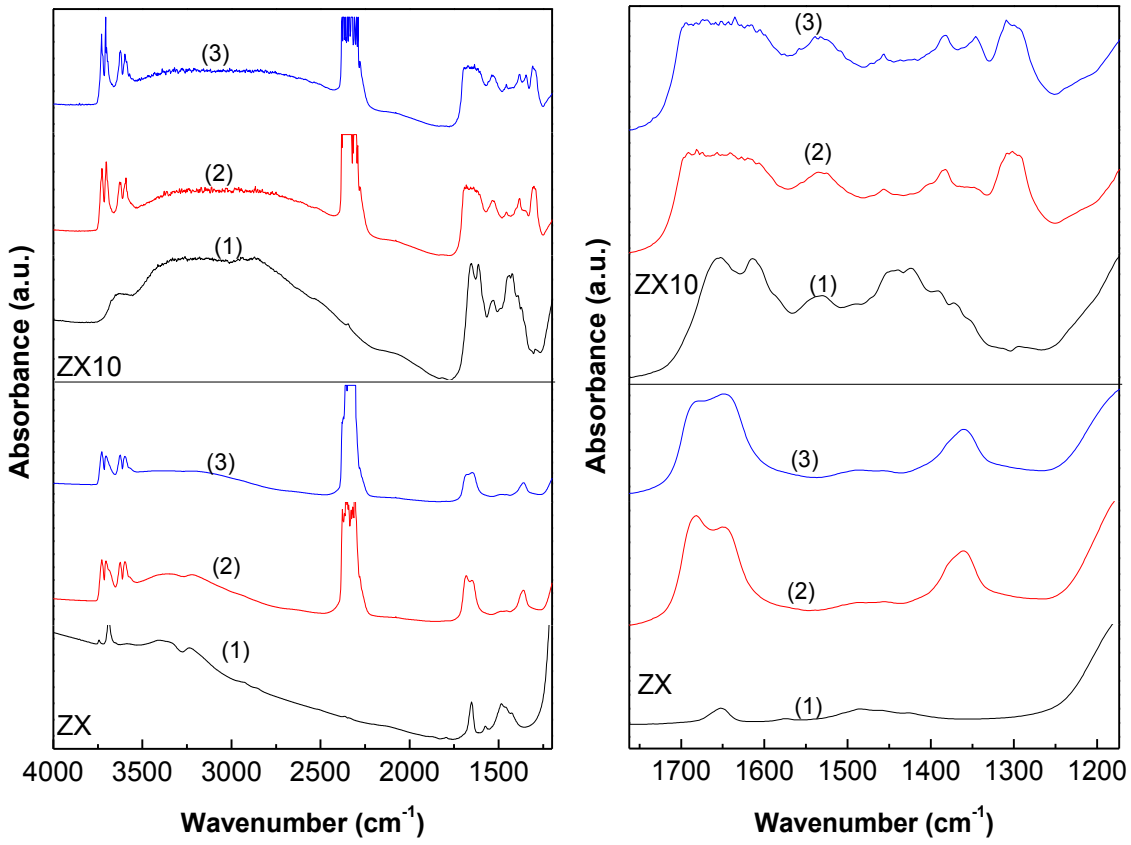

(a) (b)

Figure 4.5. In situ FTIR spectra for zeolite (ZX) sample and the amine-grafted sample ZX10 for different spectral regions (a) and (b): under vacuum at 298 K (1), with CO_2 at 298 K (2) with CO_2 at 348 K (3).

4.3.2 Adsorption Isotherms

Taking into account the results obtained from the characterization of the pristine and grafted adsorbents, the samples ZX, ZX0.2 and ZX10 were chosen to be assessed for CO_2 adsorption (**Figure 4.6**). As expected, the isotherms of conventional ZX supports show a sharp increase in CO_2 uptake at low partial pressures reaching a constant plateau at higher pressures (typical of strongly favorable isotherms).

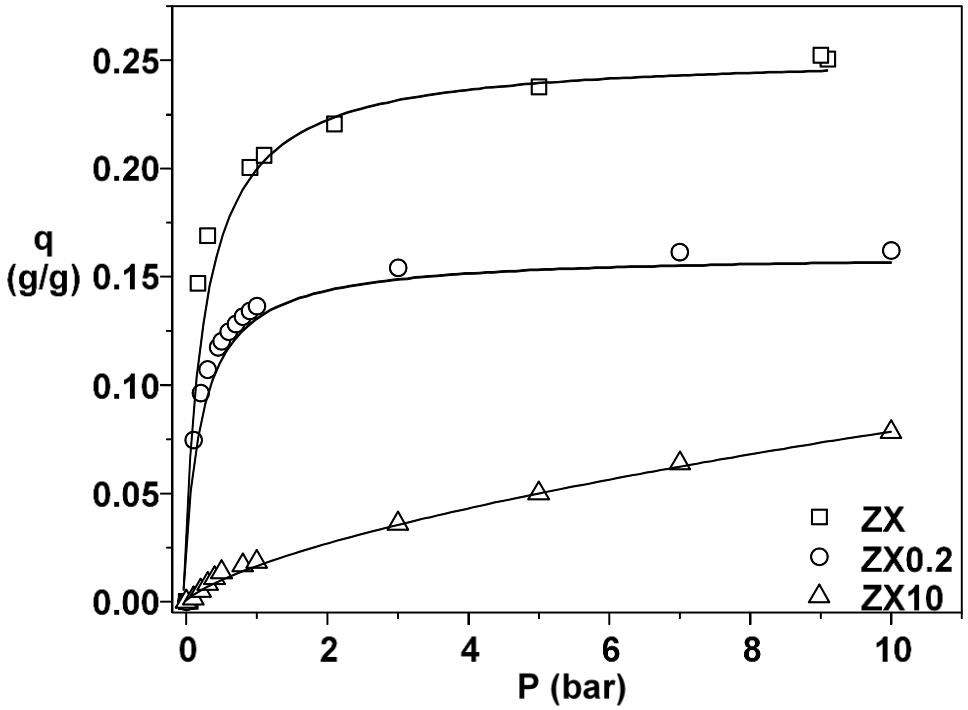

(a)

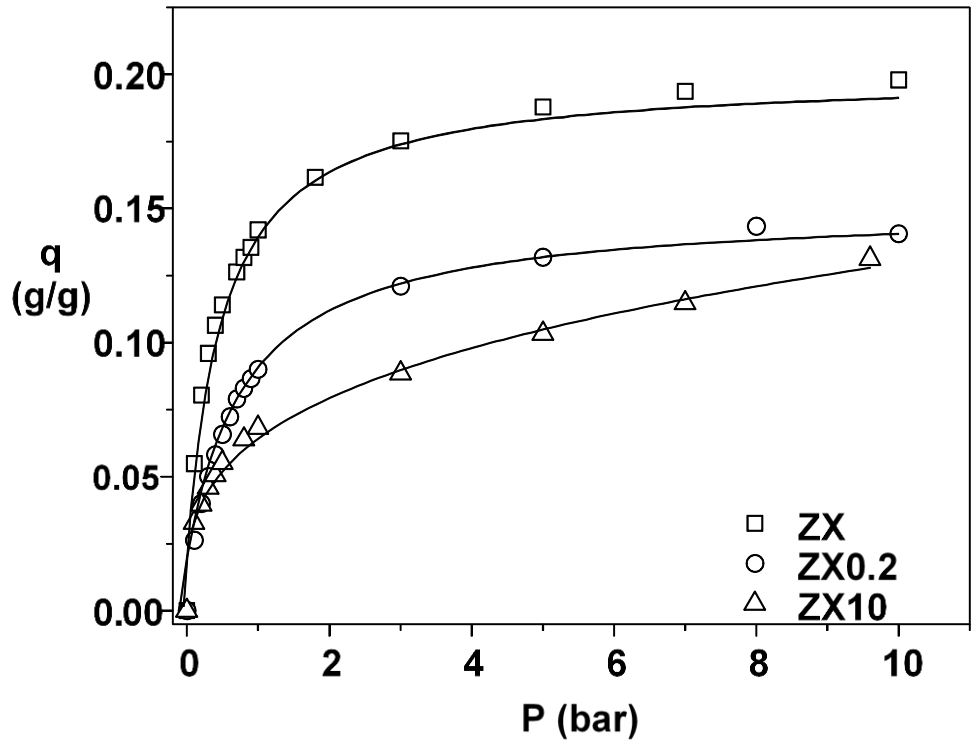

(b)

Figure 4.6. Adsorption isotherms of CO_2 in ZX, ZX0.2 and ZX10 at 298 (a) and 348 K (b).

Functionalized adsorbents show different trends regarding their CO_2 adsorption isotherms as compared to the pristine zeolite 13X, some of which had already been previously observed (**Bezerra et al., 2011**). ZX0.2 and ZX10 presented a lower CO_2 uptake in the whole pressure range under study as compared to ZX. The reduction in textural characteristics can justify the lower CO_2 uptake. However, ZX10 presented two distinct behaviors: CO_2 uptake increases at higher temperatures (348 K) and, at high pressures, CO_2 adsorbed concentration keeps rising steadily. These features are consistent with the hypothesis of CO_2 chemisorption, as suggested in XPS and FTIR results previously shown.

4.3.2.1 Effect of Regeneration Temperature

Because impregnated moieties are usually weakly attached to the adsorbent, it is important to examine the effect of the regeneration temperature of the amino-loaded sample on the CO_2 uptake. This aspect was addressed by measuring two isotherms for the same amine-loaded sample after being regenerated at two different temperatures. In **Figure 4.7**, the CO_2 adsorption isotherms obtained for the amino-loaded zeolite ZX0.2 at 348 K are shown after the sample was regenerated at 423 and 473 K. For the sake of comparison, the isotherm of the pristine zeolite ZX was also included.

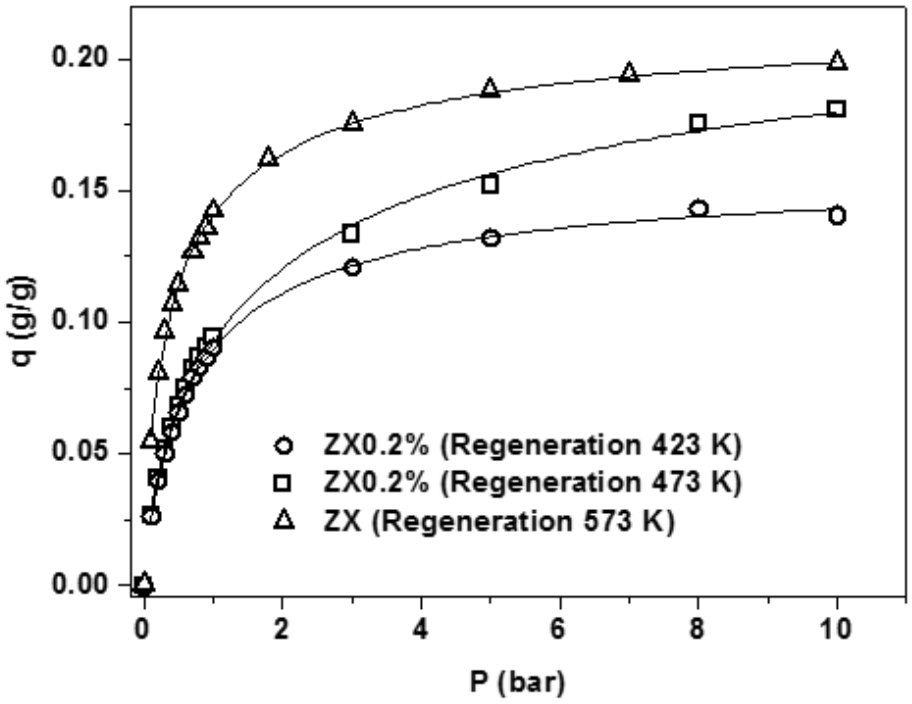

Figure 4.7. Adsorption isotherms of CO_2 at 348 K for ZX0.2 with regeneration of 423 and 473 K and ZX with regeneration of 573 K.

It may be observed that the CO_2 uptake increases when a higher temperature of regeneration is applied and approaches that of the pure zeolite ZX. These results suggest that part of the loaded amine was removed upon heating at 473 K, a temperature higher than MEA boiling point (443 K) even though TGA analysis indicates that most of the amine volatilizes only beyond 500 K (**Figure 4.3**). Nevertheless, in industrial separation units (e.g., PSA), cycles are performed under nearly isothermal conditions (at least not higher than 373 K) and regeneration is performed under pressure swings. Adsorption uptakes should ideally be constant after pressure swings.

4.3.2.2 Adsorption Reversibility

CO_2 adsorption and desorption isotherms were measured for the amino-loaded zeolite (ZX10) at two temperatures, 298 and 348 K, which are shown in **Figure 4.8a** and **4.8b**, respectively.

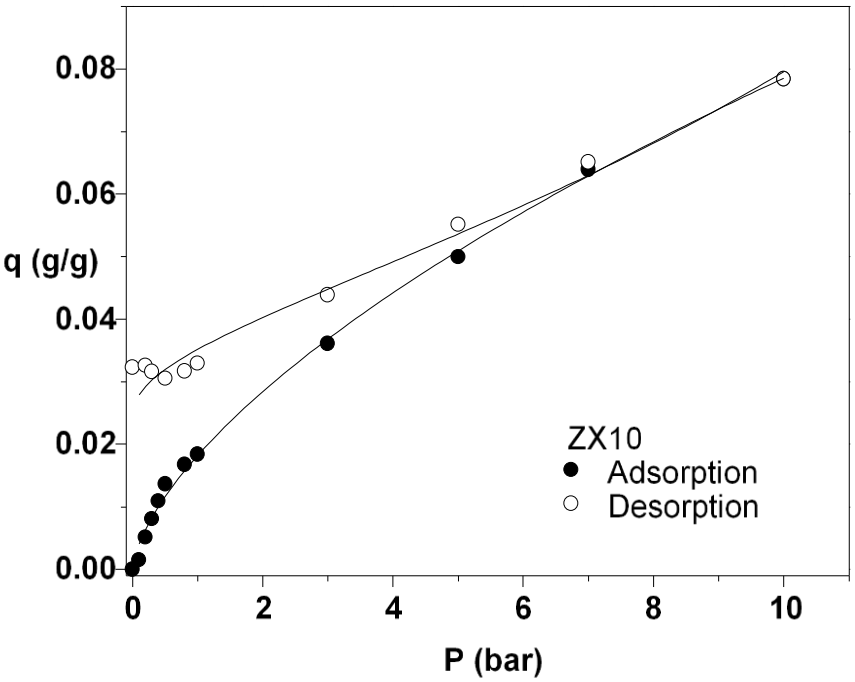

(a)

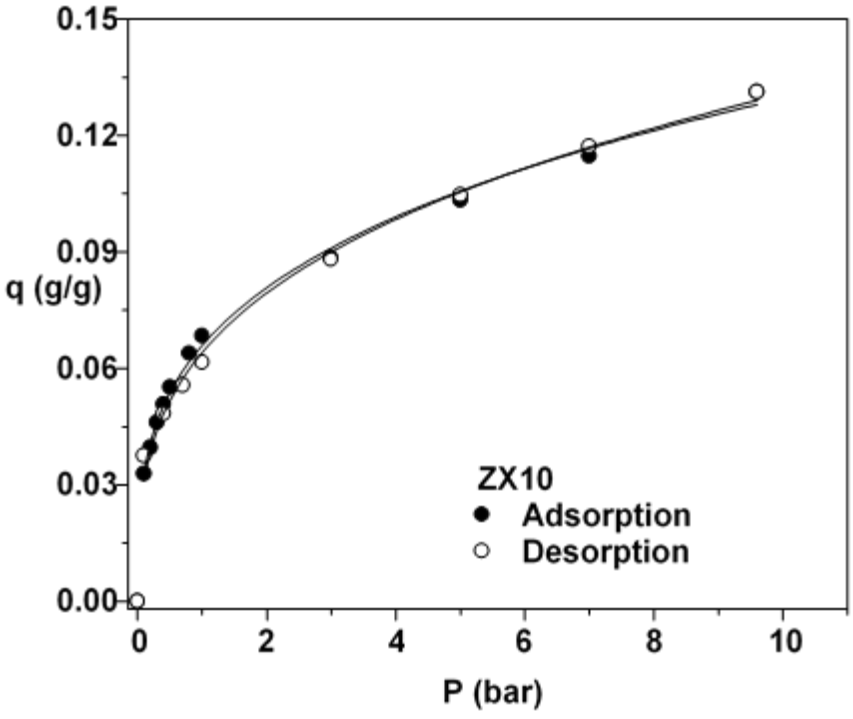

(b)

Figure 4.8. Adsorption and desorption isotherms of CO_2 at 298 (a) and 348 K (b) for ZX10.

The adsorption and desorption CO_2 isotherms at 298 K do not follow the same path and such behavior cannot be attributed to physisorption equilibrium hysteresis under the studied P and T conditions. Such behavior may be due to an irreversible reaction between CO_2 and amine sites present in the adsorbent. On the other hand, the apparent irreversibility observed in **Figure 8a** may also be attributed to diffusion limitations imposed by the pore blocking with MEA. This is consistent with the adsorption/desorption isotherms at 348 K, a higher temperature which will eventually enhance intraparticle mass transfer. In fact, both adsorption and desorption isotherms overlap at this temperature. The diffusion resistance and intraparticle mass transfer of CO_2 through filled pores may prevent the achievement of a strict equilibrium in the adsorption branch (**Olea et al., 2013**), particularly at the lower temperature (**Figure 4.8a**). At this stage, however, none of these two hypotheses may be ruled out. It is likely that both mechanisms (chemisorption and hindered diffusion) occur.

4.3.2.3 On the Occurrence of Chemisorption

In order to collect experimental evidence as to whether chemisorption of CO_2 on amine-loaded samples would take place, as suggested in a previous publication (**Bezerra et al., 2011**) and in the XPS analysis, the behavior of adsorption isotherms for sample ZX10 at different temperatures was observed. As can be seen in **Figure 4.9**, for zeolites loaded with high concentrations of amine, the usual physisorption behavior with temperature does not occur. That is to say, CO_2 uptakes apparently increase for increasing temperatures in some amine loaded samples. Nevertheless, from the discussion in the previous sections, it is also reasonable to attribute such behavior also to diffusion resistances caused by the clogging of the porous structure of the adsorbent with MEA.

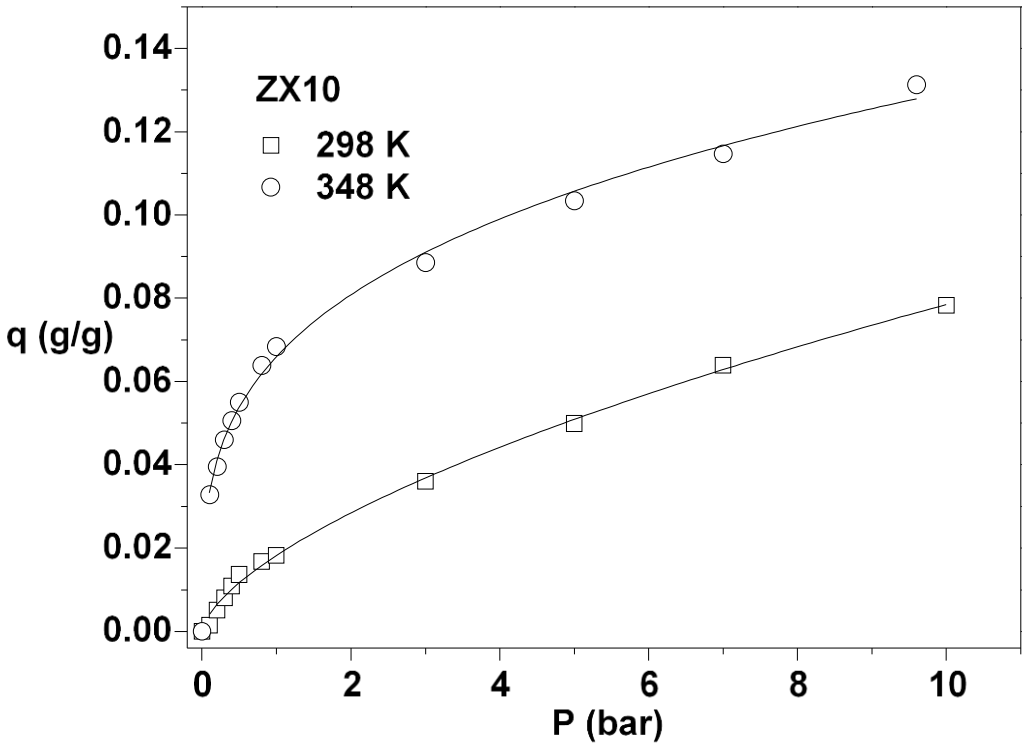

Figure 4.9. Adsorption isotherms of CO_2 at 298 and 348 K for ZX10.

In order to further examine the hypothesis of chemisorption, adsorption calorimetric experiments were carried out in a Tian-Calvet microcalorimeter coupled to an adsorption volumetric device, as described in full detail elsewhere (**Silva et al., 2012**). The calorimetric curves, which plot the differential adsorption enthalpy as a function of CO_2 loading, are shown in **Figure 4.10** for the pristine zeolite 13X and some of the amine-loaded samples. As expected for microporous adsorbents, all curves start with a relatively high value of adsorption enthalpy at nearly zero loading, which decreases for increasing CO_2 loadings and levels off at about 35 kJ/mol, which is in close agreement with reported values of adsorption enthalpy of CO_2 in zeolites (**Silva et al., 2012; Lee et al., 2002; Garcia-Cuello et al., 2008**). The most important piece of information in this kind of curve is the initial value, because it refers to the adsorption enthalpy in the stronger sites of the adsorbent and gives an idea of its surface heterogeneity. In **Figure 4.10**, it may be

observed that the zero-coverage adsorption enthalpy becomes higher as the MEA loading increases. At nearly-zero CO_2 coverage, the initial heats of adsorption are 50.0, 59.7 and 144.7kJ/mol for samples ZX, ZX0.2 and ZX10, respectively. On one hand, such values confirm that the introduction of MEA in the zeolite effectively causes new sorbate-sorbent interactions as compared to the pristine material. On the other hand, the excess MEA which fills completely the pores and deteriorates textural properties is possibly responsible for the little availability/accessibility of such stronger sites, which would explain the very rapid decrease in the calorimetric curves at relatively low CO_2 uptakes of the amine-loaded samples.

This suggests that there are few available chemisorption surface sites owing to MEA impregnation. Above 1 $mmol.g^{-1}$ of loaded CO_2, the differential enthalpy curves for the three samples reach similar values. These results show the order of magnitude of the adsorption enthalpy at zero-coverage is compatible with the occurrence of a chemical reaction between CO_2 and the amine loaded surface (**Silva et al., 2012**).

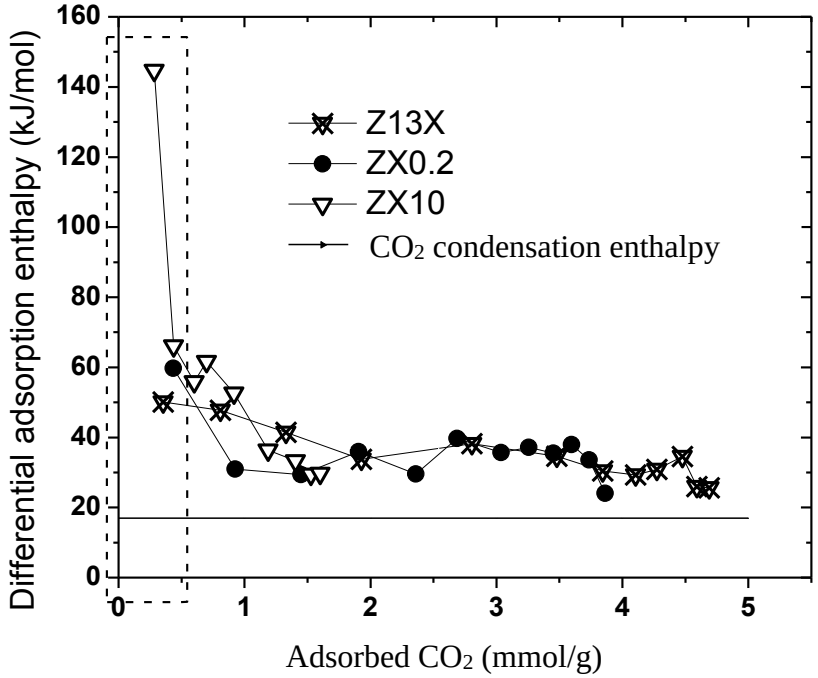

Figure 4.10. Adsorption differential enthalpies of CO_2 at 298 K.

According to **Chatti et al. (2009)**, the amino groups may act as a solvent in the confined pores of the zeolite which plays the role of microreactors for CO_2 capture. Therefore, the reactions taking place in an amine-modified adsorbent would be essentially the same as those between the liquid amine and the CO_2, wherein there is formation of carbamate species, as shown in reaction (1):

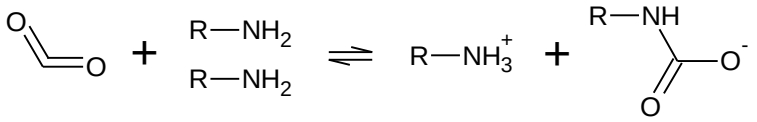

(1)

From the stoichiometry of this reaction, one CO_2 molecule reacts with two amine molecules. From the adsorption isotherm of ZX10 at 298 K (**Figure 4.6**), and considering that this sample has a molar concentration of 2.71 mmol N/g (XPS), such sample adsorbs 0.15 mol CO_2/mol N at 1 bar. The hypothesis of diffusion resistance and intraparticle mass transfer of CO_2 through filled pores may justify this behavior. At 348K, this figure

rises to 0.57 mol CO_2/mol N, probably because the temperature increase promotes/facilitates intracrystalline diffusion. This is approximately the same figure to be expected from the reaction stoichiometric in dry conditions (equation 1).

At 10 bar, this sample (ZX10) retains 0.66 mol CO_2/mol N at 298 K and 1.10 mol CO_2/mol N at 348K, which suggests that, besides chemisorption, physisorption also takes place. Note that these experiments were performed with dry CO_2, however there are indication (**Gray et al., 2004**) that in the presence of water, reaction would proceed so as to form bicarbonates, in which case 1 mol CO_2 would react with one mol N.

4.4 Conclusion

Zeolite 13X has been impregnated with monoethanolamine (MEA) from methanolic solutions with increasing concentrations. Texture and surface chemistry of the thus-prepared materials have been investigated by nitrogen adsorption/desorption isotherms, TGA, FTIR and XPS. It has been shown that MEA tends to obstruct the micropores of the zeolite. TGA and XPS analyses reveal that part of the loaded amine is firmly attached to the adsorbent surface. Nevertheless, not much of this covalently bonded amine is available for chemisorptions. As a result, amine loaded zeolites adsorb less than the pristine material at a given temperature, but they tend to increase CO_2 uptake as temperature rises. Such behavior together with measured calorimetric data confirm that there are chemisorption sites for CO_2. The amine-grafted materials did not show superior adsorption capacities than the pristine sample, however they revealed important features and adsorptive properties that can lead to new studies. Future investigation should be focused on the functionalization of mesoporous, rather than microporous matrices, so that both chemisorption and physisorption may be the driving mechanisms of CO_2 retention.

4.5 References

Aroua, M.K., Daud, W.M.A.W., Yin, C.Y., Adinata, D. Adsorption capacities of carbon dioxide, oxygen, nitrogen and methane on carbon molecular basket derived from polyethyleneimine impregnation on microporous palm shell activated carbon. Separation and Purification Technology 62 (2008) 609–613.

Aziz, B., Hedin, N., Bacsik, Z. Quantification of chemisorption and physisorption of carbon dioxide on porous silica modified by propylamines: effect of amine density. Microporous and mesoporous materials 159 (2012) 42–49.

Bacsik, Z., Atluri, R., Garcia-Bennett, A.E., Hedin, N. Temperature-Induced Uptake of CO_2 and Formation of Carbamates in Mesocaged Silica Modified with n-Propylamines. Langmuir 26 (2010) 10013–10024.

Bezerra, D.P., Oliveira, R.S., Vieira, R.S., Cavalcante Jr., C.L., Azevedo, D.C.S. Adsorption of CO_2 on nitrogen-enriched activated carbon and zeolite 13X. Adsorption 17 (2011) 235–246.

Chatti, R., Bansiwal, A.K., Thote, J.A., Kumar, V., Jadhav, P., Lokhande, S.K., Biniwale, R.B., Labhsetwar, N.K., Rayalu, S.S. Amine loaded zeolites for carbon dioxide capture: Amine loading and adsorption studies. Microporous Mesoporous Material 121 (2009) 84–89.

Choi, S., Drese, J.H., Jones, C.W. Adsorbent materials for carbon dioxide capture from large anthropogenic point sources. ChemSusChem 2 (2009) 796–854.

D'Alessandro, D.M., Smit, B., Long, R.J. Carbon dioxide capture: prospects for new materials. Angewandte Chemie 49 (2010) 6058–6082.

Du, H., Williams, C.T., Ebner, A.D., Ritter, J.A. In situ FTIR spectroscopic analysis of carbonate transformations during adsorption and desorption of CO_2 in K-promoted HTIc. Chemistry of Materials 22 (2010) 3519–2536.

Ebner, A.D., Ritter, J.A. State-of-the-art adsorption and membrane separation processes for carbon dioxide production from carbon dioxide emitting industries. Separation Science and Technology 44 (2009) 1273–1421.

Garcia-Cuello, V., Moreno-Pirajan, J.C., Giraldo-Gutierrez, L., Sapag, K., Zgrablich G. Determination of Differential Enthalpy and Isotherm by Adsorption Calorimetry. Research Letters in Physical Chemistry 2008 (2008) 1–4.

Gray, M.L., Soong, Y., Champagne, K.J., Baltrus, J., Stevens Jr., R.W., Toochinda, P., Chuang, S.S.C. CO_2 capture by amine-enriched fly ash carbon sorbents. Separation and Purification Technology 35 (2004) 31–36.

Jadhav, P.D., Chatti, R.V., Biniwale, R.B., Labhsetwar, N.K., Devotta, S., Rayalu, S.S. Monoethanol amine modified zeolite 13X for CO_2 adsorption at different temperatures. Energy Fuels 21 (2007) 3555–3559.

Lee, J.S., Kim, J.H., Kim, J.T., Suh, J.K., Lee, J.M., Lee, C.H. Adsorption equilibria of CO_2 on zeolite 13X and zeolite X/activated carbon composite. Journal of Chemical and Engineering Data 47 (2002) 1237–1242.

Lee, S.C., Hsieh, C.C., Chen, C.H., Chen, Y.S. CO_2 Adsorption by Y-Type Zeolite Impregnated with Amines in Indoor Air. Aerosol and Air Quality Research 13 (2013) 360–366.

Moliner, M. Direct Synthesis of Functional Zeolitic Materials. ISRN Materials Science 2012 (2012) 1–24.

Montanari, T., Finocchio, E., Bozzano, I., Garuti, G., Giordano, A., Pistarino, C., Busca, G. Purification of landfill biogases from siloxanes by adsorption: a study of silica and X zeolite adsorvents on hexamethylcyclotrisiloxane separation. Chemical engineering journal 165 (2010) 859–863.

Montanari, T., Finocchio, E., Salvatore, E., Garuti, G., Giordano, A., Pistarino, C., Busca, G. CO_2 separation and landfill biogas upgrading: a comparison of 4A and 13X zeolite adsorbents. Energy 36 (2011) 314–319.

Nik, O.G., Sadrzadeh, M., Kaliaguine, S.Surface grafting of FAU/EMT zeolite with (3-aminopropyl)methyldiethoxysilane optimized using Taguchi experimental design. Chemical Engineering Research and Design 90 (2012) 1313–1321.

Olea, A., Sanz-Perez, E.S., Arencibia, A., Sanz, R., Calleja, G. Amino-functionalized pore-expanded SBA-15 for CO_2 adsorption. Adsorption 19 (2013) 589–600.

Rouquerol, F., Rouquerol, J., Sing, K. Adsorption by Powders & Porous Solids. Academic Press, San Diego (1999).

Shao, W., Zhang, L., Li, L., Lee, R.L.Adsorption of CO_2 and N_2 on synthesized NaY zeolite at high temperatures. Adsorption 15 (2009) 497–505.

Silva, F.W.M., Soares-Maia, D.A., Oliveira, R.S., Moreno-Pirajan, J.C., Sapag, K., Cavalcante Jr., C.L., Zgrablich, G., Azevedo, D.C.S. Adsorption microcalorimetry applied to the characterization of adsorbents for CO_2 capture, Canadian Journal of Chemical Engineering, 90 (2012) 1372–1380.

Stevens Jr., R.W., Siriwadane, R.V., Logan, J. In situ transform infrared (FTIR) investigation of CO_2 adsorption onto zeolite materials. Energy and Fuels 22 (2008) 3070–3079.

Su, F., Lu, C., Kuo, S.C., Zeng, W.Adsorption of CO_2 on amine-functionalized y-type zeolites. Energy and Fuels 24 (2010) 1441–1448.

Sumida, K., Rogow, D.L., Mason, J.A., McDonald, T.M., Bloch, E.D., Herm, Z.R., Bae, T.-H., Long, J.R.Carbon dioxide capture in metal-organic frameworks. Chemical Reviews 112 (2012) 724–781.

Yu, J., Le, Y. and Cheng, B. Fabrication and CO_2 adsorption performance of bimodal porous silica hollow spheres with amine-modified surfaces.RSC Advances 2 (2012) 6784–6791.

Zukal, A., Dominguez, I., Mayerová, J., Cejka, J. Functionalization of delaminated zeolite ITQ-6 for the adsorption ofcarbon dioxide. Langmuir 25 (2009) 10314–10321.

Vilarrasa-García, E., Cecilia, J.A., Santos, S.M.L., Cavalcante Jr., C.L., Jiménez-Jiménez, J., Azevedo, D.C.S., Rodríguez-Castellón, E. CO2 adsorption on APTES functionalized mesocellular foams obtained from mesoporous silicas. Microporous and Mesoporous Material 187 (2014) 125–134.

CHAPTER 5 – AMINE-GRAFTED ACTIVATED CARBON

ADSORPTION OF CO_2 ON AMINE–GRAFTED ACTIVATED CARBON

Abstract

Adsorption on amine-grafted materials may be a potentially attractive alternative to capturing CO_2 from power plants. Activated Carbon (AC) has been proposed as a potential adsorbent due to its natural affinity for CO_2 and to the possibility of tailoring textural properties and surface chemistry to enhance capacity and selectivity. An AC commercial sample was functionalized with monoethanolamine (MEA) in order to obtain nitrogen-enriched AC with two different loadings (ACN10 and ACN20). Samples characterization was carried out by nitrogen adsorption/desorption isotherms at 77 K, XPS, FTIR and adsorption microcalorimetry. CO_2 equilibrium adsorption experiments were accomplished in a volumetric system in the pressure range of vacuum up to 10 bar, at 298 and 348 K. Impregnated activated carbon presented different chemical and textural characteristics with a significant reduction in the surface area, depending on the amine loading. A high adsorption capacity at room temperature and high pressure was observed for the pristine AC, as compared to the modified samples. The reduction in surface area affected the adsorption capacity of CO_2 at 298 and 348 K, except for adsorption on ACN10 at 348 K, which suggests the occurrence of chemisorption.

Key Words: adsorption, CO_2 capture, activated carbon, amine impregnation, chemisorption

5.1 Introduction

CO_2 is the major greenhouse gas (GHG) which may cause undesired consequences to environment, such as global warming. Although atmospheric CO_2 accounts for only 0.035 percent of the air, it is the most abundant among the GHGs, which also include methane, nitrous oxide and chlorofluorocarbons (CFCs) (**Yang et al., 2008**).

The main anthropogenic CO_2 emission source is the combustion of fossil fuels, particularly for power generation (**Lee et al., 2002; Grande and Rodrigues, 2008**). However, there are other scenarios where CO_2 capture is required, e.g. the purification of natural gas, biogas and syngas (**Rios et al., 2011; Rios et al., 2013**). The Intergovernmental Panel on Climate Change (IPCC) has reported that CO_2 capture systems in power plants can reduce CO_2 emissions down to 10-20 % of the current values, with an efficiency of 85-95 % (**IPCC, 2005**). Thus, different technologies have been studied to capture CO_2 from stationary sources, such as absorption, membrane based separation, adsorption and cryogenic distillation (**Ebner and Ritter, 2009**).

However, the major challenge for CCS technologies is the large required energy input associated with the capture process. Approximately 70 % of the total operating cost of CCS is related with the selective capture CO_2 from flue gas in power plants (**Haszeldine, 2009**). For separation by absorption using alkanolamines, it is well known that most of the cost is associated to the energy input required for solvent regeneration (**Idem et al., 2006**). Thus, reduction of energy consumption spent in the regeneration of the capture agent is one of the most crucial requirements to improve the overall energy efficiency of CO_2 capture (**Sumida et al., 2012**).

Regarding the CCS available technologies, adsorption may be an alternative separation technology depending on the successful development of tunable porous materials in order to capture CO_2 at particular conditions and release it with relatively low

energy consumption (**Bulánek et al., 2010**). The major difficulty in CO_2 capture from flue gases is the low partial pressure of CO_2 and fairly high temperatures (e.g., 348 K). Amine-modified materials are claimed to be potentially effective for the CO_2 capture from flue gas owing to the smaller decrease – or even increase – in adsorption capacity at higher temperatures as compared to physisorbents (**Sumida et al., 2012; Bezerra et al., 2011; Aroua et al., 2008; Choi et al., 2009**).

Various adsorbents modified with amines have been investigated as potential materials for CO_2 capture, which include activated carbons, zeolites, mesoporoussilicas, clays and metal-organic frameworks (**Sumida et al., 2012; Bezerra et al., 2011; Chatti et al., 2009; Dantas et al., 2010; Khalil et al., 2012; Kim et al., 2013**). In this context, activated carbon (AC) has been proposed as a potential support adsorbent due to its affinity for CO_2 and the possibility of tailoring textural properties and surface chemistry. **Khalil et al. (2012)** studied the adsorption of CO_2 from a gas mixture stream on activated carbon particles modified with MEA and 2-amino-2-methyl-1-propanol (AMP). Although the impregnation process led to pore filling and subsequent reduced surface area, there was an enhancement on adsorption capacity and selectivity for CO_2. However this is not a general rule, since there are other studies that show that grafting of amine groups on activated carbon has been accompanied by a decrease in CO_2 adsorption capacity at several temperatures (**Dantas et al., 2010**). In fact, it seems there is an optimal concentration at which there is a compromise between the decrease in surface area available for physisorption and the generation of amine active sites that will bind CO_2 selectively at a wider temperature range.

In this study, nitrogen functional groups were introduced on commercial activated carbon by impregnation of a primary amine in an attempt to enhance the adsorbed concentration of CO_2 at high temperatures (e.g., 348 K). Commercial AC was

impregnated by immersing it in MEA solutions under different amine concentrations (0 to 20 % v/v). In order to evaluate the textural, structural and surface modifications induced by the impregnation process, the resulting adsorbents were characterized by a variety of analytical techniques such as N_2 adsorption/desorption isotherms at 77 K, thermogravimetric analysis, X-ray photoelectron spectroscopy (XPS), Fourier transform infrared spectroscopy (FTIR) and CO_2 adsorption microcalorimetry. The potential use of these materials as CO_2 adsorbents was investigated at two temperatures (298 and 348 K) and within the pressure range from vacuum to 13 bar using a gravimetric device.

5.2 Experimental

5.2.1 Materials

Monoethanolamine (MEA, 99.9 %, VETEC, Brazil) and methanol (99.9 %, VETEC, Brazil) were used as received. The gases used in the experiments (CO_2 and He) were supplied by White Martins with purity of 99.995 % for He and 99.8 % for CO_2. The commercial activated carbon (AC) provided by Mead WestVaco (USA), was previously washed with deionised water in order to remove fines and it was then dried in an oven at 373 K for 24 h.

5.2.2 Impregnation Process of AC

Impregnated AC was prepared by immersing the sample (2 g) in a methanolic solution of MEA (50 mL) and placing the suspension inside a rotary evaporator system (VETEC, Brazil). The system was maintained at a constant temperature 323 K (close to the boiling point of the solvent) and vacuum. The impregnation process was conducted with a moderate rotation until complete evaporation of the solvent. Then, the sample was dried at 423 K under inert atmosphere (nitrogen flow). Two amine concentrations (10 and

20 % vol. in methanol, considering the wide pore size distribution of the activated carbon with micro, meso and macroporous) were studied and the thus prepared samples were denoted as ACN10 and ACN20.

5.2.3 Characterization Methods

N_2 adsorption–desorption isotherms at 77 K were measured in an automated manometric system ASAP 2000 (Micromeritics Instrument Corporation) to determine textural characteristics of the samples. Prior to the measurements, the samples were outgassed at 373 K and under vacuum (10-5 bar). Adsorption data were used to calculate BET surface area (S_{BET}) and total pore volume (V_{TOTAL}). X-ray photoelectron spectroscopy data were collected on a Physical Electronics spectrometer (model 5700) under ultra high vacuum (10-9 bar). The surface functional groups were investigated by Fourier transform infrared spectroscopy (FTIR) using a Perkin-Elmer spectrometer. To improve the reflectivity of the samples, they were diluted with KBr at a mass ratio (KBr:sample) equal to 20:1. A spectrum of pure KBr was recorded as background.

CO_2 adsorption microcalorimetry experiments were performed at 273 K and up to 101 kPa, using a Tian–Calvet type isothermal microcalorimeter coupled with a homemade manometric dosing apparatus (**Silva et al., 2012**). This microcalorimeter consists of two thermopiles with several thermocouples mounted in electrical opposition. Thus, this system allowed us to obtain adsorption isotherms and differential enthalpies as a function of the gas coverage.

5.2.4 CO_2 Adsorption Measurements

Prior to adsorption experiments, the samples were degassed for 12 h under vacuum at 373 K. CO_2 adsorption isotherms were measured at 298 and 348 K in the

pressure range of 0 – 13 bar using a gravimetric device (magnetic suspension balance by Rubotherm, Bochum, GE).

5.3 Results and Discussion

5.3.1 Adsorbent Characterization

5.3.1.1 Nitrogen Adsorption/Desorption Isotherms

The influence of the amine impregnation on the textural characteristics of the samples was investigated by analyzing the N_2 adsorption and desorption isotherms at 77 K. The N_2 isotherms of the sorbents are shown in **Figure 5.1**.

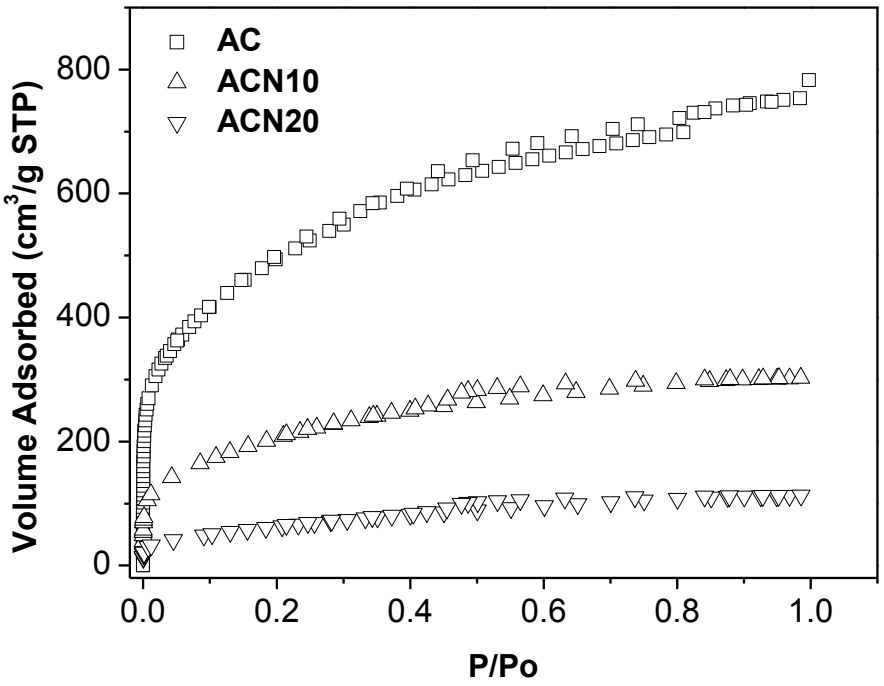

Figure 5.1. Nitrogen adsorption isotherms at 77 K of the studied samples.

All the isotherms were classified as Type I in accordance with the IUPAC classification with characteristic predominance of micropores, although the pristine AC has a rather smooth knee, which is indicative of the presence of mesopores. A high N_2

volume of nitrogen was adsorbed in the relative pressure range of 0-0.2, so it can be concluded that all adsorbents are predominantly microporous. There was a small hysteresis loop on N_2 isotherms for all the samples in the relative pressures range of 0.4-0.8, which is associated with capillary condensation of nitrogen in slit-like mesopores.

The BET surface areas of all adsorbents studied are given in **Table 5.1**. The results indicate that total surface area and total pore volume decrease with the amine impregnation process. The drastic decrease of textural properties can be assigned to the filling of the pores by amine molecules and/or destructions of pore walls, as previously observed by other authors (**Lin et al., 2013; Yaumi et al., 2013**). According to **Khalil et al. (2012)** there were many empty pores available in pristine sample which could be used to absorb N_2 molecules (on nitrogen adsorption/desorption isotherms analysis). However, for ACN10 and ACN20, the pores were blocked by amines, which may sterically hinder the diffusion of N_2 molecules. The CO_2 molecule has a smaller diameter and may eventually diffuse in the filled pores of adsorbent, despite the detrimental effect of amine impregnation on the texture of the sample. Note that, in this study, the surface area was not as drastically affected as in other studies, which report reductions in the surface area down to some tenths of m^2/g (**Khalil et al., 2012; Lee et al., 2013; Houshmand et al., 2013**). However, from another point of view, the surface area decrease also can demonstrate that amines were successfully incorporated to the surface of adsorbent.

Table 5.1. Textural characteristics of the investigated adsorbents.

Sample	S_{BET} (m^2/g)	V_{TOTAL} (cm^3/g)
AC	1727	1.204
ACN10	749	0.468
ACN20	237	0.175

Finally, the pore size distribution (PSD) of the materials was determined by using the non-linear density functional theory (NLDFT) method from the N_2 isotherms at 77 K. In **Figure 5.2**, it is seen that the carbon matrix has a wide range of pore size distribution with a major fraction in the range of micropores (<20 Å). After modification by MEA, a reduction of the pores in the microporous range confirm that the MEA was loaded into the micropores and a higher concentration of MEA solution entails a higher reduction in the range of micropores. Furthermore, it is noted that the AC PSD starts at 5 Å, whereas the PSD of the amine-modified materials begins from 9 Å. This confirms the filling of most of the micropore fraction by MEA.

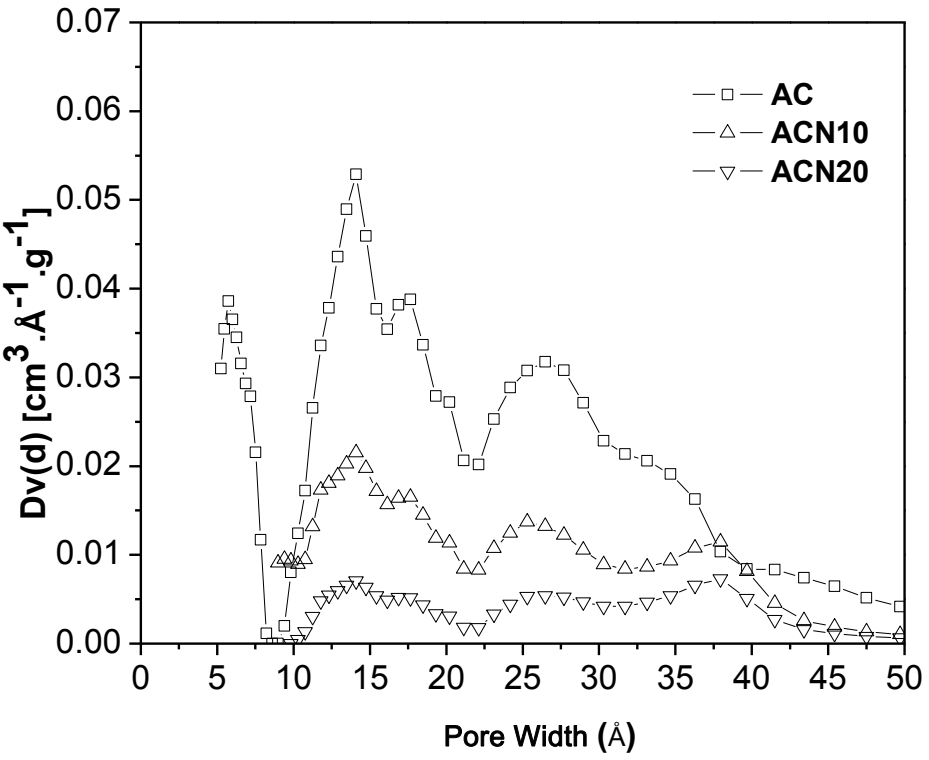

Figure 5.2. Pore size distribution from N_2 adsorption isotherms at 77 K by using NLDFT (Non Localized Density Functional Theory).

5.3.1.2 XPS Analysis

XPS measurements were performed to order to investigate interaction between MEA and the surface of activated carbon. The nitrogen functional groups were measured by XPS and could be identified by examining the C 1*s*, O 1*s* and N 1*s* core regions. Atomic concentrations and biding energies obtained from XPS are shown in **Table 5.2**. As expected, the XPS spectra indicate that the unmodified AC sample contained only C and O elements and after MEA modification, a new XPS peak appears at 400.5 eV, suggesting the presence of N in the samples.

Table 5.2. Binding energy (BE) values (in eV) of C 1*s*, O 1*s* and N 1*s* of AC, ACN10 and ACN20.

Element	BE (eV)	Atomic Concentration (%)		
		AC	ACN10	ACN20
C 1*s*	284.8 (C-C)	60.14	55.22	47.65
	286.4 (C-O)	14.82	19.24	21.09
	288.6 (COOH)	6.97	5.86	6.25
	290.7 (p–p* groups)	5.23	3.35	3.12
O 1*s*	532.8	10.56	11.02	14.04
N 1*s*	400.5	-	3.99	4.24
Impurity	-	2.28	1.33	3.62

The main C1*s* peak was deconvoluted into four peaks centered on the binding energies of 284.8, 286.4, 288.6, 290.7 eV corresponding to the bonds C–C, C–O, COOH and pi–pi*, respectively (**Guo et al., 2013; Yu et al., 2012**). The percent areas under the peaks reflect the relative concentration of each bond. This reveals that AC contains more C–C and pi–pi* bonds than the impregnated samples ACN10 and ACN20, whereas the latter samples exhibit a higher concentration of C–O bonds. This is an indication that there are amino groups attached to the carbon surface due to the impregnation. The peak

288.6 (C–OOH) presented a slight increase in the two samples (ACN10 and (ACN20) attributed to the presence of one oxygen molecule in the amine.

5.3.1.3 FTIR Analysis

In order to determine if new functional groups have been attached to activated carbon surface after impregnation, FTIR analysis was used. **Figure 5.3** shows the FTIR spectra for the pristine sample (AC) and that impregnated with the highest amine loading (ACN20) over the wave number range of 3600–600 cm^{-1}.

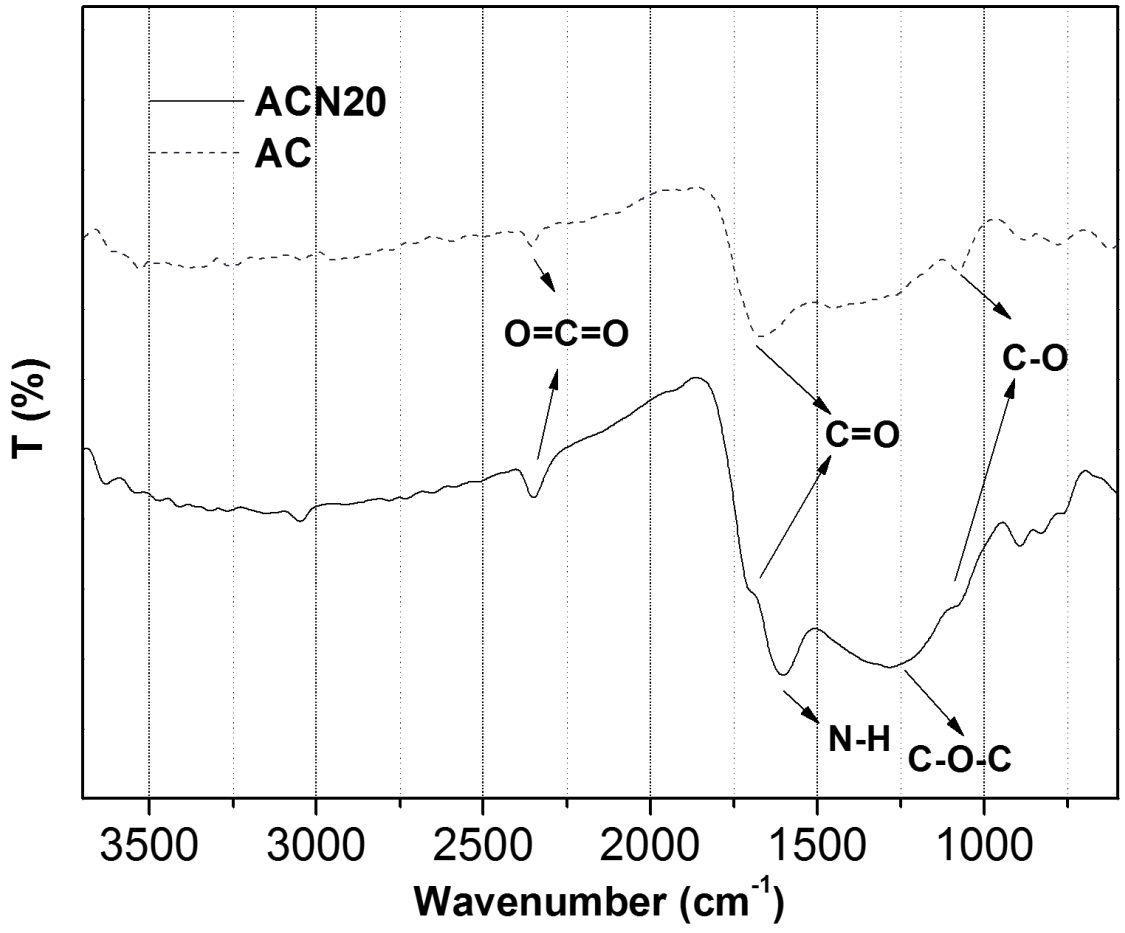

Figure 5.3. FTIR spectra for activated carbon (AC) sample and the amine-loaded sample (ACN20).

The results showed that the activated carbon has surface functionalities related with vibrational modes to oxygenated groups: a peak between 1700 and 1682 cm^{-1}, which could be assigned to the C–O groups on the surface of the carbon (lactonic, ether, phenol, etc.), and another peak at 1700-1682 cm^{-1}, which could be attributed with vibrational modes to C=O (carboxylic, anhydride, lactone and ketone groups) (**Tomaszewski et al., 2003**). For the amine-grafted carbon, the main difference observed was the appearance of two broad peaks at 1620 to 1610 cm^{-1} and at 1375 to 1175 cm^{-1}, which are indicative of the presence of N–H in the surface material (**Lin et al., 2013; Yu et al., 2012**) and C–O–C, as a result of possible dehydration reaction between two hydroxyl groups (one belonging to the amine with another from the activated carbon) taking place in amine grafting. For both samples, a peak between 2380 to 2270 cm^{-1} is observed, which is associated with the asymmetric with vibrational modes of gas-phase O=C=O, i.e., physisorbed CO_2 from the air (**Caglayan et al., 2013**). Note that such peak is significantly more intense in the amine loaded sample, which suggests a stronger interaction of the surface with CO_2 brought about by the incorporation of MEA.

5.3.2 Adsorption Isotherms

Adsorption isotherm of CO_2 on AC (pristine sample), measured at pressures up to 10 bar and two different temperatures (298 and 348 K) are shown in **Figure 5.4**.

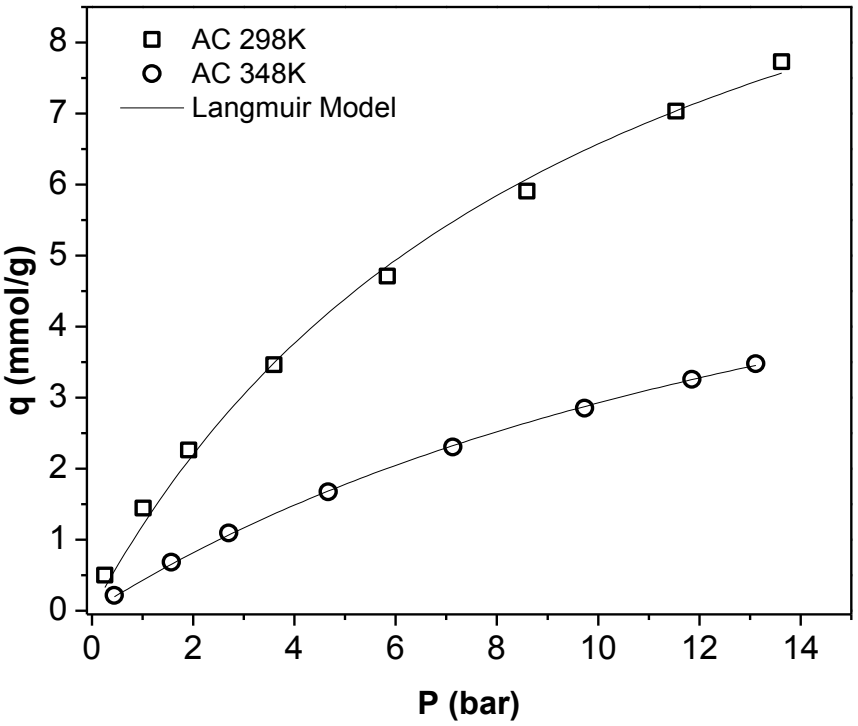

Figure 5.4. Adsorption isotherms of CO_2 in AC at 298 and 348 K.

The adsorption capacity of small molecules such as gases depends on the amount of micropores of a specific diameter and volumes as well as the chemical surface characteristics of sorbents (**Lin et al., 2013**). The superior textural properties of the pristine sample (AC) resulted in high adsorption capacity values, mainly at 298 K (indicating a predominantly exothermic process). The AC sample presented an increase in the adsorption capacity for all the pressure range studied. This is a consequence of the textural properties, which reveal a wide range of pore size distribution (micro and mesoporous) observed in **Figure 5.1**.

The CO_2 adsorption isotherm on ACN20 sample is shown in **Figure 5.5** under similar experimental conditions.

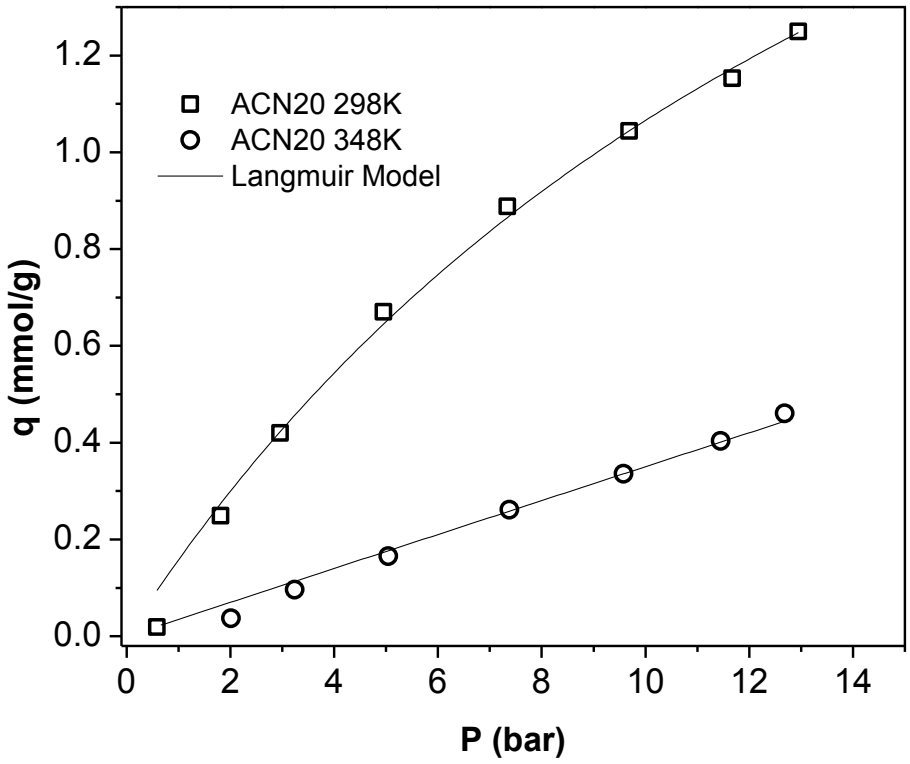

Figure 5.5. Adsorption isotherms CO_2 in ACN20 at 298 and 348 K.

CO_2 adsorption capacity of the amine-loaded AC (ACN20) was lower than that of the pristine AC, which may be explained by the fact that the surface area and porous volume of sorbents were reduced due to amine impregnation, as shown in **Table 5.1**. The pore filling of AC with amine was inappropriate and possibly led to obstruction/destructions of a considerable number of physisorption sites. Therefore, the resulting material presented low CO_2 uptake, in accordance with its low surface area, 237 m^2/g.

The great difficulty in functionalized sorbents with small pores is an adequate filling with the target functionalization moiety. The concentration of the impregnating solution and the experimental procedure are important factors that may lead to an adsorbent which will bind CO_2 predominantly either by physisorption or chemisorption.

In order to apply such materials for CO_2 adsorption from flue gases, a sorbent with both physical and chemical adsorption properties is desirable, particularly because of the temperature range of such emissions (323-353 K).

In the search of an absorbent with a balance of such properties, the sample ACN10, with an intermediate amine load, was analyzed. The adsorption data at 298 and 348 K are shown in **Figure 5.6**.

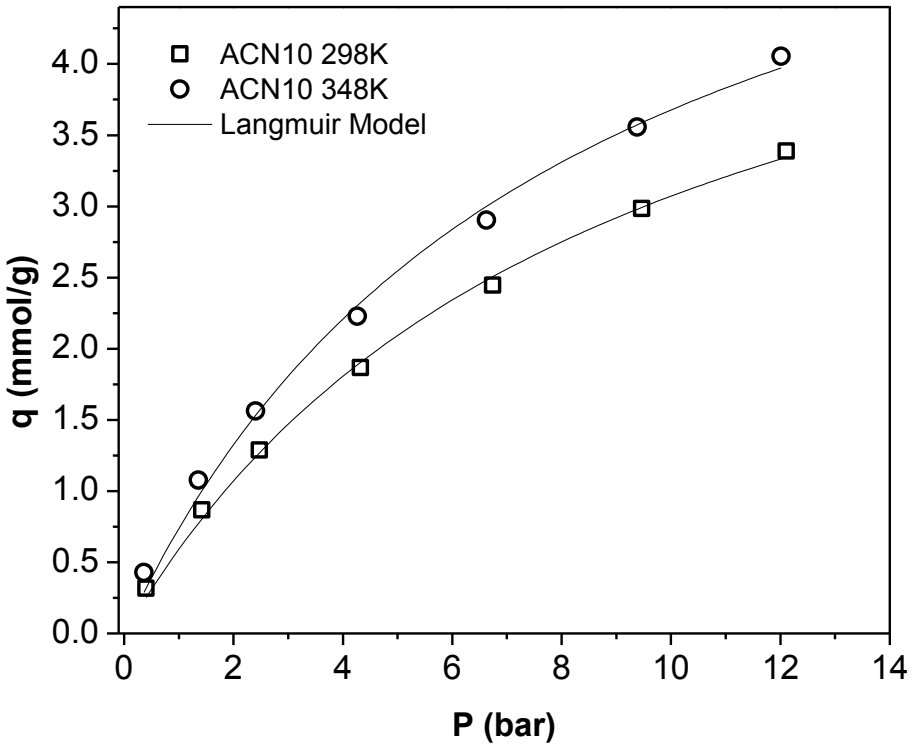

Figure 5.6. Adsorption isotherms of CO_2 in ACN10 at 298 and 348 K.

In this case, experimental results indicate that CO_2 adsorption capacity is not only determined by the BET area surface, but also by the surface properties, especially the basic functional groups. The adsorption capacity results were calculated on mmol/g and mmol/m^2 at given pressures and they were summarized in the **Table 5.3**.

CO_2 adsorption for the pristine sample was essentially due to physisorption, and hence depended only on the surface area and pore volume available in the adsorbent. The sample AC has the largest surface area, 1727 m^2/g, and the highest physisorption capacity at low temperature, over 6 mmol CO_2/g at 10 bar.

Samples ACN10 and ACN20 presented a decrease in the adsorption capacity at low temperature, 298 K, as a result of the detrimental effect of amine impregnation on the textural properties. According to a previous study in this group (**Bezerra et al., 2011**), at low temperatures, this effect may be attributed to either size exclusion or diffusion limitations imposed by the pore blocking with amine. Nonetheless, sample ACN10 presented a different behavior at the high temperature, 348 K. Its adsorption capacity (on mmol/g and mmol/m^2) were superior as compared to the pristine sample. Such behavior may be due to a temperature-controlled reaction, i.e., favored in high temperature (chemisorption). This also is consistent with the diffusion effects, i.e., at high temperatures, intraparticle mass transfer is possibly enhanced. It is likely that both mechanisms (chemisorption and resistance diffusion) occur. Also note that, in mmol/m^2, nearly all samples have the same CO_2 adsorption capacity at 298 K, which is another evidence that physisorption is the main mechanism in such temperature. At the higher temperature, ACN10 seems to have a balanced amount of loaded amine, which successfully enhanced adsorption capacity despite the much lower surface area as compared to the pristine sample.

Table 5.3. CO_2 adsorption capacity for amine-grafted on activated carbon.

Pressure (bar)	Adsorption Capacity (mmol/g)					
	AC		ACN10		ACN20	
	298K	348K	298K	348K	298K	348K
0.1	0.131	**0.045**	0.065	**0.082**	0.017	0.004
1	1.202	**0.430**	0.590	**0.737**	0.158	0.035
10	6.571	**2.926**	3.072	**3.677**	1.066	0.350
	Adsorption Capacity (10^{-3}mmol/m^2)					
1	0.696	**0.250**	0.877	**0.984**	0.666	0.148
10	3.80	**1.694**	4.101	**4.909**	4.498	1.477

CO_2 adsorption calorimetric experiments were carried in order to further investigate the hypothesis of chemisorption in the sample AC and ACN10. In **Figure 5.7** and **5.8**, the adsorption isotherms and calorimetric curves of the two samples at 273 K are shown.

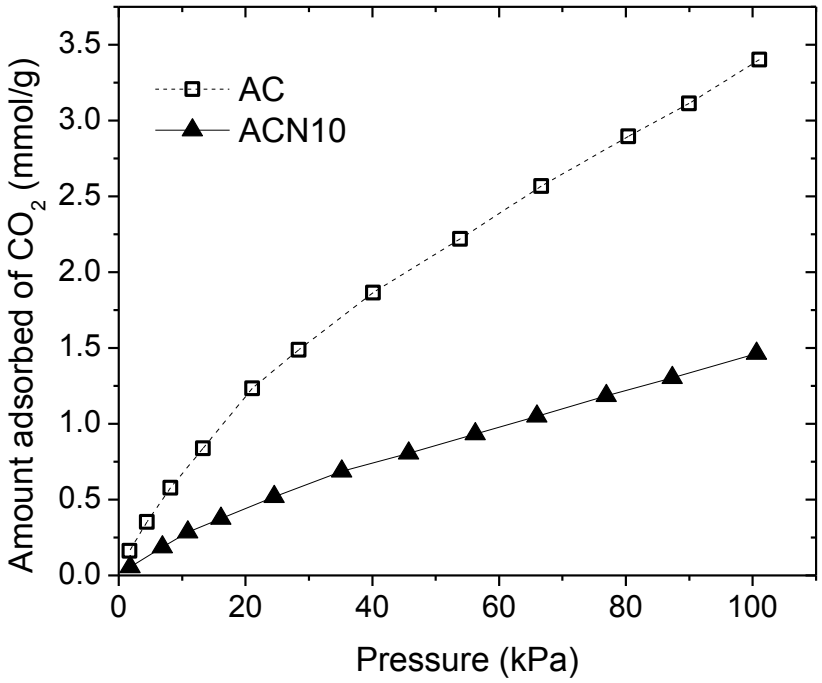

Figure 5.7. CO_2 adsorption isotherms at 273 K by joint volumetry-calorimetry.

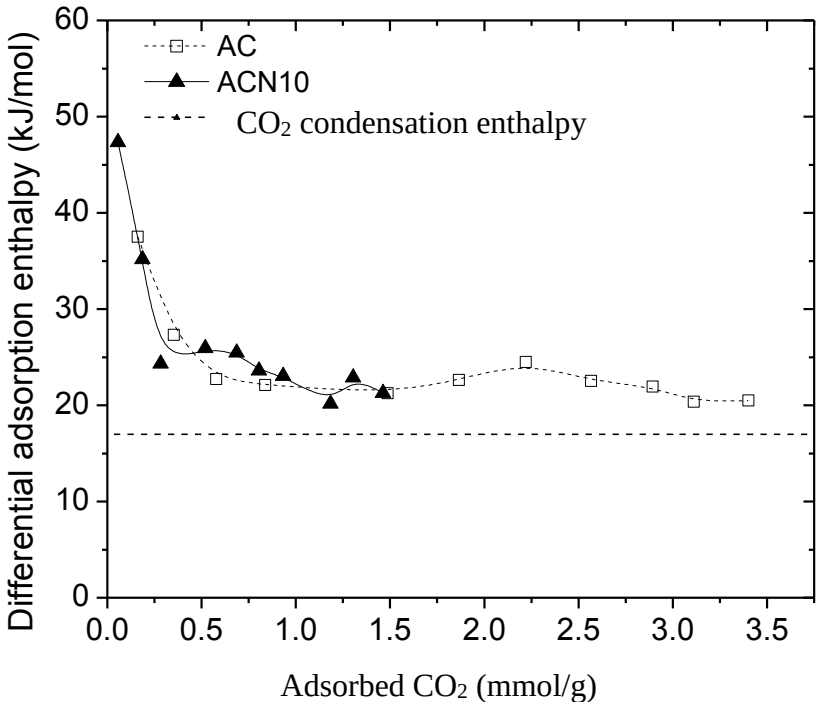

Figure 5.8. Adsorption differential enthalpies of CO_2 at 273 K.

From the volumetric-calorimetric isotherms (**Figure 5.7**), it can be seen that MEA loading have decreased CO_2 adsorption capacity compared with unmodified carbon, as previously observed in isotherms measured at other temperatures. From differential adsorption enthalpy measurements (**Figure 5.8**), it is observed that the curves of the adsorption enthalpies for AC and ACN10 are relatively similar, except for the first measured point, which is notably higher for the amine-loaded sample (-38 kJ/mol for AC and -47 kJ/mol for ACN10). This behavior suggests that chemisorption is not significant in CO2 adsorption at 273 K (except for very low coverages) and, thus, the physisorption is the dominant mechanism. As temperature increases, the role of chemisorption in amine loaded sample ACN10 becomes more evident, as can be observed in the values shown in **Table 5.3**, particularly on a mmol/m^2 basis.

5.4 Conclusion

Two modified activated carbon samples were obtained by loading the pristine sample (AC) with MEA by wet impregnation (ACN10 and ACN20). It has been shown that MEA tends to fill and eventually block the pores of the adsorbent. XPS and FTIR analyses reveal that there is nitrogen covalently attached to the adsorbent surface. At low temperature (room temperature and below), physisorption in the main bonding mechanism of CO_2, regardless the amine concentration loaded to the adsorbent. At higher temperatures, though, the presence of amine in moderate amounts seems to enhance CO_2 uptake by a synergistic combination of physisorption and chemisorption. As a result, ACN10 adsorbs more CO_2 than the pristine material as temperature rises, unlike ACN20. For the latter, loaded amine was excessive and led to such a detrimental effect on the textural properties that the expected increase in uptake by chemisorption at higher temperature could not be observed.

5.5 References

Aroua, M.K., Daud, W.M.A.W., Yin, C.Y. Adinata, D. Adsorption capacities of carbon dioxide, oxygen, nitrogen and methane on carbon molecular basket derived from polyethyleneimine impregnation on microporous palm shell activated carbon. Separation and Purification Technology 62 (2008) 609–613.

Bezerra, D.P., Oliveira, R.S., Vieira, R.S., Cavalcante Jr., C.L., Azevedo, D.C.S. Adsorption of CO_2 on nitrogen-enriched activated carbon and zeolite 13X. Adsorption 17 (2011) 235–246.

Bulánek, R., Frolich, K., Frydova, E., Cicmanec, P. Microcalorimetric and FTIR study of the adsorption of carbon dioxide on alkali-metal exchanged FER zeolites. Topics in Catalysis 53 (2010) 1349–1360.

Caglayan, B.S., Aksoylu, A.E. CO_2 adsorption on chemically modified activated carbon. Journal of Hazardous Materials 252 (2013) 19–28.

Chatti, R., Bansiwal, A.K., Thote, J.A., Kumar, V., Jadhav, P., Lokhande, S.K., Biniwale, R.B., Labhsetwar, N.K., Rayalu, S.S. Amine loaded zeolites for carbon dioxide capture: Amine loading and adsorption studies. Microporous and Mesoporous Material 121 (2009) 84–89.

Choi, S., Drese, J.H., Jones, C.W. Adsorbent materials for carbon dioxide capture from large anthropogenic point sources. ChemSusChem 2 (2009) 796–854.

Dantas, T.L.P., Amorim, S.M., Luna, F.M.T., Silva Jr., I.J., Azevedo, D.C.S., Rodrigues, A.E., Moreira, R.F.P.M. Adsorption of carbon dioxide onto activated carbon and nitrogen-enriched activated carbon: Surface changes, equilibrium, and modeling of fixed-bed adsorption. Separation Science and Technology 45 (2010) 73–84.

Ebner, A.D. Ritter, J.A. State-of-the-art adsorption and membrane separation processes for carbon dioxide production from carbon dioxide emitting industries. Separation Science and Technology 44 (2009) 1273–1421.

Grande, C.A., Rodrigues, A.E. Electric Swing Adsorption for CO_2 removal from flue gases. International Journal of Greenhouse Gas Control 2 (2008) 194–202.

Guo, Y., Li, Y., Zhu, T., Ye, M., Wang, X. Adsorption of SO_2 and chlorobenzene on activated carbon. Adsorption (2013). doi: 10.1007/s10450-013-9539-y.

Haszeldine, R.S. Carbon capture and storage: how green can black be?Science 325 (2009) 1647–1652.

Houshmand, A., Shafeeyan, M.S., Arami-Niya, A., Daud, W.M.A.W., Anchoring a halogenated amine on the surface of a microporous activated carbon for carbon dioxide capture. Journal of the Taiwan Institute of Chemical Engineers 44 (2013) 774–779.

Idem, R., Wilson, M., Tontiwachwuthikul, P., Chakma, A., Veawab, A., Aroonwilas, A., Gelowitz, D. Pilot plant studies of the CO_2 capture performance of aqueous MEA and mixed MEA/MDEA solvents at the University of Regina CO_2 capture technology development plant and the boundary dam CO_2 capture demonstration plant. Industrial and Engineering Chemistry Research 45 (2006) 2414–2420.

IPCC. Special Report on Carbon dioxide Capture and Storage.Intergovernmental Panel on Climate Change. Cambridge University Press, Cambridge, 2005.

Khalil, S.H., Aroua, M.K., Daud, W.M.A.W. Study on the improvement of the capacity of amine-impregnated commercial activated carbon beds for CO_2 adsorbing.Chemical Engineering Journal 183 (2012) 15–20.

Kim, J., Park, D-W. Ahn, W-S. Ethylenediamine grafting on a zeolite-like metal organic framework (ZMOF) for CO_2 capture. Materials Letters 106 (2013) 344–347.

Lee, J.S., Kim, J.H., Kim, J.T., Suh, J.K., Lee, J.M., Lee, C.H. Adsorption equilibrium of CO_2 on zeolite 13X and zeolite X/activated carbon composite. Journal of Chemical and Engineering Data 47 (2002) 1237–1242.

Lee, S.C., Hsieh, C.C., Chen, C.H., Chen, Y.S. CO_2 Adsorption by Y-Type Zeolite Impregnated with Amines in Indoor Air. Aerosol and Air Quality Research 13 (2013) 360–366.

Lin, C., Zhang, H., Lin, X., Feng, Y. Adsorption CO_2 on activated carbon with surface modification. Advanced Materials Research 634 (2013) 746–750.

Rios, R.B., Bastos-Neto, M., Amora Jr., M.R., Torres, A.E.B., Azevedo, D.C.S. andCavalcante Jr., C.L. Experimental analysis of the efficiency on charge/discharge cycles in natural gas storage by adsorption. Fuel 90 (2011) 113–119.

Silva, F.W.M., Soares-Maia, D.A., Oliveira, R.S., Moreno-Pirajan, J.C.,Sapag, K., Cavalcante Jr., C.L.,Zgrablich, G., Azevedo, D.C.S. Adsorption microcalorimetry applied to the characterization of adsorbents for CO_2 capture. Canadian Journal of Chemical Engineering 90 (2012) 1372–1380.

Sumida, K., Rogow, D.L., Mason, J.A., McDonald, T.M., Bloch, E.D., Herm, Z.R., Bae, T.H., Long, J.R. Carbon dioxide capture in metal-organic frameworks. Chemical Reviews 112 (2012) 724–781.

Tomaszewski, W., Gunko, V.M., Skubiszewska-Zieba, J., Leboda, R. Structural characteristics of modified activated carbons and adsorption of explosives. Journal of Colloid and Interface Science 266 (2003) 388–402.

Yang, H., Xu, Z., Fan, M., Gupta, R., Slimane, R.B., Bland, A.E., Wright, I. Progress in carbon dioxide separation and capture: A review. Journal of Environmental Sciences 20 (2008) 14–27.

Yaumi, A.L., Hussien, I.A. Shawabkeh, R.A. Surface modification of oil fly ash and its application in selective capturing of carbon dioxide. Applied Surface Science 266 (2013) 118–125.

Yu, J., Le, Y., Cheng, B. Fabrication and CO_2 adsorption performance of bimodal porous silica hollow spheres with amine-modified surfaces. RSC Advances 2 (2012) 6784–6791.

CHAPTER 6 – ION-EXCHANGED BINDERLESS X ZEOLITE

ION-EXCHANGED BINDERLESS X ZEOLITES FOR CO_2 ADSORPTION

Abstract

Ion-exchange with various ions (NH_4^+, Li^+, Ba^{2+} and Fe^{3+}) was performed in binderless X zeolite pellets. The extent of ion exchange was confirmed by TGA-MS and textural properties of the samples were measured by XRD and adsorption-desorption N_2 isotherms a 77 K. CO_2 adsorption isotherms of the ion-exchanged samples up to 10 bar were obtained at 298 and 348 K. CO_2 adsorption capacity at low pressures and high temperature decreased in the sequence of NH_4 ~ Na > Li > Ba > Fe.

Key Words: Ion-exchange, adsorption, carbon dioxide.

6.1 Introduction

CO_2 plays a significant role in global warming, contributing with more than 60% because of its huge emitted amounts (**Albo et al., 2010**). It has become necessary to think about new approaches and novel ideas for CO_2 management. Some of the strategies include reducing emissions from power plants, using clean energy (wind, solar, and tidal), CO_2 capture, utilization and sequestration. It is well-known that zeolites have the potential to separate and/or store gases. Zeolites are crystalline aluminosilicates composed of connected, cage-like structures, which are large enough to adsorb and accommodate a wide variety of molecules (**Barrer, 1978; Lin et al., 2013**). The adsorptive activity of zeolites was first related to the presence of acid sites in their cage. It is also well known that metal ions (compensating cations) are very important catalytic/adsorptive centers, because they can induce interactions with the adsorbate (**Klier, 1988; Valdés et al., 2012**).

It has been clearly established that the extra-framework cations compensating the negative charge of the zeolite (arising from the silicon and aluminum oxides), play a significant role in adsorption. The acid character of zeolites may be tuned to increase or decrease in intensity (**Barrer, 1978; Lin et al., 2013; Klier, 1988; Valdés et al., 2012; Barthomeuf, 2003**).

Walton et al. (2006) studied ion exchange on NaY and NaX zeolite crystals with alkali metal cations Li^+, K^+, Rb^+, and Cs^+ applied to the adsorption of CO_2 at 25 ºC. They observed that CO_2 capacity increased as Cs <Rb< K < Li < Na for Y zeolites. For X zeolites, the capacity for CO_2 increased in the order Cs <Rb< K < Na < Li (in other words, following the order of decreasing ionic radii). According to **Walton et al. (2006)**, this is consistent with an increased basicity of the framework as cation size increases, given that CO_2 is a slightly acid gas.

Plant et al. (2006) have also studied ion exchange on NaY zeolites with alkali metal cations Li^+, K^+ and Cs^+ applied to the adsorption of CO_2 at room temperature. The adsorption enthalpies as calculated from density functional theory show a decrease from Li^+ to Cs^+ and reproduce well experimental data obtained by microcalorimetric measurements: Li^+ (33.20 kJ.mol^{-1}), Na^+ (28.69 kJ.mol^{-1}), K^+ (21.07 kJ.mol^{-1}) and Cs^+ (17.17 kJ.mol^{-1}).

Yang et al. (2010) synthesized zeolite beta and performed ion-exchange with various alkali and alkaline earth metal ions (Li^+, K^+, Cs^+, Mg^{2+}, Ca^{2+}, and Ba^{2+}) for CO_2 capture at room temperature. CO_2 adsorption capacity increased in the sequence of $K^+ > Na^+ > Li^+ > Ba^{2+} = Ca^{2+} > Cs^+ > Mg^{2+}$. It appears that CO_2 uptake in zeolites depends of various properties, highlighting the density and distribution of the cations located in the zeolite framework structures.

In this work, we investigated the effects of ion-exchanged NH_4^+, Li^+, Na^+,Ba^{2+} and Fe^{3+}cations in X zeolite on CO_2 adsorption. The adsorption isotherms were measured gravimetrically at 298 K (for comparison with other studies) and 348 K (temperature of post-combustion process).

6.2 Experimental

6.2.1 Materials and Ion Exchange Procedure

Spherical pellets (2 mm) of binder-free zeolite KÖSTRLITH 13X BF were supplied by CWK Chemiewerk Bad Kostritz (Bad Kostritz, Germany). The zeolite samples of the current study were obtained by ion exchange following the procedure reported by **Walton et al. (2006)** with minor changes. Cation exchange in the LiX, BaX and FeX sample were performed by using 1.0 M chloride aqueous solutions (50 mL) of Li^+, Ba^{2+} and Fe^{3+} prepared from the respective chloride salts. In order to obtain sample NH_4X, a 1.0 M ammonium hydroxide aqueous solution was used.

Approximately 2 g NaX zeolite were immersed in 50 mL solution for 3 h under constant agitation at 298 K. The procedure was performed five times, each exchange batch with fresh solution. The final exchanged samples were filtered and washed with distilled water and dried in air. **Table 6.1** summarizes the solutions used in each ion-exchange procedure, the target exchanged cation, its ionic radius and the code of the sample thus obtained.

Table 6.1. Summary of cations compensating, ionic radius and code used.

Sample	Ion-exchange solution	Compensating cation	Ionic Radius (nm)	Code
X Zeolite	-	Na^+	0.095	NaX
	NH_4OH	NH_4^+	0.148	NH_4X
	LiCl	Li^+	0.068	LiX
	BaCl	Ba^{2+}	0.135	BaX
	FeCl	Fe^{3+}	0.064	FeX

6.2.2 Physical–Chemical Characterization

Textural properties of the zeolite samples (BET equivalent area and total pore volume) were obtained by nitrogen adsorption/desorption isotherms, using an Autosorb-1 MP apparatus (Quantachrome, U.S.A.) and data was treated as described elsewhere (**Rouquerol et al., 1999**). Samples were previously degassed at 573 K for 12 h under vacuum. X-ray powder diffraction (XRD) was applied to all zeolite samples in order to evaluate structural changes upon ion-exchange procedure. XRD was performed with a Rigaku (DMAXB) X-ray Powder Diffractometer.

TGA–MS analysis was employed to monitor the emissions from ion exchanged samples during pyrolysis. About 20 mg sample were placed in a TGA 2050 (TA Instruments, Newcastle, DE) and heated from room temperature to 973 K under an inert atmosphere (Ar at 10 ml/min and 7.7 mbar). This technique allows for the identification of the soft compensation cations that volatilize at temperatures lower than 973 K and ensure that they will be fixed to the solid adsorbent under the conditions of CO_2 adsorption, in other words, keep its structure intact in temperature around 373 K.

CO_2 adsorption enthalpy as a function of the adsorbed concentrations was measured using an isothermal Tian–Calvet type microcalorimeter (model CA-100 from ITI Company, Del Mar, CA) combined with a coupled volumetric equipment (**Silva et al., 2012**). The experiments were performed for samples NaX, NH_4X and LiX at 298 K up to 101 kPa.

6.2.3 CO_2 Capture Measurements

Prior to measuring adsorption isotherms, all samples were regenerated by heating under vacuum up to 573 K and maintaining this temperature for 12 h. Carbon dioxide (purity of 99.995 % vol.) isotherms were measured on all ion-exchanged samples at

pressures up to 10 bar and a temperature of 298 and 348 K. All isotherm measurements were performed on a magnetic suspension balance by Rubotherm (Bochum, Germany).

6.3. Results and Discussion

6.3.1 Adsorbent Characterization

6.3.1.1 Nitrogen Adsorption/Desorption Isotherms

N_2 adsorption–desorption isotherms at 77 K are shown in **Figure 6.1** for the cation-exchanged zeolite samples. It can be seen that all isotherms are type I, according to the IUPAC classification (**Sing et al., 1985**). Nevertheless, the typical constant plateau of type I isotherms is not reached, but rather a constant and smooth increase in uptake as the relative pressure reaches 1. It is interesting to note that no significant changes in the isotherm shape of zeolites samples were detected after ion-exchange, which suggests that the porous structure may have remained intact. In general, all ion-exchanged zeolites have lower N_2 uptake than the parent zeolite NaX. This is most noticeable for the samples with cations NH_4^+, which are those with the largest ionic radius. Their exchange with sodium cations may have reduced the available space in the pores for N_2 adsorption.

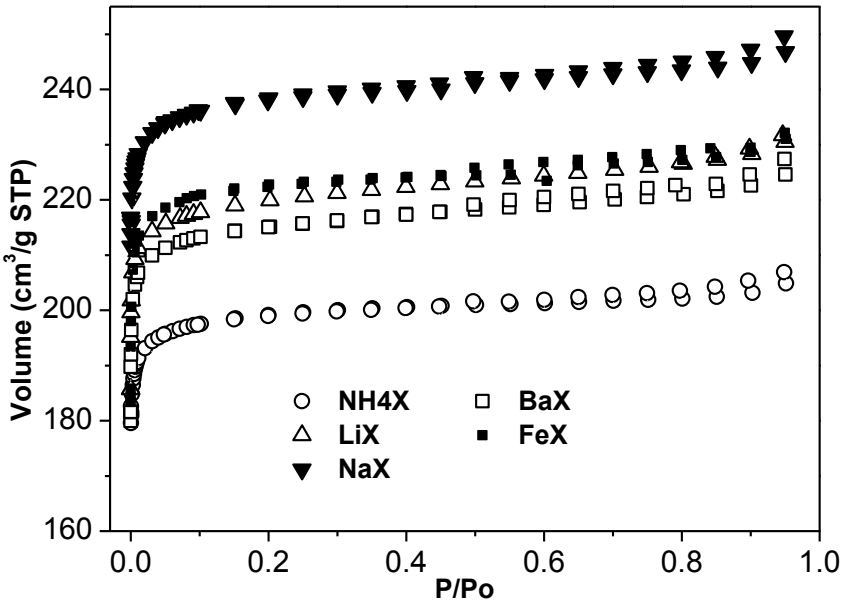

Figure 6.1. Nitrogen adsorption isotherms at 77 K of the studied samples.

The observations from the previous paragraph may be confirmed by the calculated BET equivalent area and total pore volume, which are summarized in **Table 6.2** for the parent zeolite and the cation-exchanged zeolites samples. BET equivalent area decreases down to 544 m^2/g (17 %) for the zeolite exchanged with NH_4^+. The total pore volume and pore diameter remains about the same for all samples.

Table 6.2. Textural characteristics of the investigated adsorbents.

Sample	Textural Characteristics		
	S_{BET} m^2/g	V_P cm^3/g	D_{P*} A
NH_4X	544	0.38	13
LiX	605	0.38	14
NaX	652	0.43	13
BaX	590	0.39	13
FeX	610	0.42	13

$*D_P = \frac{2 \cdot V_P}{S_{BET}}$

6.3.1.2 XRD Analysis

The XRD patterns of NaX and the ion-exchanged zeolite samples are shown in **Figure 6.2**. The similarity of peaks in the XRD patterns of NH_4X, LiX, BaX and FeX as compared to the original NaX indicates that the original zeolite crystallinity is maintained. Moreover, no new diffraction peak was observed in the sample. However, the intensity of some characteristic peaks decreased slightly, indicating a minor reduction in crystallinity of ion exchanged zeolite samples.

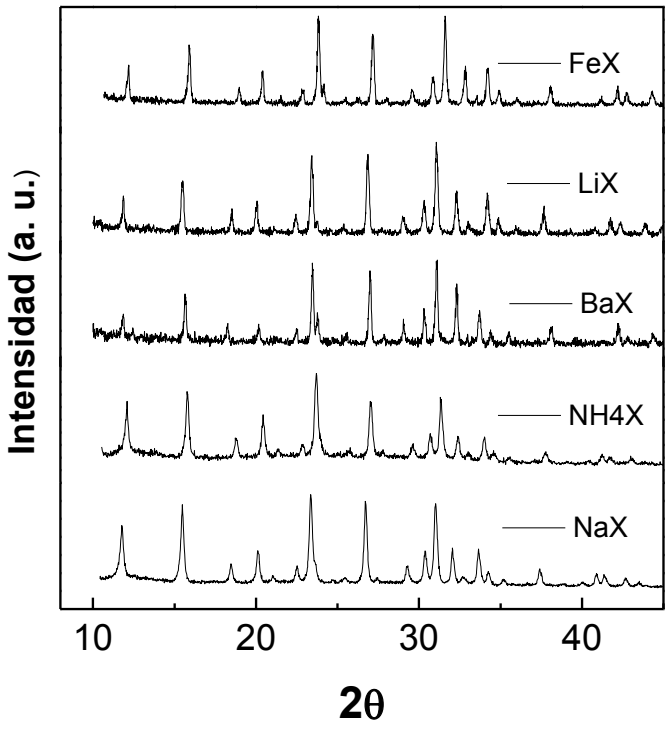

Figure 6.2. XRD patterns of NaX and ion exchanged zeolite adsorbents.

6.3.1.3 TGA-MS Analysis

The TGA curves of the cation-exchanged zeolite samples (NaX, NH_4X, LiX) in the temperature range of 50–700 ^oC are shown in **Figure 6.3**. All figures show the percent weight loss and its derivative as a function of temperature.

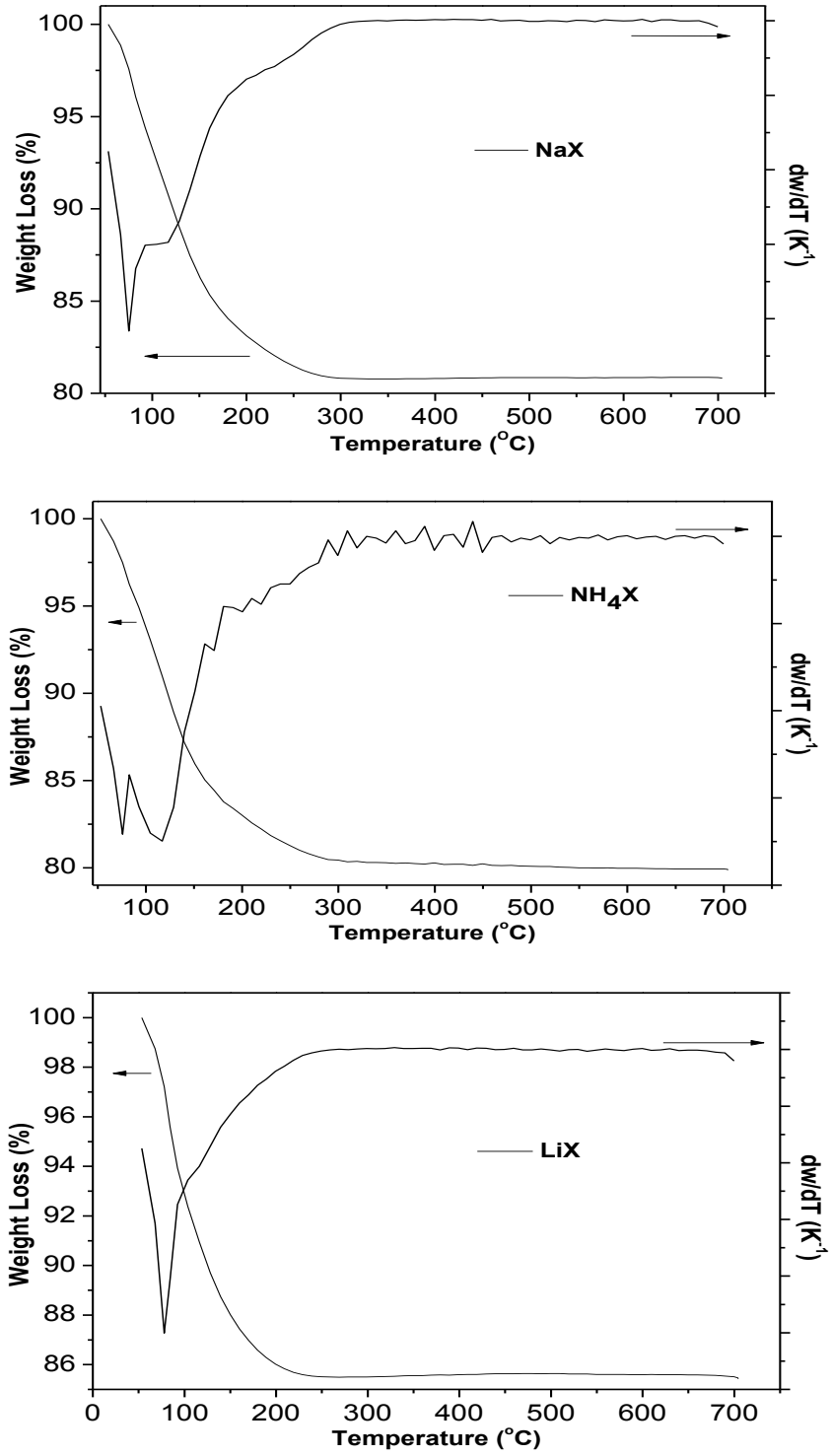

Figure 6.3. DTA/TGA curves of ion-exchanged zeolites samples (NaX, NH_4X and LiX).

The TGA curve displays a broad peak in the temperature range of 50-300 ºC, due to water desorption (**Yi et al., 2014**). This wide temperature interval can be explained by

the well-known hydrophilic character of zeolites, due to a variety of interactions of the water molecule with the solid surface, namely with non framework cations, framework oxygen ions and preadsorbed water molecules. This peak was observed for all samples. The mass loss corresponds to 20 % within this temperature interval. The NH_4X sample presented two distinct peaks, probably due to the formation of strong intermolecular interactions, such as hydrogen bonds (**Bonenfant et al., 2008**). This explains the need of a higher temperature to desorb all of the water. Furthermore, part of ammonium may also be volatilized in this temperature range. The TGA curves of the cation-exchanged zeolite samples (BaX, FeX) in the temperature range of 50–700 ºC are shown in **Figure 6.4**.

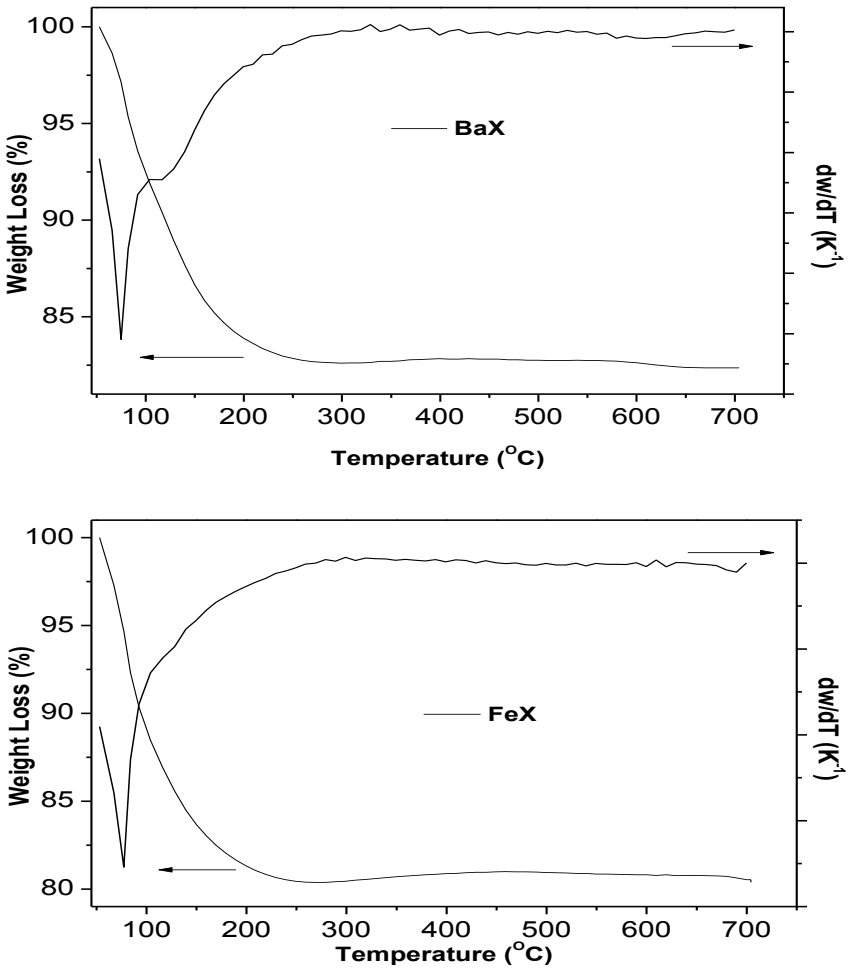

Figure 6.4. DTA/TGA curves of ion-exchanged zeolites samples.

TGA-MS also shows the release of cation from the ion-exchanged zeolites as temperature rises for NaX, LiX and NH_4X sample (see **Figure 6.5**). Several peaks or broad peaks registered at different temperatures are observed and may be related to free ion re-adsorption on vacant acid sites (**Bonenfant et al., 2008**).

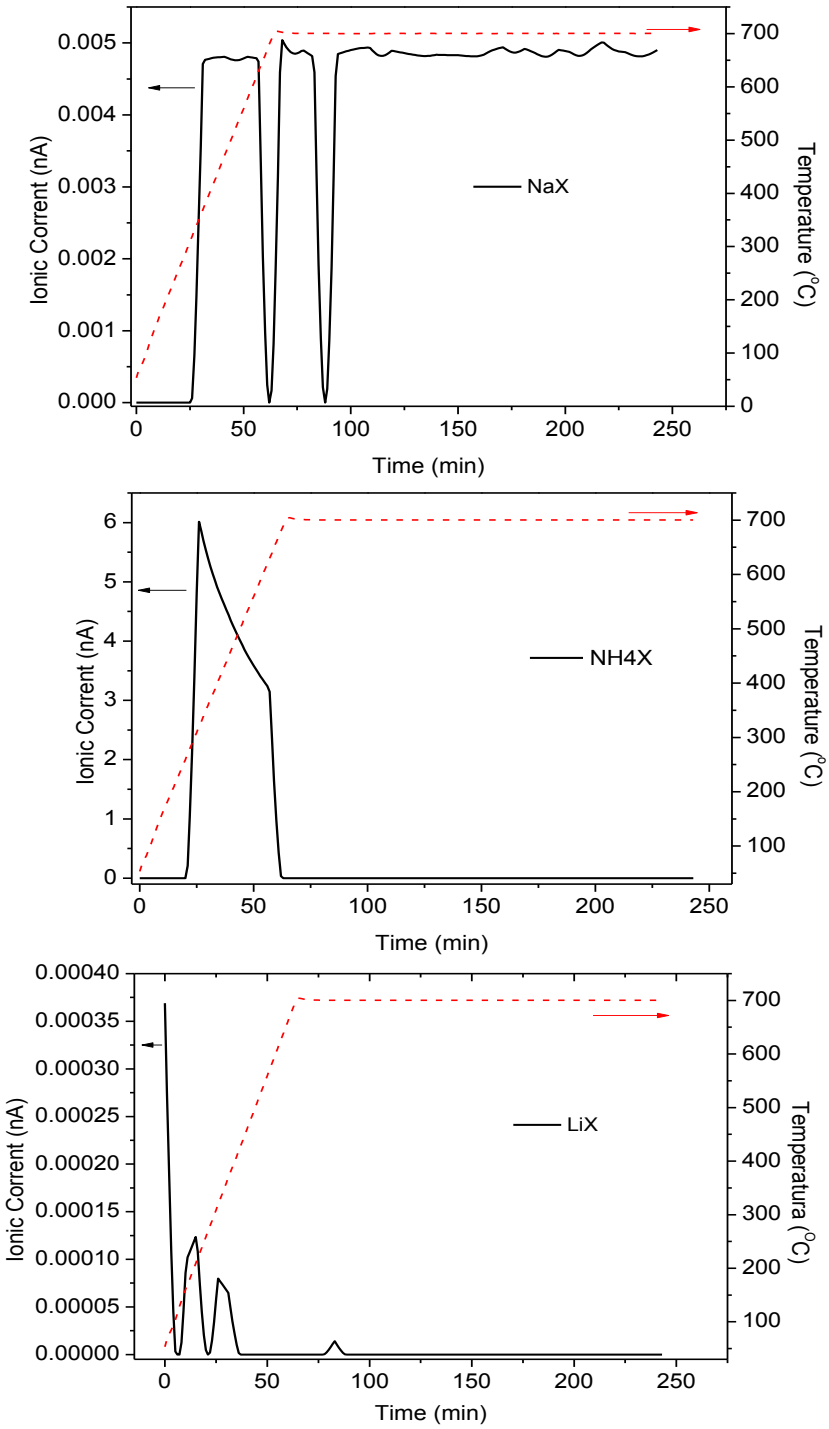

Figure 6.5. TGA-MS curves of ion-exchanged zeolites NH_4X, NaX and LiX samples.

In the case of NaX, the ions may be localized in three different sites: sites I, which are not accessible to adsorbate molecules; sites II, which are strongly bound to the zeolite lattice and the sites III, which are less bound and responsible for the heterogeneous character of CO_2 adsorption (see **Figure 6.6**).

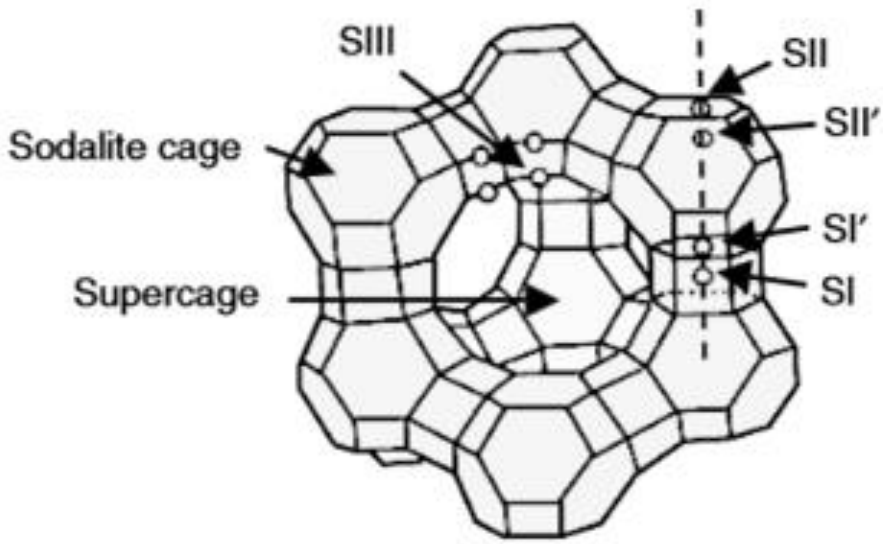

Figure 6.6. Scheme of unit cell of zeolite showing cations sites (adapted **Hutson et al., 2000**).

The ions localization in the sites II and III may cause them to interact more or less strongly with CO_2 molecules. Some ions may be quite mobile between the adsorption sites as temperature increases, mainly ammonium, because it has four hydrogen atoms bonded to nitrogen (**Bonenfant et al. 2008**). This bond favors more intense van der Waals forces, involving N, H and O atoms (hydrogen bonds). Results of the ion exchanged sample for NH_4X, LiX, BaX and FeX did not show the release of traces of sodium vapors, suggesting a complete ion exchange.

Some basic properties of zeolites brought about by compensation cations allow for a strong retention of acidic molecules (such as CO_2 and H_2S) by enhancing the electron density of the framework oxygen. Therefore, the electropositivity of exchangeable ions is very important.

6.3.2 Adsorption Isotherms

Taking into account the results obtained from XRD, N_2 isotherms and DTA/TGA-MS of the NaX and ion exchanged zeolites, the samples NH_4X, LiX, NaX, BaX and FeX were assessed for CO_2 uptake. These samples presented very different characteristics: lithium, from group 1 (charge +1); barium, from group 2 (charge +2); iron as a transition metal (charge 3+) and ammonium ion (non-metal of charge +1), which allow for the possibility of forming hydrogen bonds with CO_2 and exhibiting similar basic properties as amines (indicated for CO_2 uptake) (**Dantas et al., 2010; Chatti et al., 2009; Bezerra et al., 2011**). **Figure 6.7** shows the adsorption and desorption isotherms of pure CO_2 on the NaX, BaX and FeX at 298 (a) and 348 K (b) and pressure range of 0-10 bar.

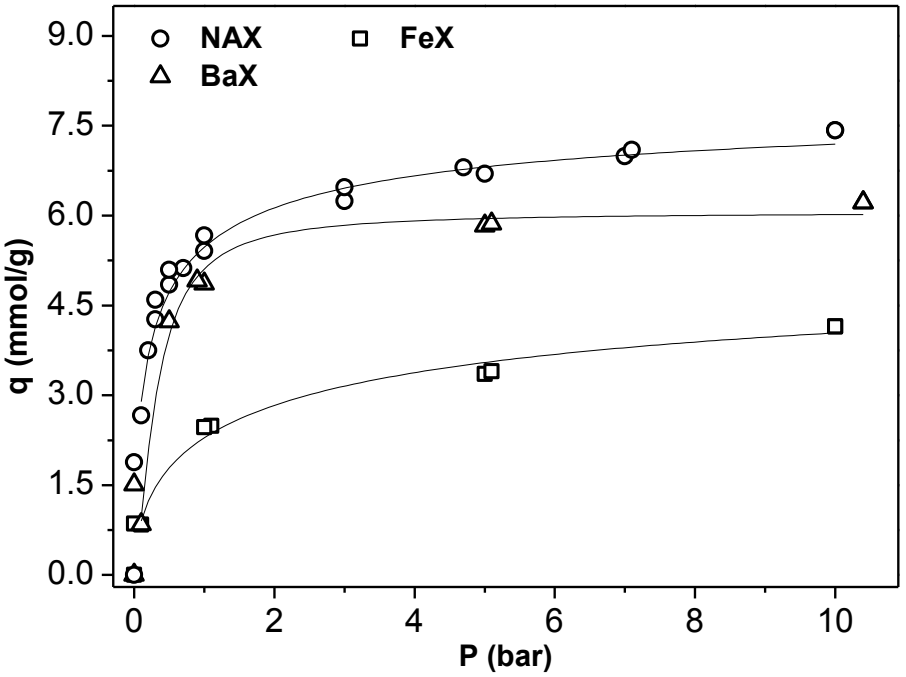

(a)

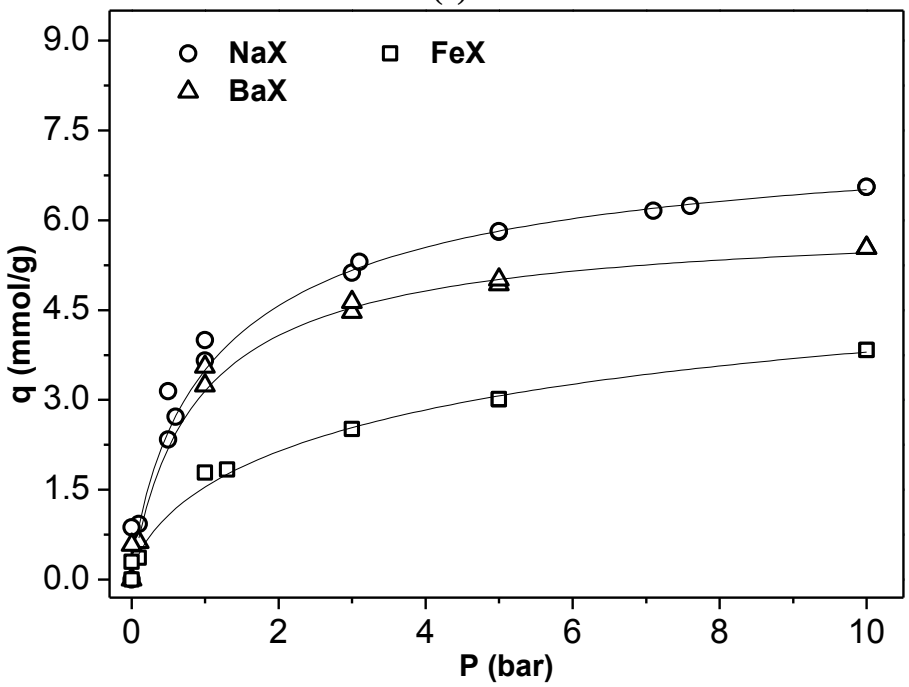

(b)

Figure 6.7. CO_2 adsorption isotherms in NaX, BaX and FeX at 298 (a) and 348 K (b).

The CO_2 adsorption isotherms are all favorable, which are typical of strong interactions between CO_2 and cations (**Walton et al., 2006**). The adsorption isotherms, in general, showed high affinity and adsorption capacity for CO_2, with NaX

outperforming the other samples by a considerable margin in the two temperatures under study (298 and 348 K). In the temperature of 348 K, CO_2 adsorption capacity suffers slight reduction for all cations. However CO_2 uptakes increase in the same order as for the lower temperature: FeX < BaX < NaX. The Fe cations triggered formation of some acid sites, while the cations Ba triggered formation of some basic sites.

These adsorption capacity trends are inversely proportional to the ionic charge (Na^+, Ba^{2+} and Fe^{3+}), possibly because fewer cations are required to balance the negative charge of the zeolitic framework. Studies (**Walton et al., 2006; Erten et al., 2008; Plant et al., 2006; Yang et al., 2010**) suggest that the ionic radii is a key factor in the adsorption capacity, but also the ion charge located in the zeolite framework structures may affect this values. In this case, it is also important to consider the effective nuclear charge and shielding effect, which in turn affect the electron in the valence shell. These electrons will interact directly with the CO_2. It is desirable that the valence shell electrons have a low effective nuclear charge, which can be further reduced by the shielding effect caused by electrons from another layer. Moreover, the iron ion prompted the formation of acidic sites, reducing the CO_2 interaction.

Figure 6.8 shows the adsorption and desorption isotherms of pure CO_2 on the NaX, LiX and NH_4X at 298 (a) and 348 K (b) and pressure range of 0-10 bar.

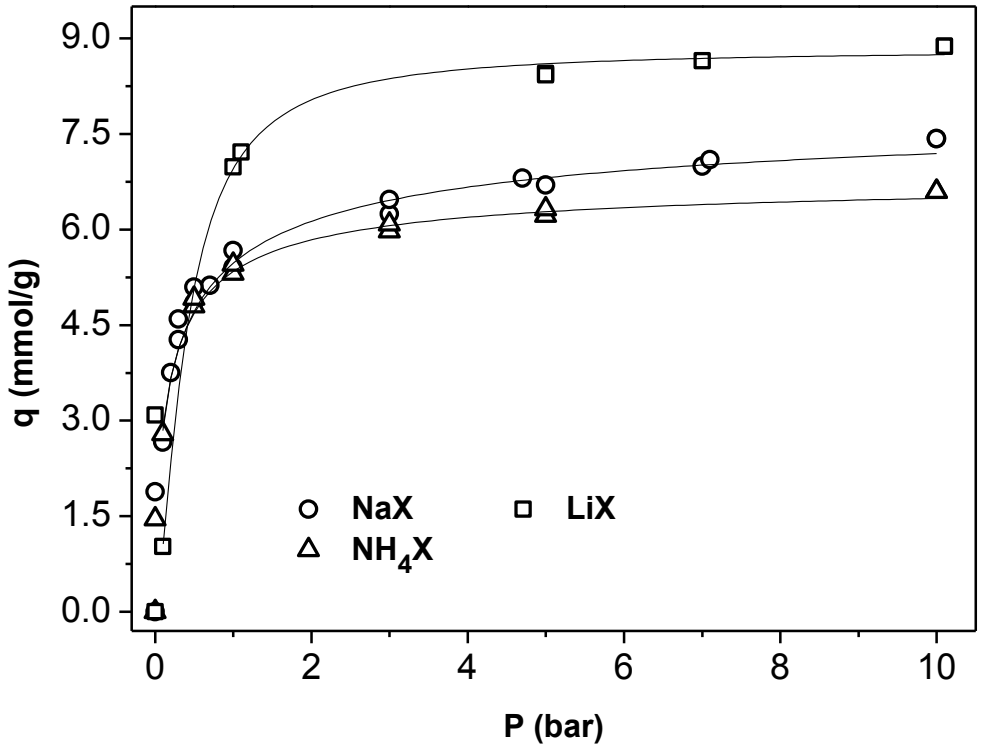

(a)

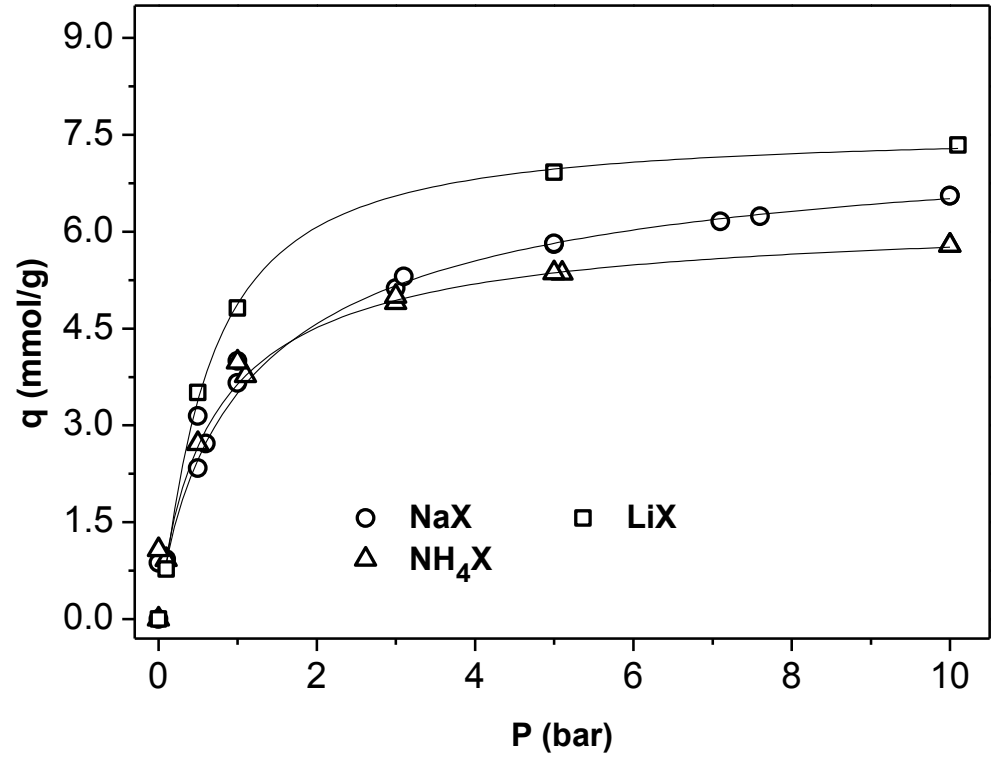

(b)

Figure 6.8. CO_2 adsorption isotherms in NaX, LiX and NH_4X at 298 (a) and 348 K (b).

LiX shows the lowest adsorption at low pressure but presents the largest capacity at 10 bar in both temperatures. This profile is in agreement with the studies of **Walton et al. (2006)**, who suggest that the intensity of the charge density (greater in Li^+) leads to a higher CO_2 adsorption capacity only at high pressure. Such behavior may also may be attributed to the existence of two types of cation sites and to the possibility that a rise in pressure might induce a penetration of greater volume CO_2 deep into the small channels of zeolite, which allows it to interact more strongly with the Li^+ cations located in type II sites of zeolite (**Bonenfant et al., 2008**).

NH_4X, unlike LiX, shows high adsorption capacity only at low pressure (see **Figure 6.9**). The formation of hydrogen bonds (N, H and O) only favors adsorption at low pressures, because the lengths and strengths of hydrogen bonds are quite sensitive to increases in temperature and pressure.

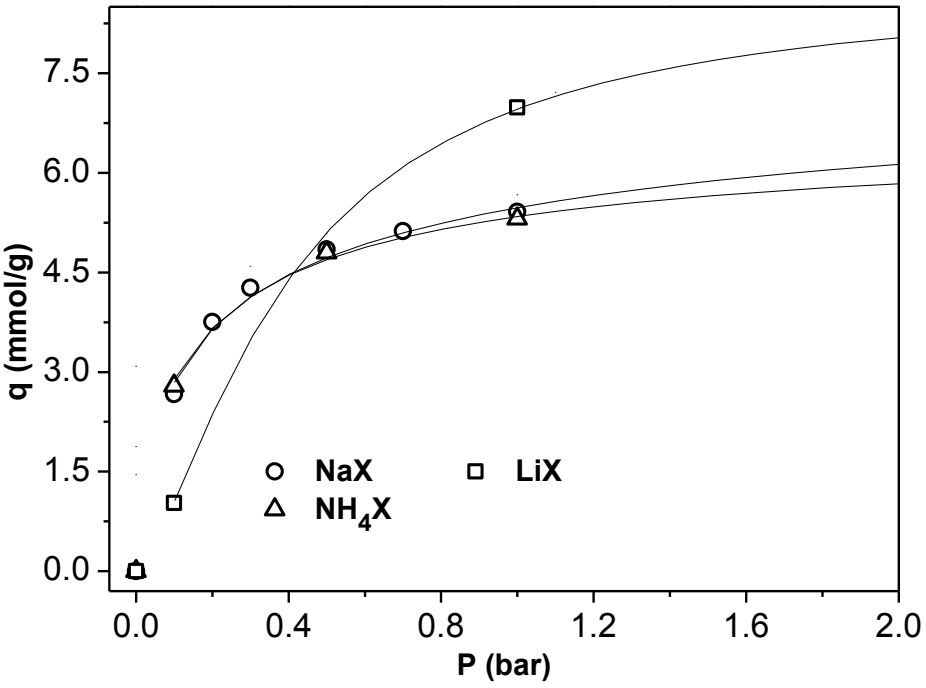

(a)

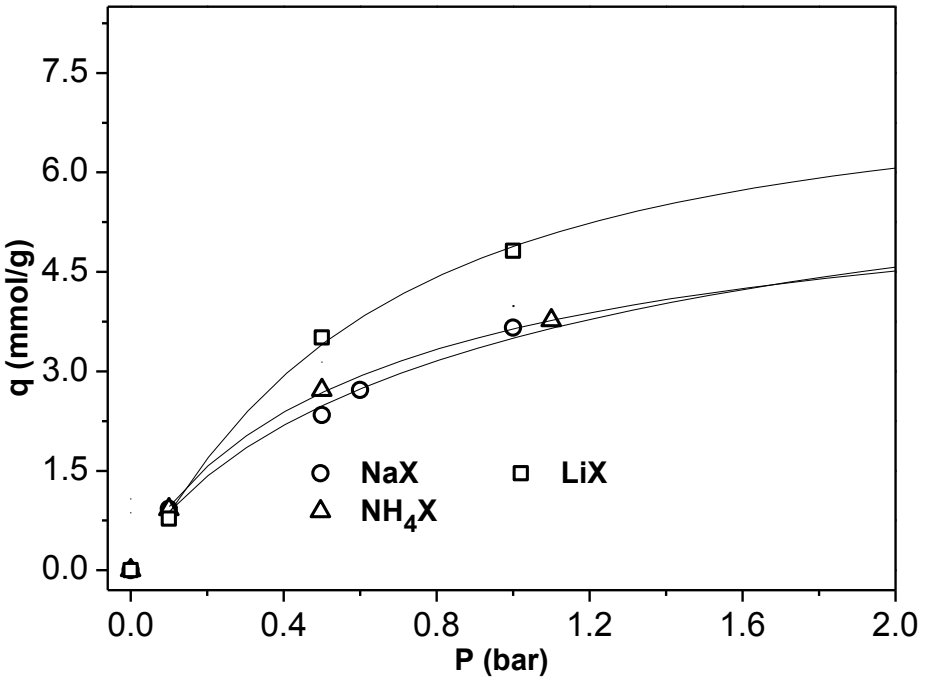

(b)

Figure 6.9. CO_2 adsorption isotherms in NaX, LiX and NH_4X at 298 (a) and 348 K (b). Magnification of the pressure range between 0 and 2 bar.

The CO_2 adsorption uptakes and working capacity at 298 and 348 K for the ion-exchanged zeolites samples are shown in **Table 6.3**. The working capacity for a gas is the difference in adsorption capacity between 0.1-1 bar or 0.1-10 bar.

Table 6.3. CO_2 adsorption uptakes and working capacities for zeolites samples with different compensating cations.

Sample	**CO_2 Adsorption Capacity (mmol/g)**						**Working Capacity (mmol/g)**			
	298 K			**348 K**			**298 K**		**348 K**	
	0.1 bar	**1 bar**	**10 bar**	**0.1 bar**	**1 bar**	**10 bar**	**0.1-1 bar**	**0.1-10 Bar**	**0.1-1 bar**	**0.1-10 bar**
NaX	2.66	5.41	7.42	0.92	3.66	6.55	2.75	4.76	2.74	5.63
NH_4X	2.79	5.31	6.59	0.92	3.77	5.79	2.52	3.80	2.85	4.87
LiX	1.02	6.98	8.87	0.77	4.82	7.34	5.96	7.85	4.05	6.57
BaX	0.84	4.86	6.22	0.62	3.24	5.54	4.02	5.38	2.62	4.92
FeX	0.84	2.49	4.15	0.36	1.78	3.83	1.65	3.31	1.42	3.47

CO_2 is significantly adsorbed in all samples, reaching adsorption uptakes around 9 mmol/g for the LiX at 10 bar and 298 K. This sample stands out in CO_2 uptakes and working capacities, and its interaction with CO_2 is relatively weak at low pressures, which may be an interesting feature for pressure-swing adsorption processes. Moreover, lithium has the lowest molar mass among all studied cations and may outperform them in terms of mmol CO_2 retained per adsorbent unit mass. Another way to compare adsorption capacity is to calculate it in terms of CO_2 retained per unit pore volume ($mmol/cm^3$). These values are summarized in **Table 6.4** and further confirm the superior performance of the LiX sample. LiX has a remarkable working capacity, followed by BaX (this only at low temperature).

Table 6.4. CO_2 adsorption and work capacity in mmol/cm^3.

Sample	CO_2 Adsorption Capacity (mmol/cm^3)					
	298 K			348 K		
	0.1 bar	1 bar	10 bar	0.1 bar	1 bar	10 bar
NaX	6.19	12.58	17.26	2.14	8.51	15.23
NH_4X	7.34	13.97	17.34	2.42	9.92	15.23
LiX	2.64	18.37	23.34	2.03	12.68	19.32
BaX	2.15	12.46	15.95	1.59	8.31	14.20
FeX	2.00	5.93	9.88	0.86	4.24	9.12

It appears that CO_2 adsorption in X zeolites depends not only on the size of the compensation cation, but also the charge ionic, shielding effect, effective nuclear charge, hydrogen bond formation, density and distribution of the cations located in the zeolite framework structures.

Lastly, samples NaX, LiX and NH_4X were tested for adsorption enthalpy as a function of CO_2 adsorbed concentration at 298 K up to 101 kPa. The calorimetric curves are shown in Figure 6.10, where the enthalpy of condensation of CO_2 at 298 K (17 kJ/mol) is highlighted. The enthalpies of adsorption are well over the enthalpy of condensation at this temperature, which is a typical behavior of adsorption in microporous adsorbents, where condensation cannot occur because there are not enough adsorbed layers to form a liquid phase. At low CO_2 loadings, sites with stronger energies are filled first and the highest values of adsorption enthalpies are reached, followed by a gradual decline as the adsorbed concentration increases. For the three samples, adsorption enthalpy levels off to a common value (oscillating around 45 kJ/mol) beyond 3 mmol/g. Among the studied samples, the lowest initial adsorption enthalpy was obtained for the LiX sample, which

indicates that, even though higher adsorption capacities are obtained, probably due to the smaller cation size as mentioned in the literature (**Walton et al., 2006**), less energy should be required to desorb CO_2 from this zeolite, as compared to the other cationic forms. NH_4X sample released slightly higher energy probably due to stronger intermolecular interactions between the ammonium ion and CO_2. Nevertheless, more calorimetric data at lower coverages than 0.5 mmol/g would be desirable for a better understanding on the different bonding energies brought about by the different cations.

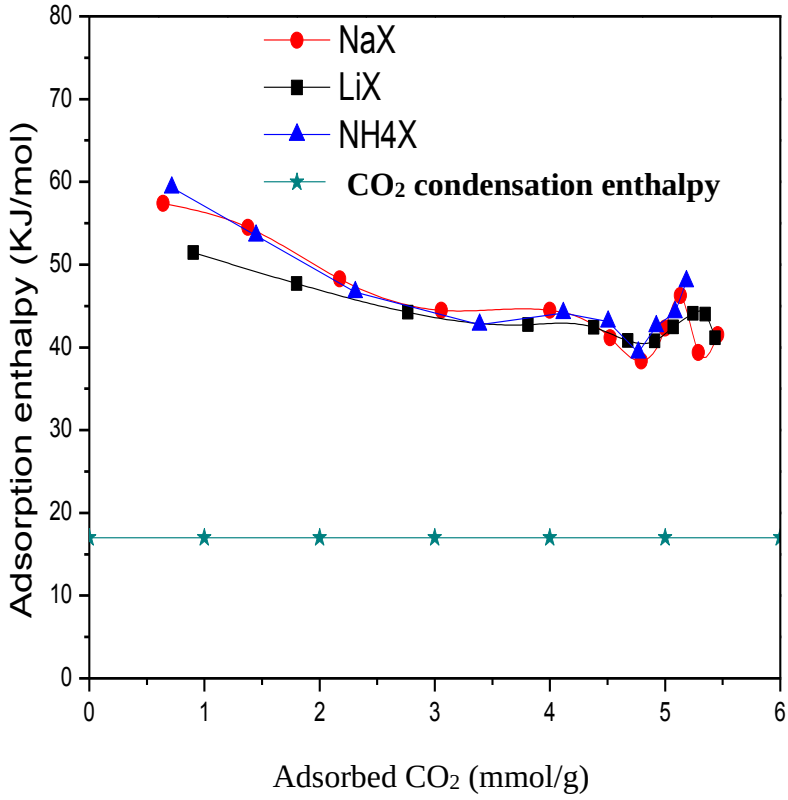

Figure 6.10. Differential adsorption enthalpy as a function of the CO_2 uptake for samples NaX, LiX and NH_4X at 298 K.

6.4. Conclusion

Ion-exchange with various ions (NH_4^+, Li^+, Ba^{2+} and Fe^{3+}) were performed in zeolite NaX binder-free pellets. The extent of ion exchange was confirmed by TGA-MS and textural properties of the samples were measured by XRD and N_2 adsorption-desorption isotherms at 77 K. CO_2 adsorption isotherms of the ion-exchanged samples up to 10 bar were obtained at 298 and 348 K. However, CO_2 adsorption capacity at low pressure and high temperature decreased in the sequence of NH_4X ~ NaX > LiX > BaX > FeX. At 298 K, the sample containing Li as the compensating cation not only binds less CO_2 at lower pressure (below 0.4 bar) and more CO_2 at higher pressures, but also has a lower adsorption enthalpy. These features may suit this sample for cyclic PSA operation better than the other studied cationic forms.

6.5. References

Albo, A., Luis P., Irabin, A. Carbon Dioxide Capture from Flue Gases Using a Cross-Flow Membrane Contactor and the Ionic Liquid 1-Ethyl-3-methylimidazolium Ethylsulfate. Industrial and Engineering Chemistry Research 49 (2010) 11045–11051.

Barrer, R.M. Zeolite and Clay Minerals as sorbents and molecular sieves. Academic Press, New York, 1978.

Barthomeuf, D. Framework induced basicity in zeolites. Microporous and Mesoporous Materials 66 (2003) 1–14.

Bezerra, D.P., Oliveira, R.S., Vieira, R.S., Cavalcante Jr., C.L., Azevedo, D.C.S. Adsorption of CO_2 on nitrogen-enriched activated carbon and zeolite 13X. Adsorption 17 (2011) 235–246.

Bonenfant, D., Kharoune, M., Niquette, P., Mimeault, M., Hausler, R. Advances in principal factors influencing carbon dioxide adsorption on zeolites. Science and Technology of Advanced Materials 9 (2008) 13007–130014.

Chatti, R., Bansiwal, A.K., Thote, J.A., Kumar, V., Jadhav, P., Lokhande, S.K., Biniwale, R.B., Labhsetwar, N.K., Rayalu, S.S. Amine loaded zeolites for carbon dioxide capture: Amine loading and adsorption studies. Microporous and Mesoporous Material 121 (2009) 84–89.

Dantas, T.L.P., Amorim, S.M., Luna, F.M.T., Silva Jr., I.J., de Azevedo, D.C.S., Rodrigues, A.E. and Moreira, R.F.P.M. Adsorption of carbon dioxide onto activated carbon and nitrogen-enriched activated carbon: Surface changes, equilibrium, and modeling of fixed-bed adsorption. Separation Science and Technology 45 (2010) 73–84.

Erten, Y., Günes-Yerkesikli, A., Çetin, A.E., Çakicioglu-Özkan, F. CO_2 adsorption and dehydration behavior of LiNaX, KNaX, CaNaX and CeNaX zeolites. Journal of Thermal Analysis and Calorimetry 94 (2008) 715–718.

Hutson, N.D., Reisner, B.A., Yang, R.T., Toby, B.H. Silver ion-exchanged zeolites Y, X, and low-silica X: Observations of thermally induced cation/cluster migration and the resulting effects on the equilibrium adsorption of nitrogen. Chemistry of Materials 12 (2000) 3020–3031.

Klier, K. Transition-metal ions in zeolites: the perfect surface sites. Langmuir 4 (1988) 13–25.

Lin, L., Lei, Z., Wang, L., Liu, X., Zhang, Y., Wan, C., Lee, D.J., Tay, J.H. Adsorption mechanisms of high-levels of ammonium onto natural and NaCl-modified zeolites. Separation and Purification Technology 103 (2013) 15–20.

Plant, D.F., Maurin, G., Deroche, I., Gaberova, L., Llewellyn, L.P. CO_2 adsorption in alkali cation exchanged Y faujasites: A quantum chemical study compared to experiments. Chemical Physics Letters 426 (2006) 387–392.

Rouquerol, F., Rouquerol, J., Sing, K. Adsorption by Powders & Porous Solids, Academic Press, San Diego (1999).

Silva, F.W.M., Soares-Maia, D.A., Oliveira, R.S., Moreno-Pirajan, J.C., Sapag, K., Cavalcante Jr., C.L., Zgrablich, G., Azevedo, D.C.S. Adsorption microcalorimetry applied to the characterization of adsorbents for CO_2 capture, Canadian Journal of Chemical Engineering, 90 (2012) 1372–1380.

Sing, K.S.W., Everett, D.H., Haul, R.A.W., Moscou, L., Pierotti, R.A., Rouquerol, J., Siemieniewska, T. Reporting physisorption data for gas/solid systems with special reference to the determination of surface area and porosity. Pure and Applied Chemistry 57 (1985) 603-619.

Valdés, H., Alejandro, S., Zaror, C.A. Natural zeolite reactivity towards ozone: The role of compensating cations. Journal of Hazardous Materials 15 (2012) 34–40.

Walton, K.S., Abney, M.B., LeVan, M. D. CO_2 adsorption in Y and X zeolites modified by alkali metal cation exchange. Microporous and Mesoporous Materials 91 (2006) 78–84.

Yang, S.T., Kim, J., Ahn, W.S. CO_2 adsorption over ion-exchanged zeolite beta with alkali and alkaline earth metal ions. Microporous and Mesoporous Materials 135 (2010) 90–94.

Yi, D., Huang, H., Meng, X., Shi, L. Adsorption–desorption behavior and mechanism of dimethyl disulfide in liquid hydrocarbon streams on modified Y zeolites. Applied Catalysis B: Environmental 148 (2014) 377–386.

CHAPTER 7 – CONCLUSION AND SUGGESTIONS FOR FUTURE WORK

7.1. Conclusion and Final Comments

The objective of this study, as described in Chapter 2, was to explore the range of adsorbents that can be used for CO_2 capture in post-combustion scenario. The commercial adsorbents show good adsorption capacity at room temperature (around 298 K); however, CO_2 uptake decreases significantly with an increase in temperature. In amino-grafted adsorbents, the reduction in adsorption capacity with an increase in temperature is less noticeable. The discussion on such effect was supported with characterization techniques used in the Chapter 3, 4 and 5, and attributed to both chemisorption and diffusion resistances for measurements at lower temperatures.

The issue of obtaining amino-grafted adsorbents with greater adsorption capacity than the pristine adsorbent (at least at room temperature) persists. Under the conditions studied and described in Chapters 4 and 5, the amino-grafted samples are not yet feasible adsorbents for their use in CO_2 capture. Grafting amines on mesoporous supports, as reported by many authors, leads to higher CO_2 uptakes as compared to the pristine supports. Nevertheless, bare mesoporous solids themselves are poor candidates for gas adsorption in general, so that any surface functionalization will appear to boost its adsorption capacity. Up to the present, and to the knowledge of this author, such mesoporous amine modified adsorbents have not outperformed microporous physisorbents at low temperatures (e.g. 298 K).

Nevertheless, further investigation under conditions similar to those of post combustion scenarios should be carried out. According to the accepted reaction mechanism between grafted amine and CO_2, the presence of water would double the

adsorption capacity of these amine-modified adsorbents. Additionally, experiments with CO_2/N_2 mixtures are necessary, because very often adsorbent selectivity towards CO_2 is enhanced in amine-modified adsorbents, despite the reduction in adsorption capacity.

The study described in Chapter 6 discloses another option for the application of physisorbents in CO_2 capture. The adsorbent LiX and NH_4X showed structural stability andsuperior capacity as compared to the commercial sample 13X (with sodium). The adsorbent containing lithium may be particularly attractive because it adsorbs less CO_2 at low pressures (below 0.4 bar) and retains more CO_2 at higher pressures, as compared to the zeolites with other cations. It also releases less adsorption enthalpy at low coverage, which implies less energy cost for desorption. Under dry conditions, this adsorbent may be potentially attractive for CO_2 separations from natural gas or biogas. At 298 K, a working capacity (0.1-1 bar) of 6 mmol/g was obtained.

Table 7.1. Comparison CO_2 adsorption capacity for sample studied.

Sample	**CO_2 Adsorption Capacity (mmol/g)**					
	298 K			**348 K**		
	0.1 bar	**1 bar**	**10 bar**	**0.1 bar**	**1 bar**	**10 bar**
ZX	3.34	4.68	5.73	1.25	3.23	4.50
ZX10	0.03	0.42	1.78	0.75	1.55	2.98
AC	0.13	1.20	6.57	0.04	0.43	2.93
ACN10	0.06	0.59	3.07	0.08	0.74	3.68
ACN20	0.02	0.16	1.07	0.00	0.03	0.35
NaX	2.66	5.41	7.42	0.92	3.66	6.55
NH_4X	2.79	5.31	6.59	0.92	3.77	5.79
LiX	1.02	6.98	8.87	0.77	4.82	7.34
BaX	0.84	4.86	6.22	0.62	3.24	5.54
FeX	0.84	2.49	4.15	0.36	1.78	3.83

7.2. Suggestions for Future Work

Microporous adsorbents obtained from MEA grafting, both activated carbons and zeolites, must be subjected to experiments under humid conditions and in the presence of N_2. It is expected that CO_2 uptakes are doubled, at least for the hydrophobic matrices (activated carbons) according to the zwitterion reaction mechanism (carbamate/bicarbonate) previously mentioned. Cyclic adsorption/desorption experiments should be carried out in order to evaluate leaching/deactivation of amines.

Binary adsorption isotherms (N_2/CO_2 and CH_4/CO_2) must also be measured for cation-exchanged zeolites in order to investigate the effect of the compensating cation on the CO_2 selectivity.